For Reference

NOT TO BE TAKEN FROM THIS ROOM

Ex libris
universitatis
albertaensis

The University of Alberta
Printing Department
Edmonton, Alberta

Digitized by the Internet Archive
in 2020 with funding from
University of Alberta Libraries

https://archive.org/details/Chary1971

THE UNIVERSITY OF ALBERTA

AN ISOTOPIC AND GEOCHEMICAL STUDY OF GOLD-QUARTZ VEINS IN THE CON-RYCON MINE, YELLOWKNIFE (N.W.T.)

by

© K. NARASIMHA CHARY B.Sc. (Hons.) M.Sc. (Tech.)

A THESIS

SUBMITTED TO THE FACULTY OF GRADUATE STUDIES

IN PARTIAL FULFILMENT OF THE REQUIREMENTS FOR THE

DEGREE OF MASTER OF SCIENCE

DEPARTMENT OF GEOLOGY

EDMONTON, ALBERTA

SPRING 1971

UNIVERSITY OF ALBERTA

FACULTY OF GRADUATE STUDIES

The undersigned certify that they have read, and recommend to the Faculty of Graduate Studies for acceptance, a thesis entitled An Isotopic and Chemical Study of Gold-Quartz Veins in the Con-Rycon Mine, Yellowknife (N.W.T.), submitted by K. Narasimhachary in partial fulfilment of the requirements for the degree of Master of Science

ABSTRACT

The temperature of formation of the gold-quartz deposits, Yellowknife, N.W.T., is obtained: 1) by studying isotope fractionation among the coexisting sulfide minerals associated with gold-quartz veins, and 2) by fluid inclusion homogenization temperatures on quartz, to be in the range of 350°-300°C.

From the thermochemical data and the knowledge of the mineral assemblages, the fugacities of oxygen and sulfur are calculated to be in the range of 10 exp. -31 to -29 and -10.5 to -8.5 respectively.

The O^{18} of the hydrothermal fluids is calculated assuming equilibrium between quartz-calcite-water (O^{18}_{water} = 5.0-6.8‰) and this value is very close to the established isotopic compositions of magmatic waters.

From the derived fugacities of CO_2 and CH_4, the total carbon isotope values are calculated to be in the range of -4.2 to -0.5‰, based on the mole fractions of CO_2 and CH_4, assuming $CaC)_3$-CO_2-CH_4 equilibria.

By comparing the frequency plot of Na/K ratios obtained on the fluid inclusions from quartz with the established plots of different aqueous solutions the ore-forming fluids are concluded to have been derived, most likely, from a magmatic source.

ACKNOWLEDGEMENTS

The author would like to acknowledge the advice and supervision given to him by Dr. R. D. Morton during the preparation of this thesis.

Dr. Baadsgaard's instructions and discussions in the flame photometric determinations are gratefully acknowledged. Thanks are due to Drs. H. Ohmoto and P. Fritz for introducing the author to the various techniques and for their discussions and constructive criticism throughout this work.

Mass spectrometric facilities were made available by the Department of Physics through the courtesy of Dr. H. R. Krouse.

Particular thanks are due to Mr. D. E. Jardine, Geologist, Con-Rycon Mines, Cominco Limited, for providing suitable samples for isotope studies. Special thanks are due to Dr. I. Kota Reddy, Department of Physics, for his suggestions in the computer programming.

Technical and other facilities were made available by the Department of Geology, University of Alberta. Financial assistance was provided by the University of Alberta in the form of a graduate assistantship; and finally, the thesis was typed by Miss P. Lumsden.

TABLE OF CONTENTS

LIST OF FIGURES

LIST OF TABLES

APPENDICES PAGE

INTRODUCTION

Yellowknife is situated on the northern shore of Great Slave Lake (lat 62°30'N, long 114°30'W) in the North West Territories. The Con-Rycon Mine is located nearly 2 miles South of the Yellowknife town site (Fig. 1). The Con-Rycon Mine, which began production in 1938, is the major gold producer of the district and is the property of Consolidated Mining and Smelting Company of Canada. The other producing mine operating in the area is the Giant Mine, situated about 3 miles North-east of the Con-Rycon Mine.

The topography of the Yellowknife area is typical of the Pre-Cambrian Shield. The country is almost flat. Numerous lakes and muskegs are quite common in the area. Permafrost conditions exist in most parts of the area.

Objectives of the Thesis

Laboratory investigations, including optical, isotopic and fluid inclusion studies have been conducted on the samples collected from the Campbell Shear System, Yellowknife. It is the purpose of the thesis to reconstruct a possible geological environment in the light of the physico-chemical factors that would have influenced ore deposition.

The techniques used in this study were: (a) sulfur isotope studies, (b) fluid inclusion work, (c) carbon and oxygen isotope work, (d) K/Na ratio distributions in fluid inclusions, (e) mineral associations, and (f) application of the principles of thermodynamics in natural systems and isotope geochemistry.

CHAPTER I

REGIONAL GEOLOGY

The mineral potential of the Yellowknife area has resulted in extensive detailed mapping of this district of the Slave Province since 1938 (Henderson, 1939; Henderson and Brown, 1949, 1952, 1966; Lord, 1942; Fortier, 1947; Folinsbee, 1947; Moore, 1956; Boyle, 1961; Baragar, 1966; and Kretz, 1967).

The Precambrian rocks of the Yellowknife group have been broadly divided into two major rock units: Division A and B (Joliffe 1938). Division A consists of a series of dark green, metamorphosed Volcanic rocks which includes meta-andesites, meta-basalts and intercalated meta-dacites with associated pyroclastics. Division B consists predominantly of conglomerates, arkosic quartzites (sub-greywackes) and acid volcanic rocks resting more or less unconformably on the rocks of Division A (Table 1). Palimpsest volcanic structures are often preserved in the rocks of Division A, especially pillow and flow-structures, which are quite noticeable on the surface as well as at the underground levels of the mines. Slight modifications in categorizing the various rocks have been introduced by later authors (Henderson and Brown, 1966; Green, 1968), however, the major distinction between Divisions A and B has been retained in all cases. The volcanic and sedimentary rocks (Division A and Division B) are intruded by many sills and dykes of meta-gabbroic and meta-dioritic character.

FIGURE 1

Regional Geology, Yellowknife Area,
Northwest Territories
(After Boyle 1961)

Regional Geology, YELLOWKNIFE AREA

Northwest Territories

Legend:

- Diabase, Gabbro
- Prasperous Lake Granite
- Western Granodiarite, Southeast Granodiorite
- Diarite
- Graywacke, Argillite, Quartzite, Slate, Phyllite
- Nodular Quartz-Mica Schist and Hornfels
- Dacite, Trachyte, Rhyolite, Qtz-Porphyry and Tuff
- Andesite, Basalt, Metogabbro
- Conglomerate and Quartzite
- Drift-covered area
- Fault

Scale in miles

0 2 4 6

Scale in kilometers

0 4 8 12

Location Map

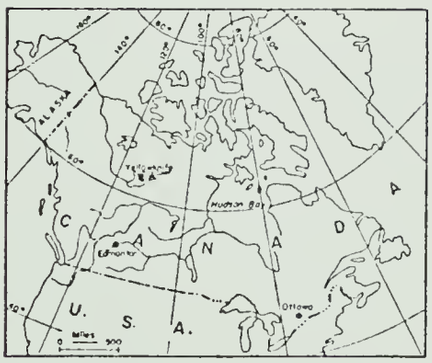

MAP ADAPTED FROM BOYLE, 1961, FIG.1.

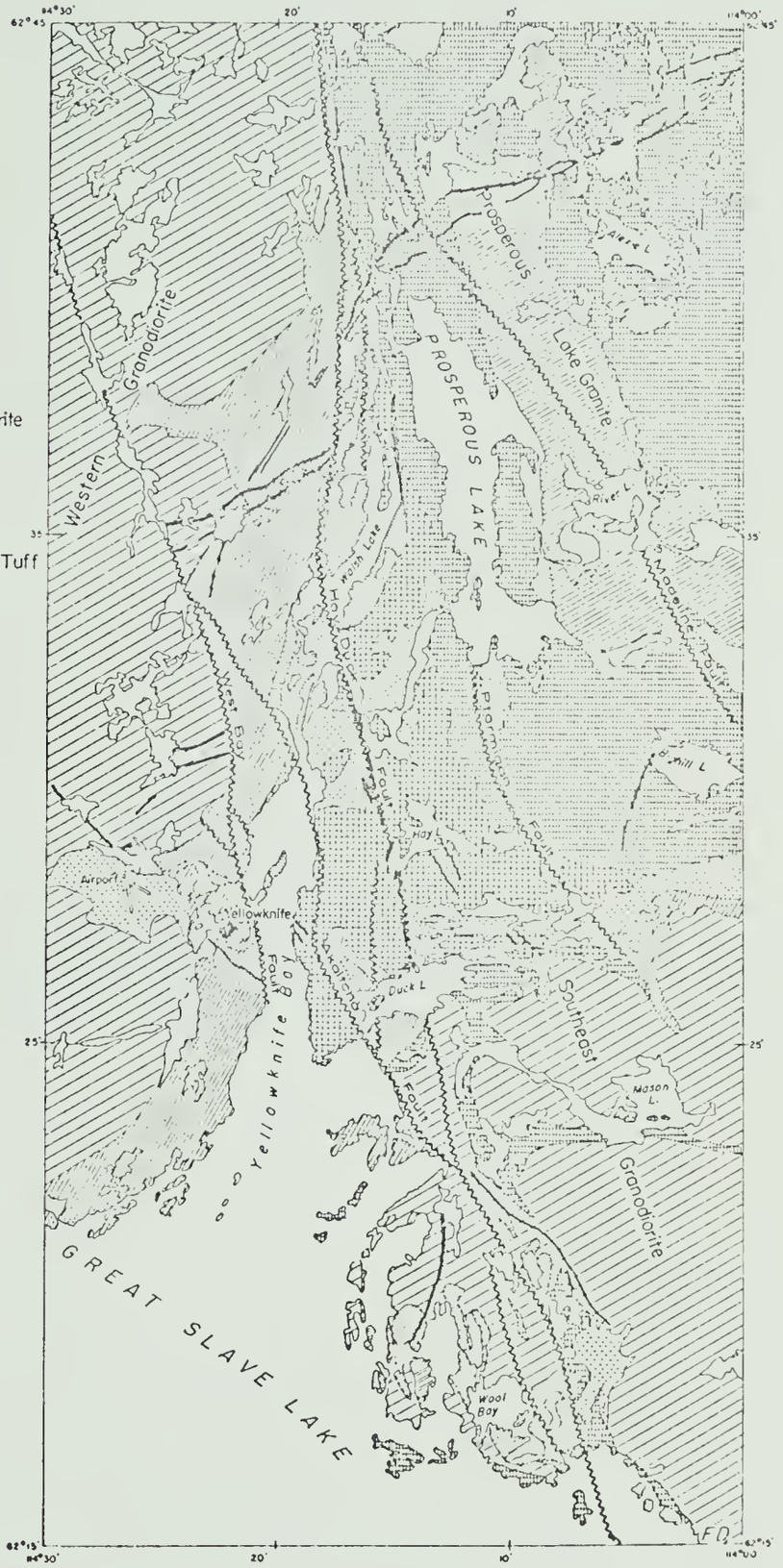

TABLE 1

Table of Formations (Pre-Cambrian)
Yellowknife Area, Northwest Territories
(adopted from Green 1968)

AGE	FORMATION	DESCRIPTION	REMARKS
PROTEROZOIC		Diabase dykes	
		Granite, granodiorite Nepheline-sodalite syenite	(Hudsonian)
		Diabase, picrite-gabbro dykes	(Leech 1966)
	Snare Group	Finely bedded, alternating siltstone and shale and metamorphic equivalents. Dolomite, arkose	(Lord 1942) (Ross and McGlynn 1963)
	UNCONFIRMITY		
ARCHAEAN		Redout Lake, Prosperous Lake granites and associated pegmatites	
		Western granodiorite (? Ross Lake granodiorite) Stock Lake stock, aplites (? South-east granodiorite)	
		Quartz feldspar porphyries	
		Second phase of metadiorite and meta gabbro intrusion	
	Yellowknife Group Division B	Graywacke, argillite, phyllite, quartzite etc. and their metamorphic equivalents. Dacite, trachyte rhyolite, quartz porphyry, pyroclastics and their metamorphic equivalents.	(Overlie Div. A with apparent regional confirmity)
	Unclassified (stratigraphic position uncertain)	Conglomerate and quartzite	
	----- Local Unconformity		
	? (South-east granodiorite)		(Folinsbee et al. 1968)
		First phase of metadiorite and metagabbro intrusion	
	Yellowknife Group Division A	Basalt, andesite, dacite rhyolite, cherty tuff and their metamorphic equivalents	
		(Ross Lake Granodiorite)	(Baragar 1966)

1.1 METAMORPHIC FACIES - YELLOWKNIFE GROUP

The volcanic rocks of the Yellowknife group have been considerably altered during regional metamorphism. These basic volcanics exhibit three metamorphic grades, the isograds, which are almost parallel to the Western granodiorite greenstone contact (see Fig. 1). The amphibolite facies rocks adjoining the Western granodiorite grade into epidote-amphibolite lithologies followed by rocks of green schist facies, when one traverses from West to East.

The rocks of amphibolite facies grade are mainly fine-grained, meta-basalts and meta-andesites. Horenblende, plagioclase (andesine) and epidote are the major constituent minerals. Quartz, ilmenite and sphene occur in small quantities. In contrast the rocks of the epidote amphibolite facies are relatively massive and contain light-green, fibrous amphibole, plagioclase (albite to oligoclase) and epidote. Quartz and small amounts of carbonate minerals are also almost ubiquitous.

The rocks of the green schist facies are of relatively limited occurrence in the district. One of the areas where these rocks are exposed is the so-called Giant-fault block East of Bow Lake. The constituents of the green schist lithologies are green chlorite, epidote plagioclase (albite) and carbonate minerals. The most characteristic feature of the meta-volcanics is that they have often retained the original pillow structures. According to Henderson and Brown (1966) there are two varieties of volcanics: massive flows and pillowed flows. Gradations between these two varieties are often seen. The massive flows are relatively coarser grained. The dimensions of the pillows range in length from a few inches to more than 1-2 feet. Each pillow is separated from its neighbouring pillow by a strong alteration rim surrounding each

pillow.

Henderson and Brown's (1966) petrographic study and Boyle's (1961) chemical studies on these meta-volcanics may be summarized as follows: SiO_2 and CaO show little difference from a typical basalt, whereas Al_2O_3 and Fe_2O_3 show a slight depletion and H_2O, CO_2, K_2O, and Na_2O exhibit a minor enrichment above a normal basaltic composition. There are different opinions on the origin of the pillowed structure in the pre-Cambrian volcanics. None of the theories would provide a clear explanation of the origin of the pillow structures. Lewis (1941) suggested that these pillow-lavas have originated due to sub-aqueous conditions. Recent views of Henderson and Brown (1966) on the mode of formation of the pillows are that each pillow has been emplaced as an individual unit, and in most cases, the upper pillow is deposited when the lower pillow is still in semi-solid, flexible plastic state. It is believed by most of the authors that pillow structure would probably have resulted from sudden chilling action at the contact.

Meta-dacites and associated meta-agglomerates, meta-tuffs and meta-breccia are exposed West of the old town-site, near the West-Bay fault. Apparently these flows are displaced North to South by more than three miles by the West-Bay fault and their continuation could be seen at the Giant C shaft. These dacites are generally fine-grained, white to buff-colored when weathered and often contain phenocrysts of feldspar and quartz. Henderson and Brown (1966) have pointed out that it is often difficult to assess the exact, original mineralogical composition of these rocks. In Henderson's opinion (1966), the more siliceous and porphyritic types might have been derived from original normal basalts and the meta-andesites could be the result of later processes of alter-

ation and metasomatism involving albitisation, silicification and chloritization.

1.2 PLUTONIC INTRUSIVES

Certain plutonic intrusive masses in the district have been studied in detail by Green (1968). The Western granodiorite is a relatively large intrusive body which abuts against the greenstone belt and extends more than 50 miles westwards. The composition of this intrusive varies from granite, adamellite, granodiorite to quartz diorite. Compositional variations in Na/K ratios have been recorded by Boyle (1961) who interpreted the higher Na/K ratios along the eastern margin of the intrusive body (compared with the ratios in the interior portions) as being due to K^+ mobilisation into the metavolcanics. In the northern part of the area, the contact between the granodiorite and metavolcanics is gradational whereas in the southern parts it is quite sharp and irregular. Green's modal analyses (1968) shows a gradational variation from granite to granodiorite and adamellite. The Stock Lake granodiorite is similar to the Western granodiorite in texture and composition (Henderson and Brown, 1966). There is clear evidence of assimilation of the bordering greenstones by the intrusives at their contacts. The composition of the Stock Lake granodiorite varies from quartz diorite to quartz monzonite (Green 1968). The southeast granodiorite ranges in composition from normal granodiorite to trondhjemite (Green 1968) but it is predominantly biotite-bearing granodiorite. The Ross Lake granodiorite, the Redout Lake granite and the Prosperous Lake granite are the other intrusive bodies identified in the area, and their relationships with the metavolcanics remain to be worked out in detail.

CHAPTER II

GEOLOGY OF THE SHEAR ZONES AND ORE DEPOSITS

Detailed descriptions of the shear zones and the nature of the ore deposits have been provided by Boyle (1961) and this work serves as the basis for the descriptions and discussions embodied in this thesis. The shear zones in the greenstone belt apparently fall into two structural groups, namely (a) those which parallel the strike of the volcanic flows and tuff beds, and (b) those which transect these horizons. The shear zones paralleling the flows and tuffs are narrow, discontinuous entities which do not carry any economic deposits. In contrast, those shear zones which transect the greenstone belt often contain potential economic ore deposits.

Boyle's detailed descriptions (1961) of the shear zones and their internal nature may be summarised as follows: two types of internal features may be distinguished: (a) Breccia zones, and (b) Schist zones. Breccia zones which are well developed in the Negus-Rycon and Con systems are characterised by lithologies broken into spindle-shaped fragments locally cemented by carbonates. The fragments are rarely greater than 6 inches in any dimension and the majority of them are about the size of brazil nuts, which they simulate in shape. The fragments in these breccias are massive to slightly schistose in character and seldom exhibit the marked schistosity or extreme alteration of the rocks which comprise the schist zones. Where quartz lenses occur in this type

of shear zone, a buff colored, dense and dyke-like alteration zone is present in which the outlines of the original breccia fragments can be discerned upon close examination.

The schist zones are characterized by linear zones of extremely schistose rock with very strong lineations, characterized by abundant chlorite and/or sericite. Schistose zones are especially common in the ore bodies of the Con and Negus-Rycon systems and are the principal features of the Giant-Campbell shear zone system. In nearly all cases the dips and in some cases the strikes of the schistose planes intersect the walls of the shear zones at a small angle.

In most of the transecting shear systems, gradational contacts between schist zones and breccia zones are common. This feature is well illustrated in the Negus-Rycon system where the gradation can be traced with some degree of confidence. In some of the shear zones, the ideal breccia shear zones grade imperceptibly to schist zones along strike and in some cases down dip. In the transition from the breccia type zone to schist zones the fragments of the breccia become elongated and flattened, alteration increases concomitantly and the fractures separating the fragments are partly or completely obliterated. The end result is a well-developed schist in which traces of fragments may appear, but in general no hint of the original breccia remains. The transition from breccia to schist can be seen in schist zones, but in others no such genetic origin for the schist zone can be evoked. The internal features of the schist zones paralleling the flows and those of the Giant-Campbell and portions of the Con systems suggests that extensive brecciation was not a major factor in their development.

2.1 THE CON-RYCON SYSTEM

Detailed descriptions of the main shear zones have been supplied by Campbell (1949), Lord (1951) and Sproule (1952). The structure has been traced southwest along the southeast end of Pud Lake and up to the Kam fault zone (Fig. 1). Brown and Henderson stated that the Con system has branched out into two or more zones and is a part of the Campbell system. However, no positive evidence for such a suggestion is apparently available at present and any conclusions remain speculative. On the other side of the Pud Lake, the Con shear system exhibits quite distinct characteristics. On the southern part of the shear zone, it is characterized by the coalescence of numerous shear zones whereas in the northern part of the system, it exhibits a multiple branching effect into series of small shear zones. But on the 500 ft level of the Con mine all these structures merge to form the so-called C-4 schist zone and again at deeper levels the shear system splits into minor shear zones separated by several minor blocks of barren meta andesitic lithology. As Henderson and Brown (1966) pointed out, the ore bodies are quartz lenses, pods and replacement bodies mineralized with pyrite, arsenopyrite, chalcopyrite, sulfo salts, galena and native gold.

The general strike of the system is N80°E and the dip 53°W. The Negus-Rycon system strikes N10-25° and dips 45-65°W. Henderson and Brown (1966) suggest that the Negus-Rycon system was probably formed by thrust movements generated by the same forces which produced the Giant Campbell and Con shear systems. The veins are quite discontinuous, small and contain a wide variety of metallic minerals: e.g., pyrite, gold, arsenopyrite, chalcopyrite, stibnite, various sulfo salts, sphalerite and galena.

2.2 THE GIANT-CAMPBELL SYSTEM

Extensive work has been performed by many authors on different aspects of the Campbell shear system (e.g. Henderson and Brown, 1952b; Dadson and Bateman, 1948; Dadson, 1949; Campbell, 1949; Lord, 1951; Bateman, 1952; Boyle et al. 1961; and Henderson and Brown, 1966). The Campbell shear system is one of the district's longest ore-producing systems. The northern extensions of the Campbell shear system, on the eastern side of the West Bay fault, have posed a controversial problem to many geologists. Campbell's (1949) location of the extensions of the shear zone on the southern part of the West Bay fault was a noteworthy step to economic development of the area.

The southern extension of the Giant-Campbell system, south of the West Bay fault is known as the Campbell shear system and is exposed for 8000 ft in the underground workings of the Negus and Con mines at the 2300 ft level. Examination of the mine plans and sections at varous levels, indicates that the width of the shear zone at the 2300 ft level is in excess of 200 ft, whereas at the 4500 ft level the width is only around 95 ft (Fig. 2). Moreover, the shear zone at the 2900 ft level is quite complex with intertwined zones separated by a barren zone of massive andesite. The massive included block of andesite is almond shaped. The shear zone maintains a strike direction of N25°E and dips vary from hanging wall to foot wall. The foot wall dips are generally steeper and the hanging wall dips vary from 45° to 65°W.

In the Campbell shear system, drag-folded and contorted schist zones apparently acted as susceptible locations for accumulating hydrothermal solutions which induced silicification, sericitization and metallic mineralization.

FIGURE 2

Typical Geological Section of the Campbell Shear Zone showing the relationship between the Gold-Quartz Lenses and the Alteration Zones

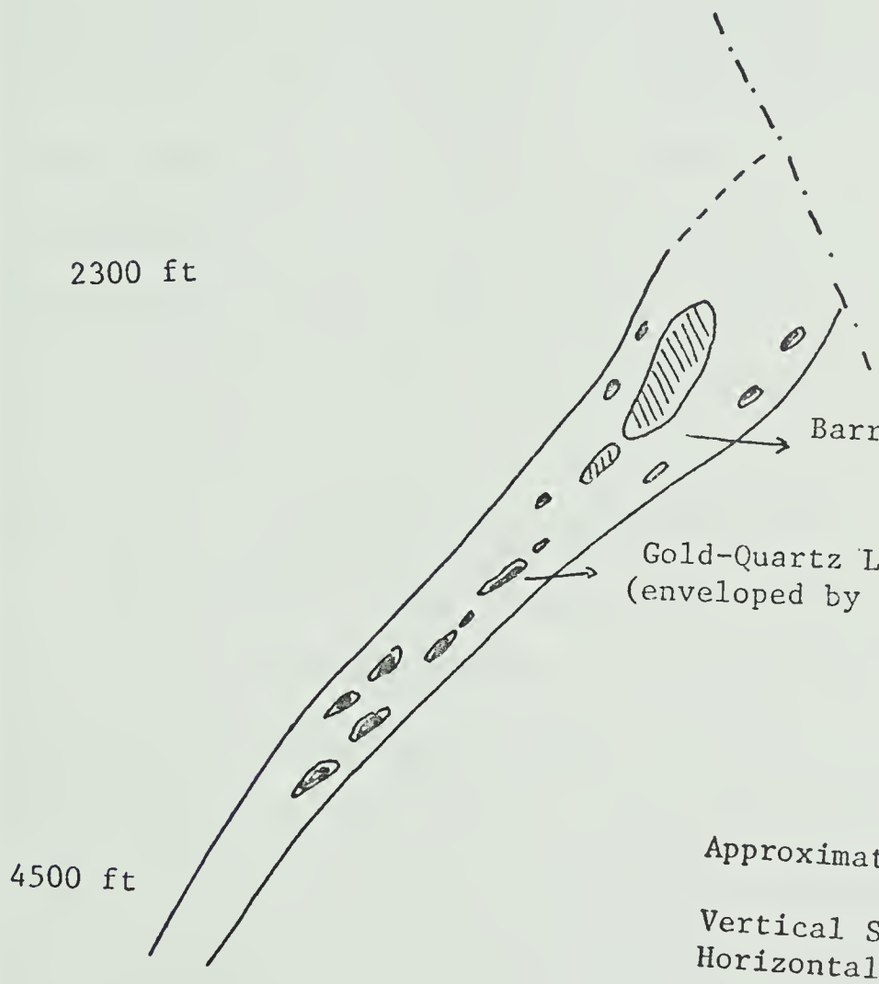

Approximate

Vertical Scale: 1 cm : 300 ft
Horizontal Scale: 1 cm : 10 ft

The mineralogy of the schist zone is comparatively complex, being composed of quartz, albite, carbonate and sericite.

2.3 QUARTZ LENSES AND THE VEIN PATTERN IN THE SHEAR ZONE

Quartz lenses enclosed within an envelope of sericite-chlorite schist constitute the main ore bodies in the shear zone. Two generations of quartz have been identified (Boyle 1961). The first generation of quartz occurs as complex, gold-bearing lenses and veins. The second type occurs as small stringers cutting the shear zone. The gold-bearing lenses range from a few inches in width to 3 ft or more. However, smaller en echelon lenses are more common and these only occasionally merge to form larger, richer lenses. Small stringers of carbonates cutting across the quartz lenses as well as the schistosity of the chlorite schist and sericite schist are quite common. The nature and mineralogy of the alteration zone are discussed elsewhere.

Many different opinions exist concerning the origin of the shear zone. The internal structures of the schist zones, particularly the ore-bearing sericite and quartz zones, show clear indications of folding (Brown, Dadson and Wriggleworth, 1959) which might be the result of simple folding of the green schist belt. Secondly the schist zone might have originated due to shearing rather than folding, as the schist zone transects the regional strike of the flows at a low angle.

The Giant-Campbell system, a complex, intricate system of shear zones (Henderson and Brown, 1966) is visualized as a result of the principal folding process. It is believed that ore deposition accompanied the last stages of development of the shear zone system. No definite metamorphic or structural event for the development of dilated zones in

the shear zone has been pointed out, however, it is suggested that the shear zone has originated as a result of thrust faulting along which the shear zone has developed (Henderson and Brown, 1966).

CHAPTER III

MINERALOGY AND PARAGENESIS

The principal objective of the microscopic examination of the specimens discussed herein was the study of textural relationships between the co-existing phases in various samples collected at different elevations in the mine, thereby interpreting the stages of deposition, the paragenetic sequence and the physico-chemical conditions prevailing during the period of mineral deposition. At the same time the microscopic examination of the ores served to check the purity of the mineral separates utilized in isotope analyses and to indicate the optimum size for the separation of pure fractions. X-ray methods were concluded to be inapplicable to these samples owing to the very low percentages of contamination, likely to be encountered in the mineral separates used for analysis.

The ore minerals identified were in order of abundance: pyrite, galena, sphalerite, arsenopyrite, chalcopyrite, native gold and pyrrhotite. The major gangue minerals were found to be quartz, calcite, sericite and chlorite. Especially in the mineralised lenses, quartz is the major phase, sulfides representing 5 to 8% by volume. Among the sulfides, pyrite constitutes 70-80% of the fraction.

3.1 DESCRIPTION OF THE MINERALS

Pyrite:

Pyrite occurs as large euhedral to subhedral grains ranging from 0.5 to 2.0 mm in diameter. Most of the specimens contain euhedral pyrite crystals exhibiting no replacement textures. However, the pyrite, in some instances does exhibit replacement textures in which pyrite is replaced by galena, sphalerite and chalcopyrite. Arsenopyrite does not seem to have replaced pyrite in any specimens.

Arsenopyrite:

Arsenopyrite occurs mainly as euhedral grains. It is generally believed by many of the mine geologists that wherever arsenopyrite is present, higher values of gold should be expected. Actually there does not seem to be any genetic relationship between gold and arsenopyrite and in a mumber of instances, native gold was identified associated with quartz and pyrite in sections devoid of arsenopyrite. The general grain size of arsenopyrite ranges from 0.2 mm to 1 mm diameter.

Galena:

Galena was always associated with sphalerite and pyrite and in parts the mineral was observed replacing pyrite. However, other specimens showed alternating bands of galena and pyrite in apparent equilibrium. The galena grains were euhedral to subhedral, 0.5 mm to 2 mm in diameter.

Chalcopyrite:

Chalcopyrite is in most cases associated with pyrite, essentially replacing pyrite. Generally the grain size of the chalcopyrite ranges from 0.2 to 1 mm and the mineral is subhedral.

Pyrrhotite:

Pyrrhotite was also noted in a few sections occurring as grains always associated with pyrite. It is possible that pyrrhotite may be cogenetic with the pyrite.

Gold:

Gold is apparently present in two distinct phases: (a) in the form of the native element, and (b) in the form of auro-complexes. Native gold could be identified very easily in hand specimens. Some of the alteration zones as well as the lenses show very high assay values, even though no visible gold is present. In these alteration zones, most of the gold is probably present in sulfo-complexes.

Quartz:

Boyle (1961) distinguished two types of quartz in the ore bodies of Yellowknife region; viz. earlier quartz which is massive, white in colour and commonly occurs in small, narrow, irregular lens-like ore bodies grading into the alteration zones. A later quartz occurs in small and narrow veinlets or stringers cutting earlier quartz and alteration zones.

In thin sections the quartz is medium to coarse grained and most of the sections show highly strained and crushed grains with intermittent clear patches of unstrained quartz between them. The fluid inclusions in quartz are mainly of two sizes, the majority being 0.05 mm to 0.1 mm in diameter whereas others range from 0.2 to 0.3 mm. The smaller inclusions present considerable difficulties to determine the homogenization temperatures.

Calcite:

Calcite is the major carbonate mineral occurring in the quartz-carbonate lenses as well as the sericite-carbonate schist of the alteration zones. Many phases of carbonates have been identified (Boyle 1961). Other carbonates present are ankerite and dolomite: the fluid inclusions in these carbonates are very small and it is most difficult to obtain a consistant temperature determination with calcite. The calcite exhibits a well crystalline nature and is transparent.

3.2 PARAGENESIS

A description of the ores from different shear zones was given by Ridland (1941) and by Graham and Kaiman (1951). These authors proposed that the mineralization within the shear zone might have taken place in many distinct stages. Ridland identified 33 mineral species and in his opinion the mineralogy of the ores is quite complex. The mineral species identified by Ridland (1941) were gold, pyrite, sphalerite, galena, chalcopyrite, arsenopyrite, chalcocite, covellite, gudmundite, tenantite, pyrrhotite, leucopyrite, cobaltite, stibnite, nagyagite, sylvanite, tantalite, altaite, calaverite, rickardite, malachite, siderite, limonite and hematite. Sulfosalts recognised were boulangerite, meneghinite, jamesonite, berthierite, bournonite and tetrahedrite. Coleman (1957) postulated that gold mineralization took place during the latter stages of mineralization. As can be seen from Fig. 3, pyrite and arsenopyrite are the earliest phases followed by sphalerite, chalcopyrite, galena, stibnite and sulfosalts forming in the late stages.

Ridland (1941) related the whole process of ore deposition to a single ore-bearing solution, introduced into the shear zone, from which

FIGURE 3

Paragenetic Relationships of the Ore and
Gangue Minerals from Con Mine, Yellowknife

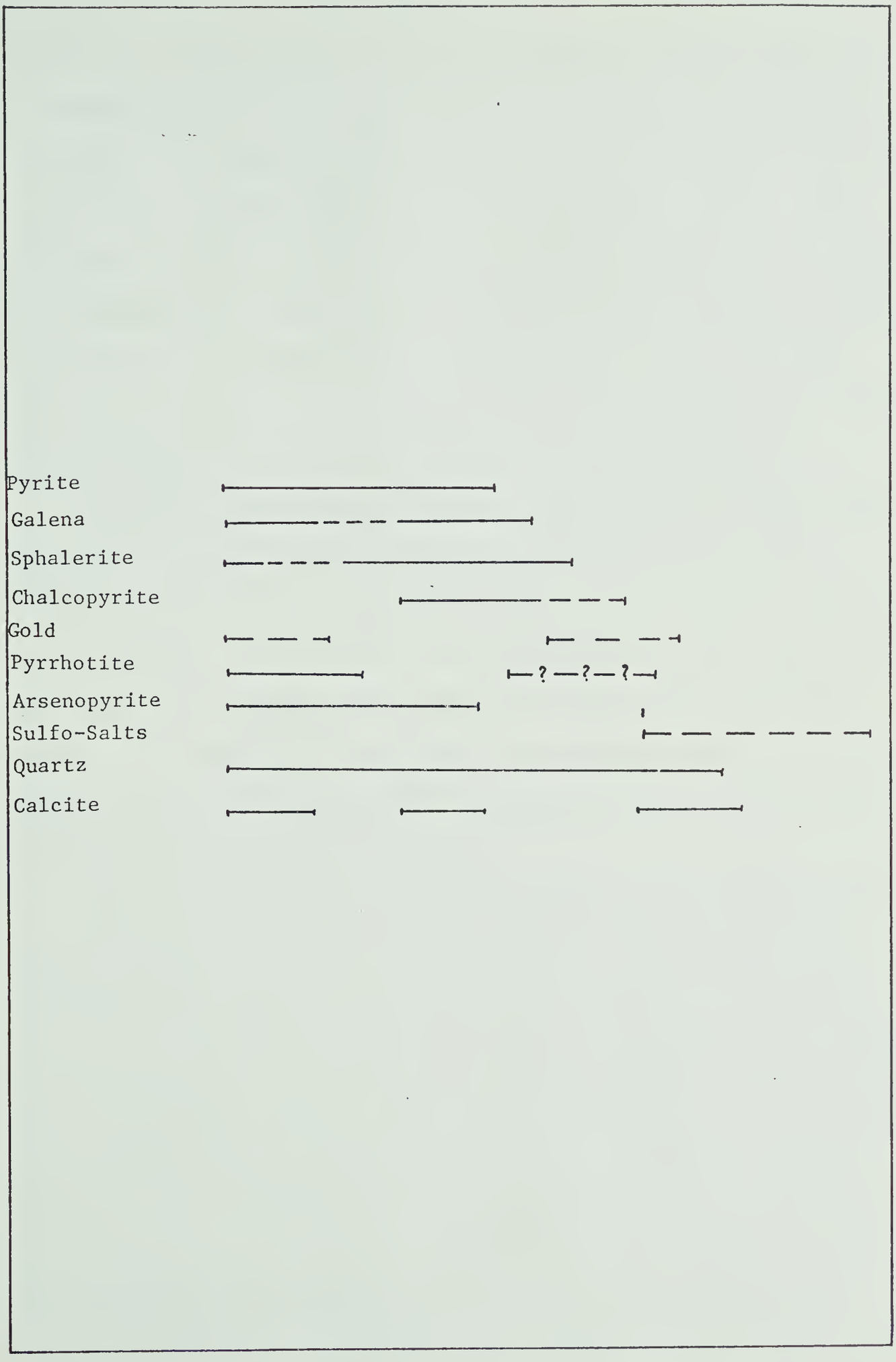
Pyrite
Galena
Sphalerite
Chalcopyrite
Gold
Pyrrhotite
? ? ?
Arsenopyrite
Sulfo-Salts
Quartz
Calcite

all the ore minerals were formed, whereas Graham and Kaiman (1951) outlined two main periods of mineral formation, separated by a period of fracturing. The authors did not mention whether the two phases were related to two different generations of ore solutions or not. Coleman (1957) envisioned three distinctly different and separate stages of mineralization, each involving the introduction of a solution having a composition different from those which preceded them, or two main stages, with a sub-phase during the second stage. He explained the manner of emplacement to be by filling susceptible zones by ore-fluids, accompanying deformation.

During the present study a suite of samples from the Campbell shear zone were examined. Particular attention was paid to the textural relationships between the ubiquitous sulfides, pyrite, galena, sphalerite and chalcopyrite. The results of these investigations have supported the previous work of Ridland (1941), Graham and Kaiman (1951) and Kaiman (1951). The paragenetic relationship of the sulfide minerals, gold and gangue minerals is diagramatically represented in Fig. 3 and pertinent illustrations and descriptions follow.

Pyrite and arsenopyrite, along with galena and sphalerite apparently belong to the primary phase of mineralization. Pyrite, like quartz is ubiquitous in the system and appears to have continued to be deposited during all phases of ore-deposition. Galena and sphalerite were probably deposited during two distinct phases of mineralization. The very characteristic feature noticed in some of the samples is the presence of minute crystals of pyrite enclosed and oriented parallel to the vein pattern in which sphalerite is the major phase (matrix mineral). Chains of pyrite crystals parallel the boundaries, as well as the centre parts of the sphalerite veinlets in quartz (Fig. 4a). Various sulfides present in the

FIGURE 4 (a)

Euhedral crystals of pyrite isolated and parallel to the walls of the sphalerite vein (light grey). Quartz (dark grey) is present on both sides of the vein .

FIGURE 4 (b)

Replacement vein of galena (light grey) and chalcopyrite (dark grey) in pyrite. Galena and pyrite show mutual mineral boundary relations

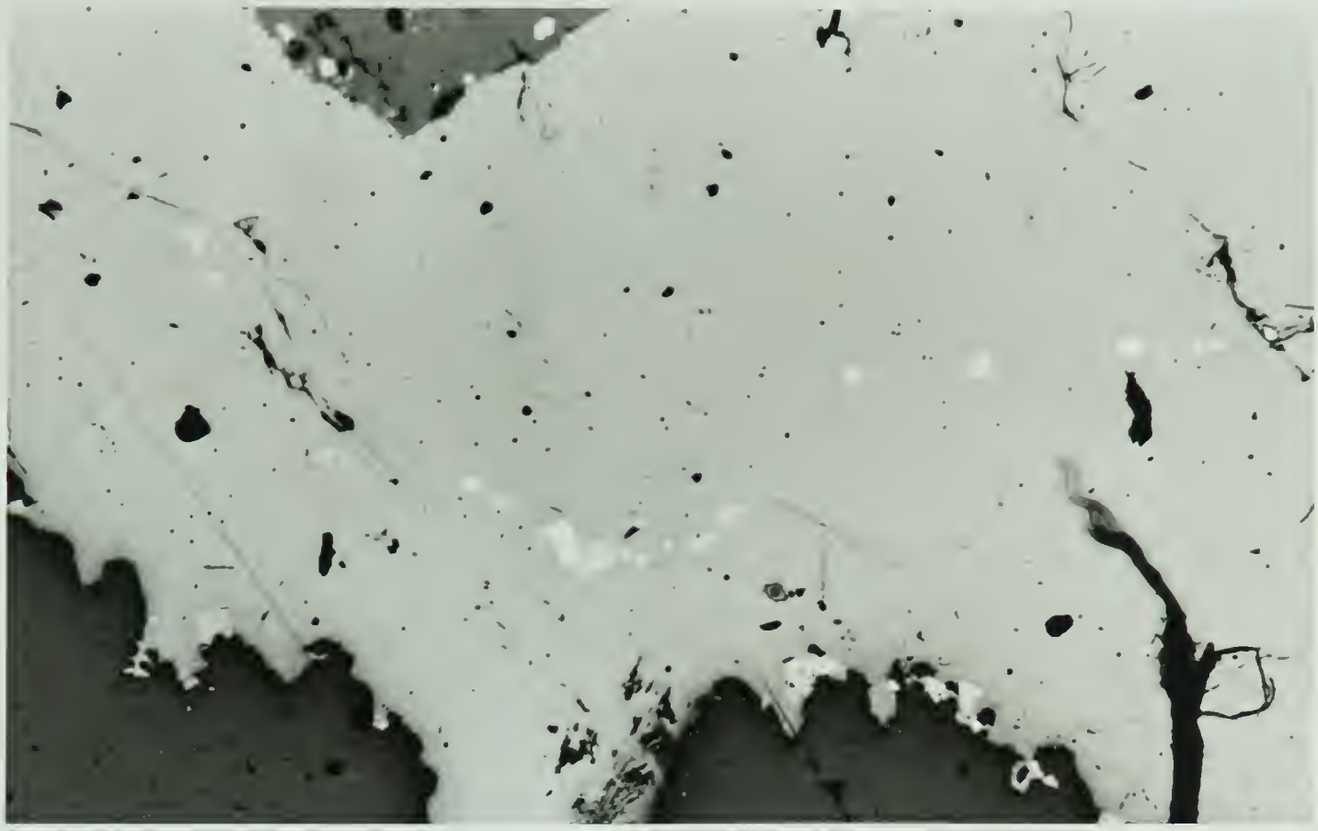

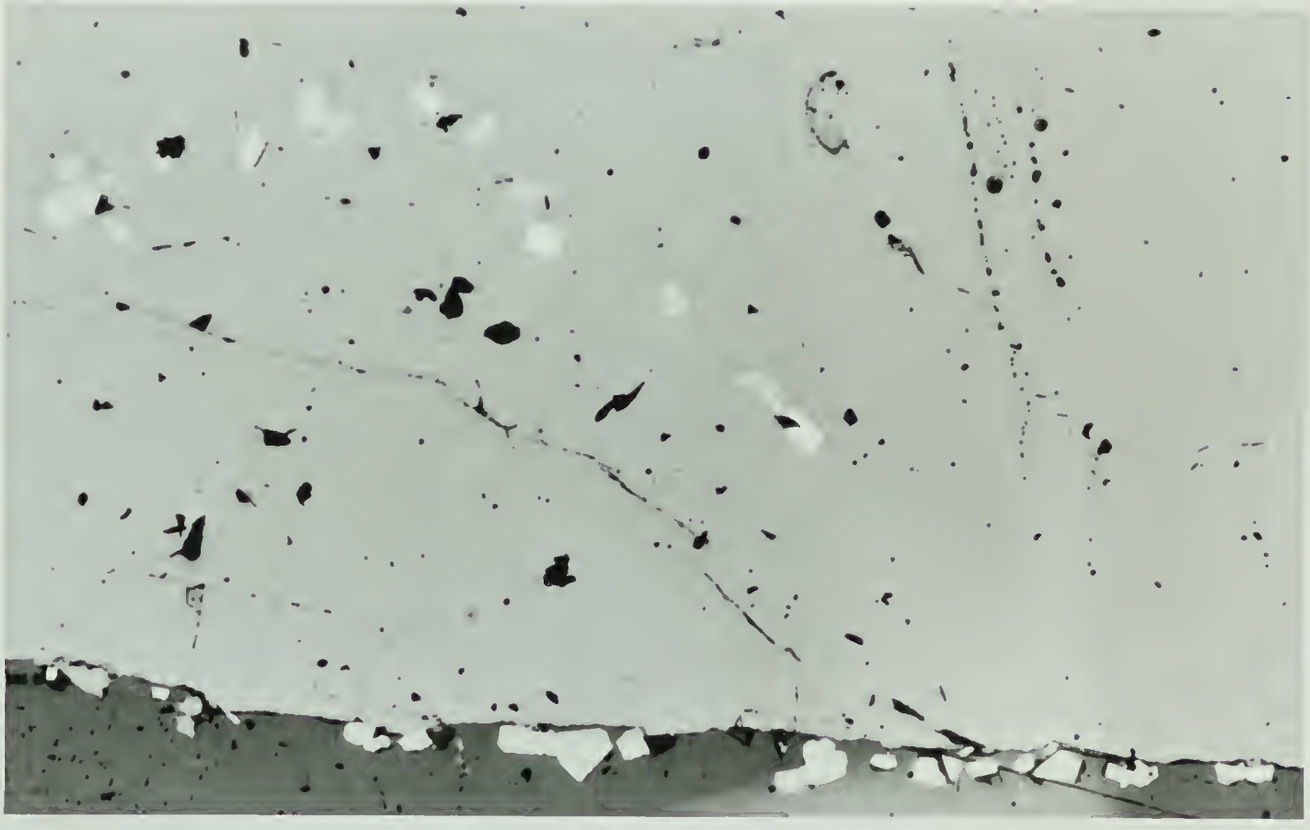

FIGURE 5

Pyrite and sphalerite - rhythmic banding associated with quartz (dark grey)

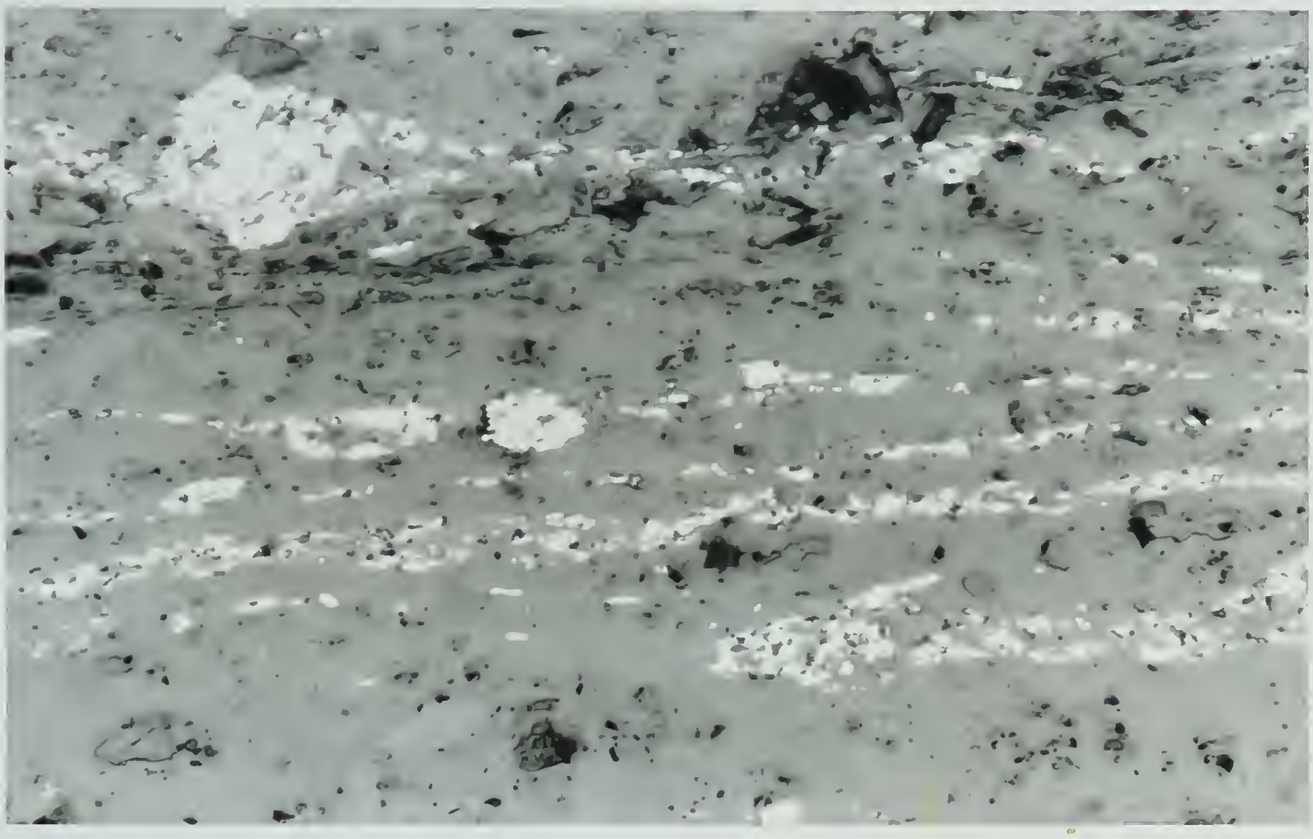

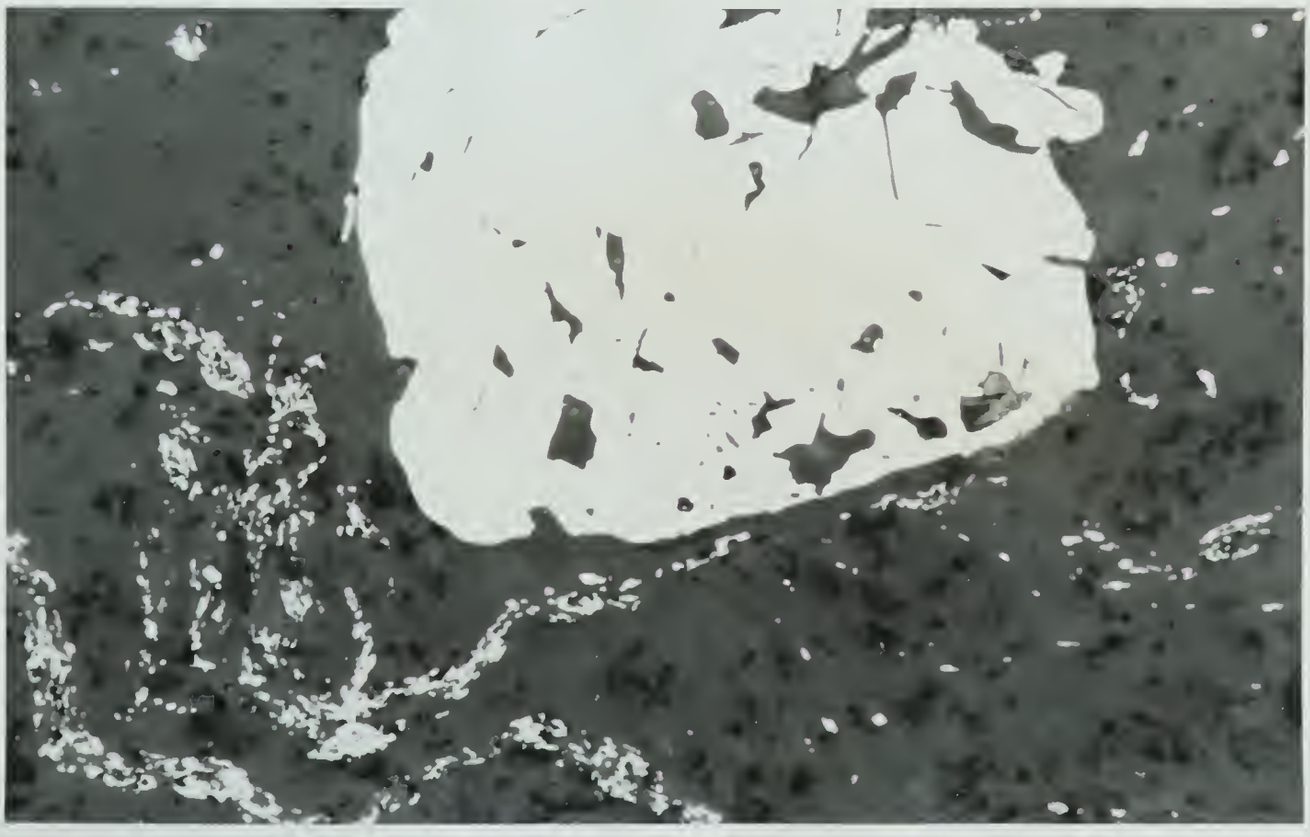

hydrothermal solutions might attain the necessary degree of saturation thus resulting in the precipitation of that particular phase. It is thought that even though all the sulfides may be contemporaneous, it is probable that the parochial precipitation of sulfides in certain sectors might have been influenced by local physico-chemical factors. As a result, replacement textures and vein deposition of other sulfides in pyrite grains might occur (Fig. 4b). Some conflicting mutual relationships were also noted. However, in the opinion of Coleman (1957) the minerals formed at any single period of mineralization exhibit, for the most part, conflicting mutual relationships or else relationships that suggest contemporaneity. The terms 'time of mineralization', 'early' and 'late' are strictly used in a relative sense.

Successive deposition inferred by crustification of two or more minerals has been interpreted by Edwards (1965) as being due to fractional crystallization and could be regarded as a special varient of simultaneous crystallization. In Fig. 5, it is shown that pyrite and sphalerite show quite distinct alternate banding with clear-cut boundaries. This is presumably because of different salts in aqueous solution attaining saturation with a rhythmic periodicity. In Bastin's opinion (1931), it is not possible to envisage solutions changing their compositions radically for the deposition of each layer, but it could be reasonably interpreted as being caused by delicately changing conditions of individual saturations. Thus crustification, probably, represents local modifications of physico-chemical factors as mentioned earlier.

Sphalerite was observed showing local variations in colour at different elevations. The type of sphalerite sampled at 3512 E displays a dark reddish to dark yellow colour, indicating higher percentages of Fe, where

as light yellow to honey yellow low Fe sphalerite was collected at the 3300 ft level. Further work obviously needs to be performed on the study of this mineral from the mine to determine the physico-chemical controls on its composition.

3.3 PARAGENETIC RELATIONSHIP OF GOLD TO OTHER MINERALS

The association of gold with vein-quartz is so common and well known that no detailed textural studies were attempted. The gold ores of the Yellowknife area have been extensively studied by various authors (e.g., Coleman 1953) and diverse opinions have been forwarded regarding the paragenetic position of gold deposition. Coleman (1953) stated that the gold is mainly associated with sulfosalts of a late stage in the paragenetic sequence. Ridland (1941) stated that the gold is commonly associated with the metallic minerals and quartz which were introduced during the first stages of ore deposition, whereas the carbonates were introduced during the second stage. A long period of gold deposition is postulated by Ridland (1941), as the gold occurs in two different forms, namely (a) as finely segregated particles distributed within fractures or along grain boundaries and (b) associated with sulfosalts. Another mode of occurrence of the gold was reported by Coleman (1953) who noted the gold occurring as minute blebs in homogenous pyrite, sphalerite or arsenopyrite. These blebs do not exhibit any connection with the minute fractures in the quartz. Probably this might be the gold cogenetic with arsenopyrite. However Coleman (1953) believes that the earlier coarse-grained gold might have been partly remobilized and redeposited by later mineralizing fluids as auro complexes.
It is noteworthy that at Kolar, India, much of the gold occurs within

narrow veins associated with other minerals in quartz, which underwent fracturing and recrystallization prior to the advent of gold (Pryor, 1924).

CHAPTER IV

EXPERIMENTAL WORK

4.1 SULPHUR ISOTOPE STUDIES:

(a) Introduction

Studies of variations in sulfur isotope distribution within an ore-body may be employed to elucidate the physico-chemical factors influencing ore deposits and consequently provide clues as to the genetic relationships of the ores (Sakai 1968). During ore transport and deposition, isotope exchange can be visualized to have been operative between coprecipitating sulfide minerals, as well as between the precipitates and the sulfide ions in the surrounding fluids. Recently sulfur isotope fractionation theories have been utilized in geothermometric studies (Kajiwara et al., 1970; Rye, 1970) and in the investigation of the conditions of deposition of various sulfides and the nature and isotopic composition of the hydrothermal fluids.

(b) Experimental procedure:

The sulfide phases for analysis were separated by crushing, taking the 170-230 mesh fraction, and separating the various components utilizing a Franz isodynamic separator, heavy liquid methods (tetrabromethane) and final purification by hand picking.

A 10 mg sample of the sulfide was then mixed thoroughly with 100 mg of CuO (pre-treated) and inserted into a quartz tube with quartz wool

loosely packed on both sides of the sample. This sample was then heated in vacuum at 1040°C for at least 10 minutes and the evolved H_2O, O_2 and CO_2 fractions were then removed by using freezing traps of liquid air, and a mixture of acetone and dry-ice. The SO_2 analysis line is illustrated in Fig. 6. The pure So_2 was then trapped into a standard break-seal.

The sulfur isotope analyses were performed on a 12", 90° radius Neir-type Mass-spectrometer employing the YKS-GMIA pyrrhotite of S^{34} -1.94‰ as the laboratory standard (relative to Cañon Diablo), by introducing the standard and the sample alternately and collecting masses 64 and 66. The ratios of these masses were obtained by direct printout.

The results of the isotopic analyses are represented in the usual permil notation defined by:

$$S^{34}‰ = \left[\frac{(S^{34}/S^{32})_{sample} - (S^{34}/S^{32})_{standard}}{(S^{34}/S^{32})_{standard}} \right] \times 1000$$

by applying the following corrections: (a) a correction factor 'B' against the working standard which was derived to be 0.0^5 in this case, (b) a fractionation correction for the standard gas with time (0.99820), and (c) a correction factor of oxygen which was taken to be 1.0907.

Certain samples were tested for reproducibility by replicate analysis and the range obtained was ±0.07 to 0.18‰. For the purposes of comparison with other published S^{34}/S^{32} values, all the values obtained were recalculated with respect to the common standard of troilite from the Canon Diablo meteorite, which has a ratio of S^{32}/S^{34} = 22.21‰ or (S^{34}/S^{32} = 0.0‰). The standard derivation of the results was calculated individually for all the samples. For 90% of the samples the standard

FIGURE 6

Schematic Diagram representing the
So_2 Extraction Train
(in the Geology Department, University of Alberta)

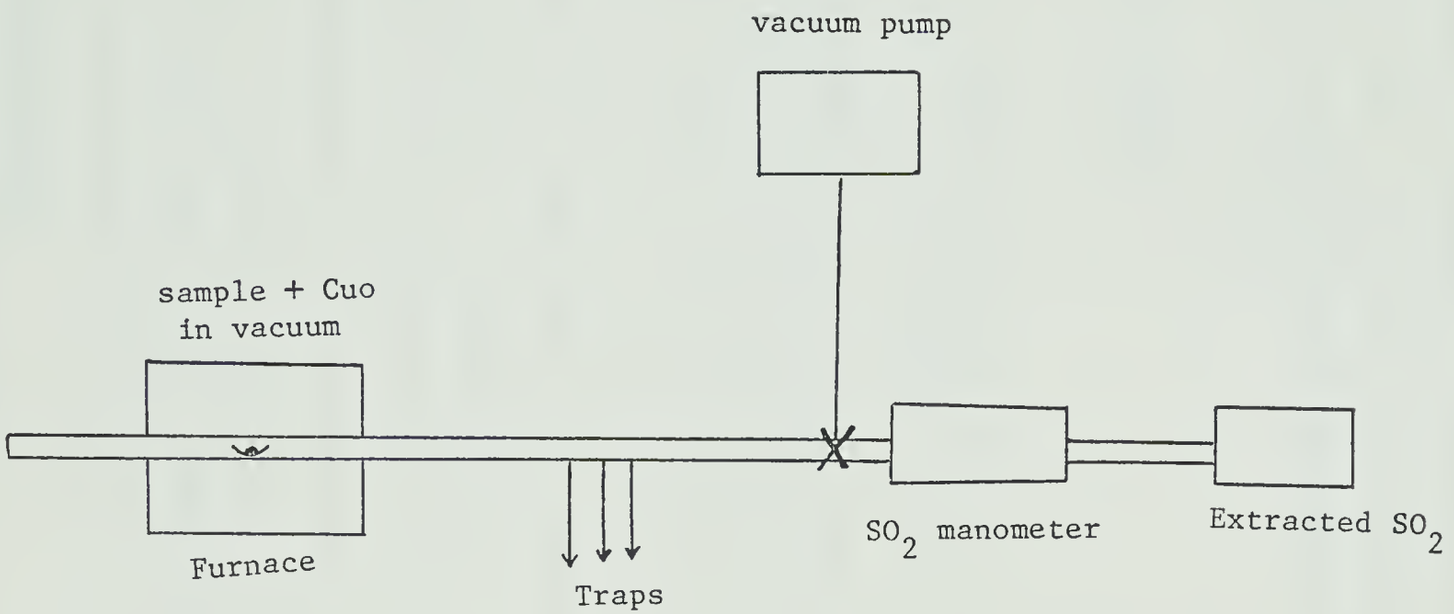
vacuum pump
sample + Cuo
in vacuum
Furnace
Traps
SO_2 manometer
Extracted SO_2

deviation falls in the range of 0.01 to 0.07‰ whereas for the rest, the standard deviation ranges from 0.09 to 0.12.

(c) Results

The analytical results of the isotopic studies on various sulfide minerals from the Con Mine together with the descriptions of those minerals are presented in Table 2. The sample locations also being indicated on the longitudinal section Fig. 7. The results are diagrammatically represented in Fig. 8. In the table, depth indicates the stopes or drift at a particular elevation represented by the figure.

4.2 FLUID INCLUSION STUDIES

(a) Introduction

Homogenization temperature determinations on the fluid inclusions in quartz and calcite have long been utilized to confirm the data obtained from other methods of geothermometry and to discuss some of the related physical parameters in the light of the fluid phase and gas phases present. The validity of the data obtained from fluid inclusion studies has long been debated on the basis of the fact that the filling temperatures obtained may not actually represent the temperatures of ore deposition, even after applying the pressure corrections. In addition to that, the analyses of the extracted fluids from the fluid inclusions were doubted to be the representatives of the true composition of the soluble salts within the ore solutions. However, the results of considerable experimental work concerning epithermal deposits in Russia (Borina 1963) exhibit a high degree of consistence, indicating that the above-mentioned determinations are quite meaningful.

(b) Homogenization Temperatures

The filling temperatures were determined on a heating stage designed by Ohmoto. Few samples were found to be suitable for filling temperature

TABLE 2

Analytical Results and Sample Descriptions
(Sulphides mainly Pyrite, Galena, Sphalerite
and Chalcopyrite from Con Mine, Yellowknife)

SAMPLE NO	MINERAL	S^{34}%	LOCATION DEPTH	(LAT)	DESCRIPTION
1.	Pyrite	+1.5	2927 Ay-1	(19200)	Py with quartz, chip sample
2.	Pyrite	+0.7	3512 E -1	(19700)	Py with other sulfides + qutz
3.	Pyrite	+1.2	4111 Ax-1	(19100)	Py + quartz + sulfides
4.	Pyrite	+1.4	4111 Ax-2	(19100)	Py with quartz
5.	Pyrite	+1.3	4311 Ax-2	(19050)	Py with other sulf + quartz
6.	Sphalerite	-0.5	3322 Ay-1	(19600)	Sph, gal and quartz
7.	Sphalerite	-0·6	4311 Ax-1	(19050)	Sph with quartz
8.	Galena	-1.6	3322 Ay-1	(19600)	Galena with quartz
9	Galena	-2.6	3512 E -1	(19700)	Galena with other sulf + qutz
10.	Galena	-2.8	4311 Ax-1	(19050)	Gal and other sulf + qutz
11.	Pyrite	+0.4	4511 DS-1	(18900)	Pyrite + quartz
12	Sphalerite	+0.9	4311 Ax-4	(19100)	Pyrite + sph + quartz
13.	Pyrite	+1.6	3512 A -1	(19450)	Pyrite + quartz
14.	Pyrite	+1.4	4513 DS-1	(18700)	Pyrite and quartz
15.	Galena	-3.4	4311 Ax-2	(19050)	Gal + quartz asso py
16.	Pyrite	+1.1	4311 Ax-2	(19050)	Py + other sulf + quartz
17.	Pyrite	+1.2	3512 E -3	(19700)	Py + other sulf + quartz
18.	Pyrite	+0.4	3322 Ay-1	(19600)	Pyrite + quartz
19.	Chalcopyrite	+0.5	3512 E -4	(19700)	Cpy + pyrite + quartz
20.	Pyrite	+0.6	3512 E -5	(19700)	Pyrite + sulf + quartz
21.	Pyrite	+1.4	3512 E	(19700)	Py + massive sulf + qutz
22.	Pyrite	+1.6	3711 Ax-2	(19100)	Py assoc qutz and sulf
23.	Galena	-0.7	3711 Ax-2	(19100)	Gn assoc py and quartz

(continued...)

(continued)

SAMPLE NO	MINERAL	S^{34}%	LOCATION DEPTH	(LAT)	DESCRIPTION
24.	Pyrite	+1.2	4311 Ax-1	(19050)	Pyrite + quartz and sulf
25.	Chalcopyrite	+0.4	4311 Ax-1	(19050)	Cpy assoc with py and qutz
26.	Galena	-1.9	3321 Ay-1	(19250)	Galena + qutz + pyrite
27.	Sphalerite	+1.0	4311 Ax-T	(19100)	Sph + qutz + sulf minor
28.	Sphalerite	+0.9	3511 H -T	(20140)	Sph + qutz + minor sulf
29.	Pyrite	+1.9	3512 A -T	(19440)	Pyrite + quartz
30.	Pyrite	+0.4	4115 Av-T	(18830)	Pyrite + quartz
31.	Pyrite	+1.6	3711 Ax-1	(19100)	Pyrite + quartz
32.	Galena	-2.7	3322 Ay-1	(19600)	Galena with quartz
33.	Galena	-2.0	3511 H -T	(20140)	Gal + qutz + minor sph
34.	Galena	-3.0	4115 Av-T	(18830)	Gal + qutz + minor py
35.	Pyrite	+1.7	4311 Ax-T	(19100)	Pyrite + quartz + sulf
36.	Pyrite	+1.3	2927 Ay-T	(19140)	Pyrite + quartz
37.	Galena	-0.8	3321 Ay-1	(19000)	Gal + other sulf + qutz
38.	Pyrite	+1.4	4311 Ax-4	(19050)	Py + other sulf + qutz
39.	Sphalerite	+0.5	4311 Ax-4	(19050)	Sph + qutz + minor sulf
40.	Pyrite	+1.6	3512 A	(19450)	Pyrite + quartz
41.	Pyrite	+1.3	3312 A	(19700)	Pyrite + quartz
42.	Pyrite	+1.7	3711 Ax-2	(19100)	Py + other sulfides
43.	Pyrite	+1.7	3511 H T	(20140)	Py + qutz + minor sulf

FIGURE 7

Longitudinal Section Campbell Shear System
Con Mine, Yellowknife
(The first two digits refer to the depth in 1000's of feet
and the rest the S tope location with respect to
foot wall - hanging wall relationship)

(map enclosed in the pocket)

FIGURE 8

Distribution of Sulfur Isotope Values
in different Sulfide Minerals,
Con Mines, Yellowknife

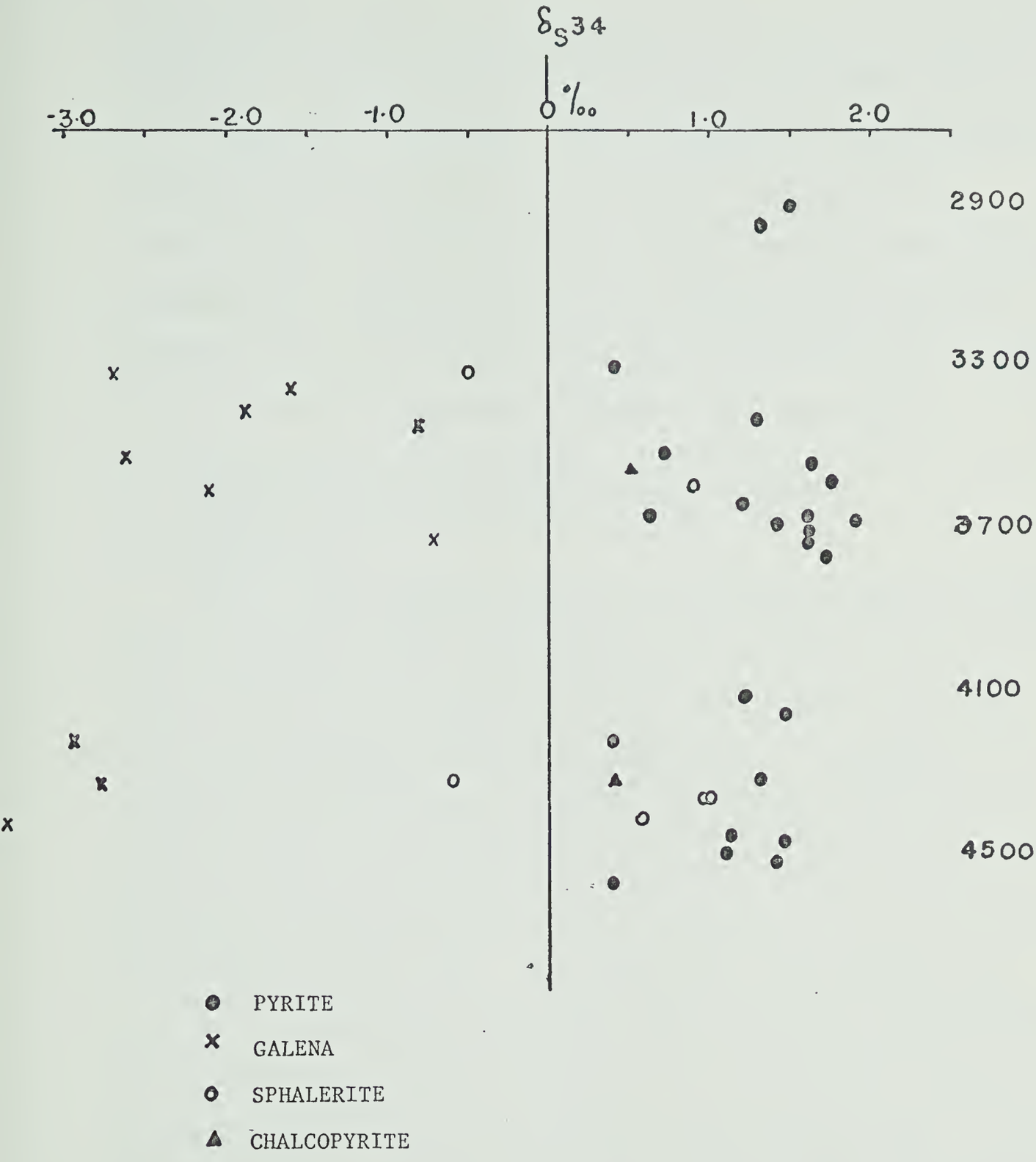

DISTRIBUTION OF SULFUR ISOTOPE VALUES IN DIFFERENT SULFIDE MINERALS.

determinations as most of the fluid inclusions were almost beyond the resolution of the microscope and therefore gas-liquid phases could not be distinguished. Furthermore, since the quartz is so often strained, polished sections tend to be rather opalescent and translucent. However, four of the fluid inclusions observed in quartz showed filling temperatures of 270±10°C and the inferred temperatures of the ore solutions, when corrected fall in the range of 300-350°C for an average pressure of 400-500 atmospheres (Lemmlein and Kletsov, 1961).

4.3 INVESTIGATIONS OF K/Na RATIOS IN FLUID INCLUSIONS

(a) Introduction

Sawkin (1966) indicated that there is a relative variation of K/Na ratios in natural waters with temperature. The empirical plot of White (1968), when Gammon's experimental data is superimposed, also showed a relationship between temperature and K/Na ratios. An increase in the temperature of chloride water in contact with feldspar and micas will apparently shift the fluid-mineral equilibria, thereby increasing the K/Na ratio in the fluid phase, as Na is exchanged for K in the minerals (Orville 1963 Hemley 1967). When hydrothermal fluids evolved from granite melts, react with the country rock, exchange type reactions can be expected, and equilibrium is obtained as a result of the formation of alteration zones in the form of aureoles surrounding the veins. In general the Na/K ratios for solutions in contact with rhyolitic volcanic rocks during hydrothermal alteration were found to range from 10 to 15 at 250°C to approximately 4 at 500°C (Ellis and Mahon, 1967). Thus it can be shown that there is an influence of temperature on the K/Na ratios in the ore-fluids. Furthermore, K/Na ratios would help to elucidate the

depositional history, temperature gradients and equilibrium relations which will be discussed in detail later in this thesis.

(b) Experimental procedures

K/Na ratios of the fluid inclusions in quartz from the Con Mine were determined using a leaching procedure after Sawkins (1966) and Grooves and Soloman (1969). In order to determine the relative amounts of K and Na in the fluid inclusions from the samples collected at different elevations in the Campbell shear system, six quartz samples were carefully cleaned and crushed separately in a clean tungsten-carbide mixer mill for four minutes. The crushed material was leached with distilled and demineralized water, washing the mixer about six to eight times for every sample. Final washings were performed with 1.0 mole nitric acid. The resulting slurry was kept overnight and filtered. The filtrate was heated gently to dryness. The volume of all the samples as well as the two blank runs, were adjusted to 25 cc and K and Na concentrations of these solutions were determined on the flame-photometer.

The experimental accuracy of these determinations was determined by two blank runs, namely (a) following the same procedure with demineralized water without any sample, and (b) by following the same procedure using synthetic quartz as blank. The results obtained should be viewed in the light of the following limitations.

(i) The accuracy of the results is difficult to estimate owing to the ubiquity of secondary inclusions in all samples.

The higher concentrations of K in these secondary inclusions might be expected to be due to latter metamorphic and metasomatic effects, however. Such conclusions are merely speculative unless certain geological evidences are shown. No specific limitations are possible to impose on the extent of contamination by this factor at this stage.

(ii) The number of fluid inclusions in the quartz samples varied considerably from one sample to the other. Thus the presence of variable concentrations of secondary inclusions in the same samples causes the results obtained to show a lack of internal consistency. Extreme caution was taken throughout the experimental procedure, however, unanticipated contamination might have been present in any one of the individual samples.

(iii) Even though most of the quartz was hand-picked for this purpose, the quartz might still (in certain cases) contain muscovite as very fine-grained inclusions; (some of the samples contained fine muscovite associated with quartz. Some of the samples contained fine muscovite associated with quartz and this contamination is believed to have contributed a major proportion ion the higher K/Na ratios obtained).

(c) Results

The results of the determinations are tabulated in Table 3. To obtain an overall value of K/Na ratio, a plot is drawn between K and Na (ppm) (Fig. 9) and it appears that some correlation exists between the K concentration and the corresponding Na concentration in any given sample. All the values have been corrected for blanks. The final values obta-ned from the graph is 0.66 ± 0.05 (atomic ratio).

4.4 OXYGEN-CARBON ISOTOPE STUDIES - CARBONATES

(a) Introduction

Oxygen isotope fractionation studies have been applied to the study of hydrothermal processes and facilitated the determination of temperatures of formation of minerals and the determination of the origin and source of the solutions involved. Furthermore, in the light of oxygen isotope fractionation studies, the validity of the assumption of equilibrium among the mineral species, has been discussed. It has also been demonstrated that the O^{18}/O^{16} of water in equilibrium with the mineral assemblages at a given temperature could be calculated by applying the experimentally determined mineral-water relations (Clayton 1969).

TABLE 3

Concentration of K and Na in the Leached Solutions
from Quartz Samples, Con Mine, Yellowknife
(all the readings are corrected for the blank)

NO	SAMPLE SPECIFICATION	K (ppm)	Na (ppm)	K/Na (at ratio)	Na/K (at ratio)
1.	2927 Ay	27.0	26.5	0.599	1.67
2.	3322 Ay	45.0	31.0	0.853	1.17
3.	3512 E	33.0	39.5	0.491	2.03
4.	3711 Ax	13.5	11.0	0.721	1.39
5.	4111 Ax	41.0	40.0	0.602	1.66
6.	4511 DS	26.5	23.5	0.663	1.51
7.	Blank 1	0.0	0.0		
8.	Blank 2	3.5	4.5		

FIGURE 9

Plot showing the Relationship between the K^+ and Na^+ (experimental data) determined by flame photometry, in the leached solutions from quartz samples from the Con Mine. The general trend of K and Na concentration is shown by the straight line.

The K^+/Na^+ (atomic ratio) from the plot is 0.66

DISTRIBUTION OF K - Na (in ppm.) IN FLUID INCLUSIONS OF QUARTZ

[Note: to obtain K/Na atomic ratio, multiply weight ratio by 0.588.]

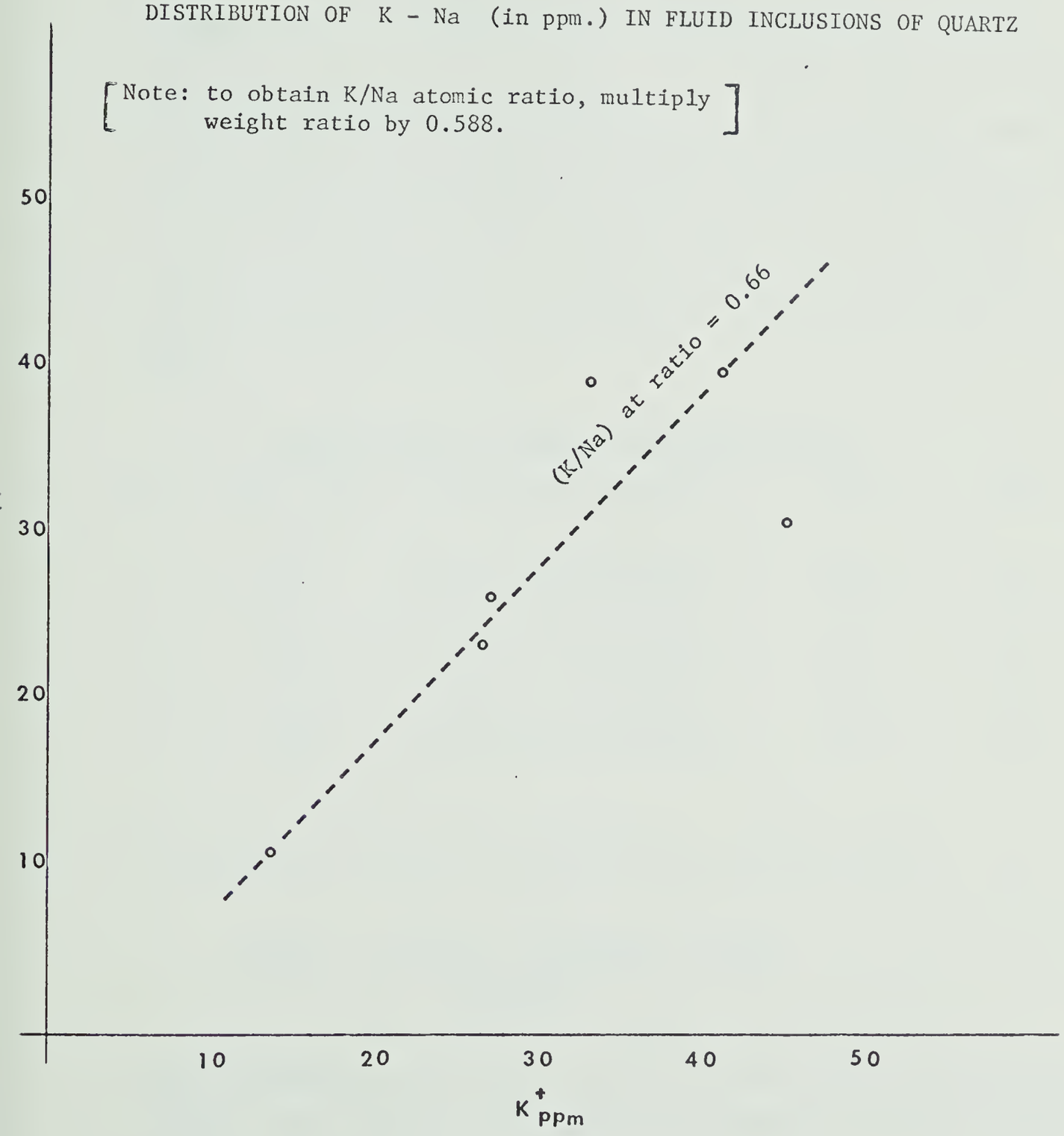

(b) Results

Six carbonate samples were collected from various parts of the mine workings and Co_2 was extracted by using an oxygen line for carbonates designed and constructed by P. Fritz at the University of Alberta. The carbondioxide gas was analyzed on a 1/2", 90° radius Nier-type, mass spectrometer using a laboratory standard of Fisher scientific company calcium carbonate. The following results for the isotopic composition of oxygen and carbon in the hydrothermal carbonates were obtained after correcting for (a) tail effects, (b) background, and (c) mass contribution effects. All the values are reported in the standard ‰ permil notation with reference to the standards mentioned below:

(Against SMOW for Oxygen and PDB for Carbon)

SNO	Prep. No.	Collection (locality)	O^{18}‰	C^{13}‰
1	1453	3511 St ReX[1] calcite	+10.6	-4.2
2	1284	2900 Drift X[1] calcite	+8.4	-3.6
3	1376	3511 St X[1] calcite	+9.6	-0.5
4	2900	2900 Drift X[1] calcite	+8.7	-2.9

The results are reported in the familiar notation, where

$$\delta O^{18}‰ = \left[\frac{R_{sample} - R_{standard}}{R_{standard}} \right] \times 1000$$

where R represents the O^{18}/O^{16} or C^{13}/C^{12} ratio of Co_2 from carbonate samples. The standards recalculated for are SMOW for oxygen isotopes and PDB for carbon isotopes.

CHAPTER V

INTERPRETATIONS - DISCUSSION

5.1 GEOTHERMOMETRY - SULFUR ISOTOPES

Isotopic fractionation of sulfur between synthetic sulfide mineral pairs (FeS_2-PbS, ZnS-PbS and FeS_2-Zns) as a function of temperature and duration of reaction time has been investigated by many authors (Kajiwara 1969, 1970; Rye 1969; Grootenboer 1969). From the results shown in the table 2, the isotopic composition of coexisting sulfide pairs have been utilized to calculate the per mil deviations between the specific sulfide pairs; the computations being given in the table 4. With respect to the selection of the appropriate geothermometric plots, shown in Fig. 10, all these plots were taken into consideration in the initial stages and subsequently comparative values were obtained by employing other geothermometric procedures, such as fluid-inclusion filling temperature methods. Experimental and theoretical plots are presented in Fig. 10 and 11.

The nature of the distribution of isotopic composition of sulfur in pyrite, sphalerite, chalcopyrite and galena shows a general fractionation trend as theoretically calculated by Sakai (1968) based upon the partition ratios for crystalline FeS_2, PbS and ZnS. The theoretical trend of fractionation of sulfur isotopes in coexisting, cogenetic sulfide species, as postulated by Sakai (1968), is that the S^{34} enrichment would be: pyrite > pyrrhotite > sphalerite > chalcopyrite > galena. This same

TABLE 4

Temperature determinations based upon the experimental plots of sulfur-isotope fractionation among sulfides (Kajiwara 1970; Rye 1969, and theoretical plots Sakai 1968; Houlston 1958)

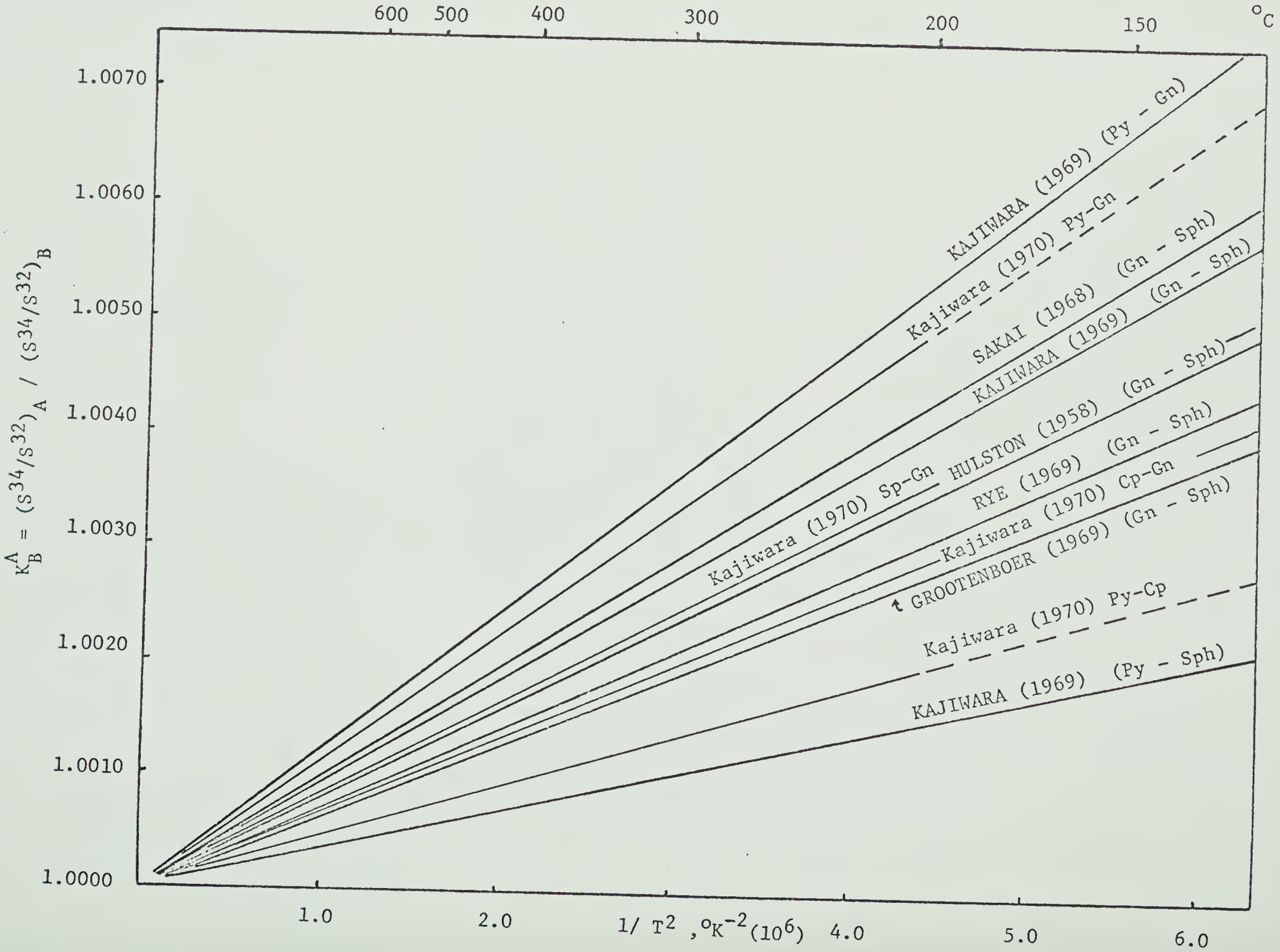
600 500 400 300 200 150 °C
1.0070
1.0060
1.0050
1.0040
1.0030
1.0020
1.0010
1.0000
$K_B^A = (S^{34}/S^{32})_A / (S^{34}/S^{32})_B$
KAJIWARA (1969) (Py - Gn)
Kajiwara (1970) Py-Gn
SAKAI (1968) (Gn - Sph)
KAJIWARA (1969) (Gn - Sph)
Kajiwara (1970) Sp-Gn
HULSTON (1958) (Gn - Sph)
RYE (1969) (Gn - Sph)
Kajiwara (1970) Cp-Gn
GROOTENBOER (1969) (Gn - Sph)
Kajiwara (1970) Py-Cp
KAJIWARA (1969) (Py - Sph)
1.0
2.0
$1/T^2$, $^oK^{-2}(10^6)$
4.0
5.0
6.0

FIGURE 10

Graph showing the results of calculations and experimental data by Kajiwara et al. (1969, 1970), Sakai (1968), Hulston (1958), Rye (1969) and Grootenboer (1969) for the variation with temperature of sulfur isotope fractionation between different sulfide pairs (specified).

NO	SAMPLE LOCATION	SAMPLE PAIR	MINERALS	S^{34} K_B^A	TEMPERATURES °C			
					Kajiwara (1970)	Sakai (1968)	Hulston (1958)	Rye (1969)
1.	3322 Ay-1	6-18	Sph-Py	1.009	330°-340°			
		18-32	Py-Gn	1.0031	320°-330°			
		6-32	Sph-Gn	1.0022	300°-310°	370	330	305 - 310
2.	3511 H -T	43-28	Py-Sph	1.008	320°-340°			
		43-33	Py-Gn	1.0037	280°-290°			
		33-28	Sph-Gn	1.0029	260°	310	250	230 - 240
3.	3512 E -1	2- 9	Py-Gn	1.0033	310°-320°			
4.	4111 Ax T	30-34	Py-Gn	1.0034	300°-310°			
5.	4311 Ax-4	38-39	Py-Sph	1.009	330°-340°			
6.	4311 Ax-1	24- 7	Py-Sph	1.0019	Abnormally low			
		7-10	Sph-Gn	1.0022	300°-310°			
		24-10	Py-Gn	1.0041	270°-280°			

N.B. 1. Sample locations refer to the specified working stopes on the levels, represented by the left two digits in thousands of feet depth.

2. Numbers specified under 'sample pair' represent the same in Table 3 (isotopic compositions of sulfides).

3. Py-pyrite; Sph-sphalerite; Gn-galena.

FIGURE 11

Theoretical sulfur-isotope fractionation curves for pyrite-galena, pyrite-sphalerite, sphalerite-galena, based upon Sakai's (1968) estimates of partition function ratios for crystalline FeS_2, PbS, ZnS. is approximately equal to 1000 ln α and for the exchange reactions given, is identical to the equilibrium constant K.

Isotope data obtained from co-existing sulfides (Con Mine, Yellowknife) are also presented on the plot.

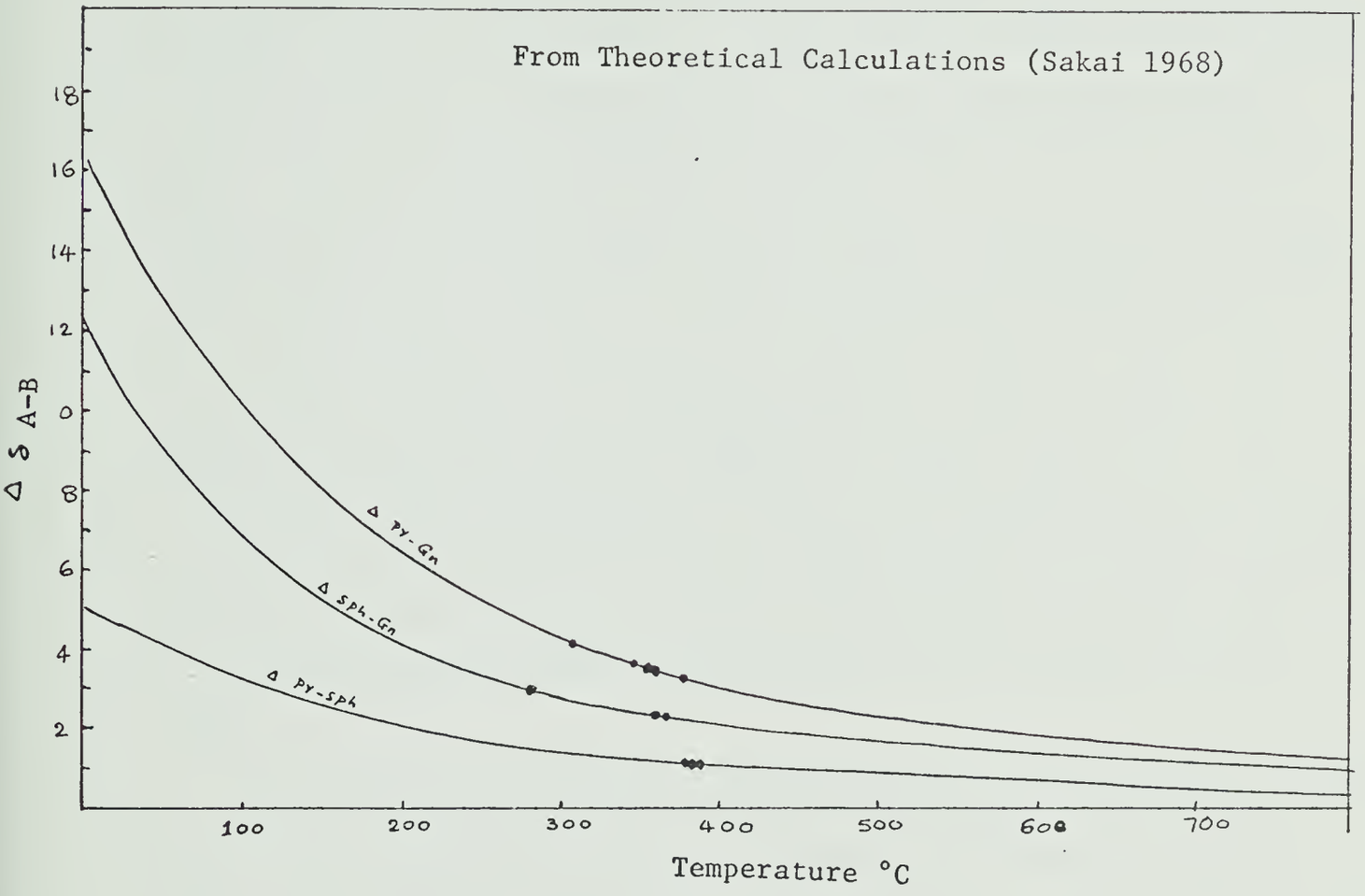
From Theoretical Calculations (Sakai 1968)
18
16
14
12
0
8
6
4
2
Δ δ A-B
Δ Py-Gn
Δ Sph-Gn
Δ Py-Sph
100
200
300
400
500
600
700
Temperature °C

trend is clearly observed in the samples collected from the Campbell shear system. The trend might imply that the mineral pairs have attained equilibrium or closely approached it. However, sphalerite and chalcopyrite show a slight variation which could be either due to local isotopic variations or due perhaps to experimental errors (Fig. 12).

A close observation of the spread of sulfur isotope composition of the three major sulfides (Fig. 9), namely pyrite, galena and sphalerite, together with corresponding textural studies on these three mineral pairs, indicate a probable history of precipitation of the sulfides which may be as follows: pyrite was ubiquitous within the shear system and no temperature gradient was attained during the precipitation of the sulfides. However, other physico-chemical factors, such as the hydrogen-ion concentration and fugacity of oxygen, might have varied considerably, effecting changes in the isotopic composition of the sulfur species within the aqueous solutions. This has been treated theoretically by Ohomoto (personal communication) and is to be discussed in detail later.

The galena and sphalerite exhibit features of simultaneous precipitation along with pyrite and the corresponding S^{34} values of galena and sphalerite show a range of -2.9‰ to -2.0‰ and -0.6‰ to -0.5‰ respectively, while pyrite showing an isotopic composition ranging from +0.5 to 1.0‰. However, where there are veins and replacement features, namely sphalerite and chalcopyrite replacing pyrite, and galena replacing pyrite, the isotopic compositions of sulfur of these sulfides are distinctly heavier, relative to those described earlier. The values of the isotopic compositions of sulfur in galena and of sphalerite would have been considerably modified during the second phase of precipitation indicated

FIGURE 12

Plot showing the mutual relationship between the pyrite-sphalerite and pyrite-galena (theoretical data of Sakai 1968) and superimposed Con Mine data.

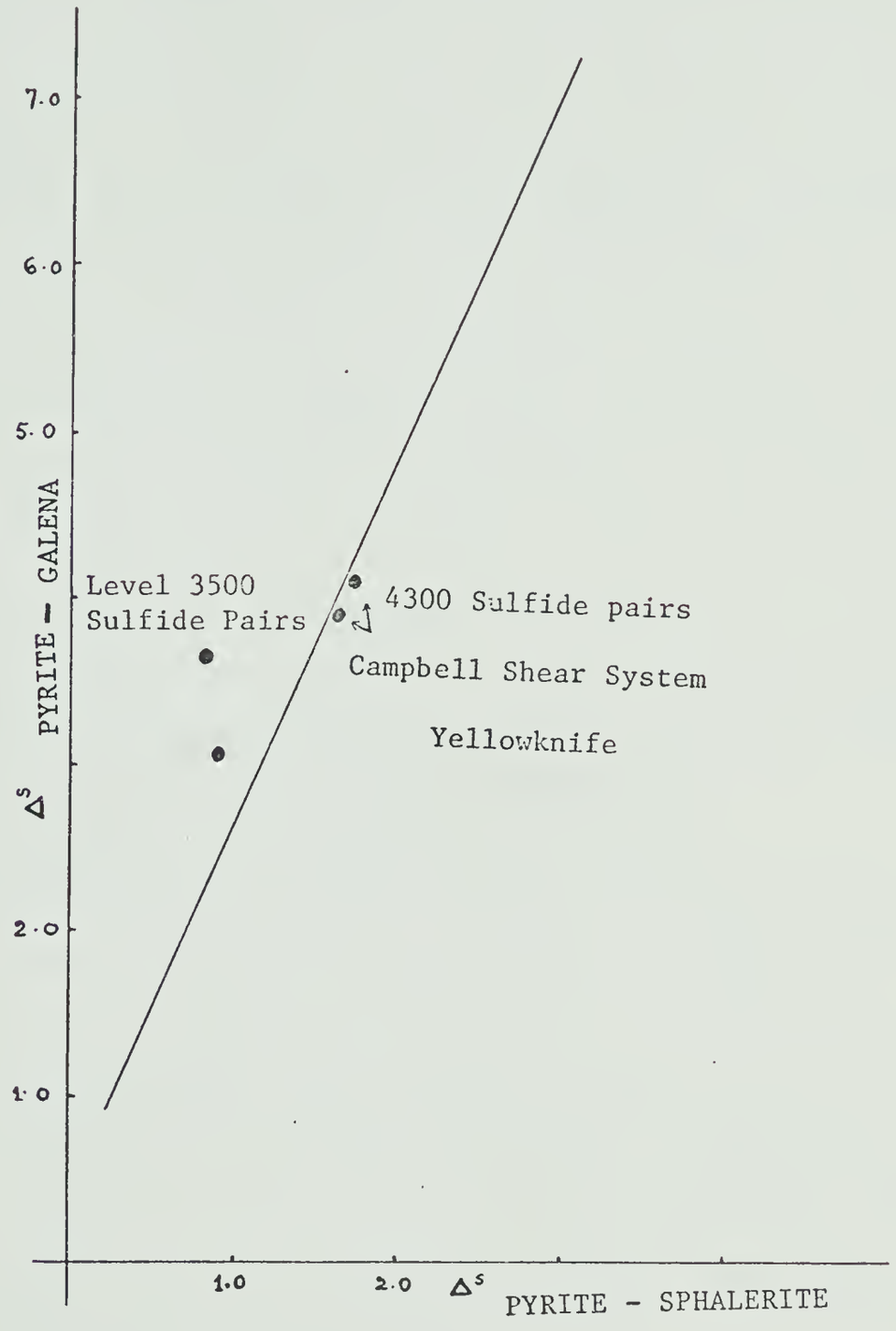
7.0
6.0
5.0
2.0
1.0
Δ^S PYRITE - GALENA
Level 3500
Sulfide Pairs
4300 Sulfide pairs
Campbell Shear System
Yellowknife
1.0
2.0
Δ^S
PYRITE - SPHALERITE

by the textural studies. Likewise the pyrite also shows relatively heavier S^{34} values ranging from 1.3 to 1.8‰. When the earlier sulfide pairs are accepted as having been precipitated simultaneously, the temperature determinations on these pairs would reveal the temperature of formation of cogenetic sulfide pairs if the other factors are the same during the precipitation of all the sulfides. The highest temperatures determined on the pairs range from 340°-360° whereas the lowest values could be considered to be within the range of 310°-300°, a temperature range which is apparently quite common in hydrothermal deposits. The range of temperatures determined for the Con Mine deposit is between 300-350°C, i.e., the temperature interval might indicate the interval during which the sulfides and other minerals have been precipitated from the hydrothermal solutions. The temperatures obtained for the ore deposits of the Campbell shear zone seem to be quite meaningful in the light of the earlier studies (Kaiman et al. 1964).

As the precipitation of pyrite continues, toward the latter phase of the depositional episode, sphalerite and galena would have reached supersaturation due to the changing physico-chemical characteristics, and hence had developed heavier characteristics, compared with the previous galena and sphalerite. The isotopic composition of galena and sphalerite range from -1.5‰ to -1.0‰ and 0.4‰ to 0.9‰ respectively, while pyrite shows an isotopic composition ranging from 1.0‰ to 1.7‰. This is illustrated schematically in Fig. 13.

The geochemistry and the origin of the Yellowknife belt has been investigated and critically discussed by Boyle (1961), who interpreted the quartz and gold as being epigenetic in character and being formed from silica released during mineralogical and chemical changes occurring within the country rocks during the development of the schist zones.

FIGURE 13

Schematic diagram showing the relationship between the sulfur isotope variations and paragenetic sequence in pyrite, sphalerite and galena (Con Mine, Yellowknife).

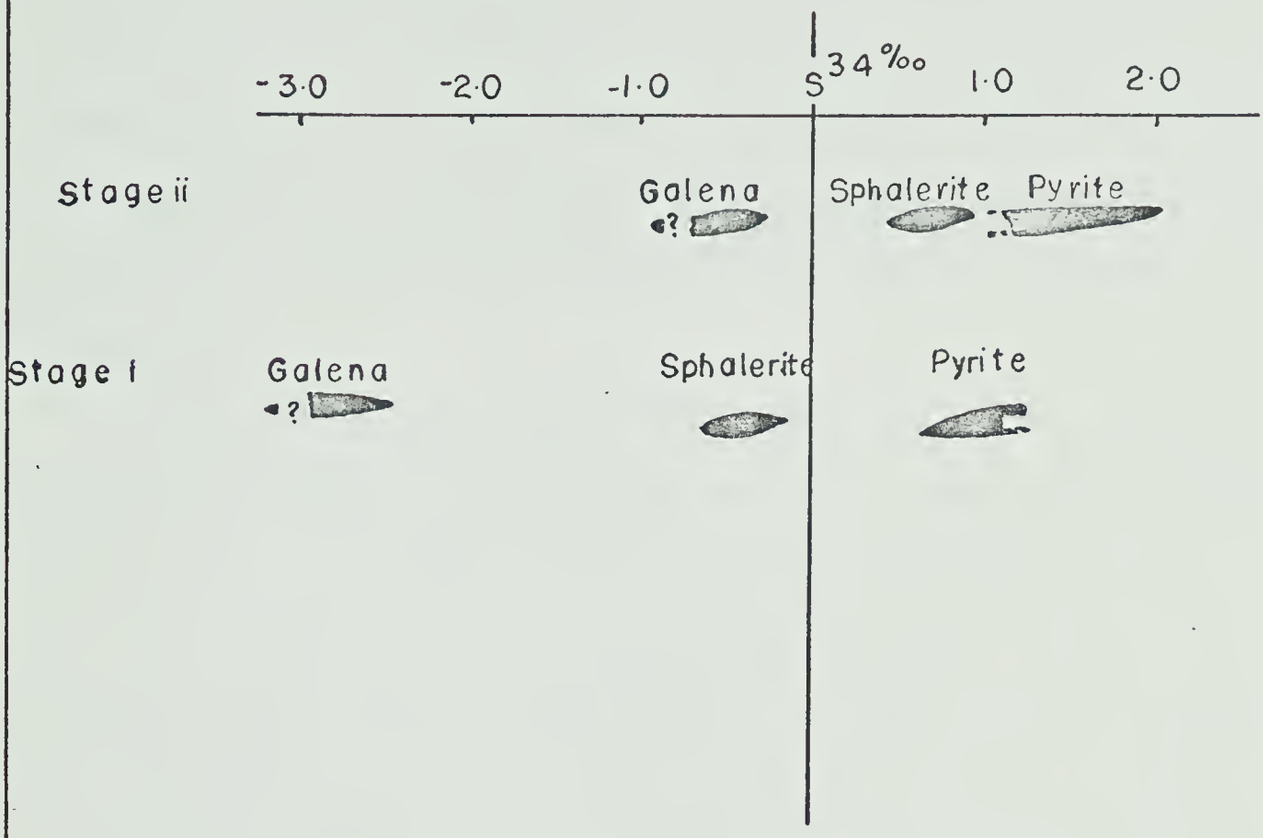
-3·0
-2·0
-1·0
S 34‰
1·0
2·0
Stage ii
Galena
?
Sphalerite
Pyrite
Stage i
Galena
?
Sphalerite
Pyrite

The sulfides in the shear zones are thought by Boyle (1961) to have originated by redistribution of sulfo-phile elements during metamorphism of the basic greenstone suite and partly as the result of chemical changes which took place during the development of schist zones. The elements present in the shear zone were therefore interpreted as being derived from the country rocks and were supposedly concentrated by the interaction of metamorphic processes within dilatent structures in the shear zones.

Wanless, Boyle and Lowden (1960) studied the sulfur distribution in different phases of the lithological units. Their work is summarized in the table 5 and diagrammatically represented elsewhere (Fig. 14 and 15). The following conclusions were drawn from their results: the available sulfur-isotope proportions in the source area were assumed to be in the same proportions as those found within meteoric troilite and thus variations in the isotopic compositions were interpreted to be due to temperature, pressure and compositional gradients.

(a) The greatest enrichment of the heavier sulfur isotope took place where high temperatures prevailed and the lighter sulfur isotope migrated to the relatively cooler portions of the lithological units. The gradients show higher values when the greenstones show lighter sulfur isotope concentrations.

(b) Pressure gradients are responsible for modification of the sulfur isotope distribution. Sulfides in the isolated lenses filling tension fractures in the epidote-amphibolite facies of the rocks always contain more S^{34} than in the sulfides in the enclosing rocks.

(c) When the quartz-gold bodies formed, the shear-zone was subjected to intense chemical activity and S^{32} diffused out of the shear zone into the associated country rock.

TABLE 5

Sulfur isotopic compositions of pyrite collected and analyzed by Wanless et al. (1960) from various lithological units (adopted from Wanless et al. 1960).

ROCK UNIT	NUMBER OF SAMPLES	SPREAD OF $\delta S^{34}‰$	AVERAGE OF VALUES (as given in Wanless et al.1960)
Granitic Rocks	5	+2.9 - +6.8	+4.0
Greenstone Belt	8	+0.6 - +2.2	+1.4
Graphic Tuffs	6	+2.0 - +5.6	+3.5
Siliceous Tuffs	4	-2.7 - -0.3	-1.2
Early Pre-quartz lenses in the tension fractures	3	+0.3 - 1.4	+0.8
Con System Ore-deposits	13	+2.4 - +6.2	+3.8
Negus-Rycon System	29	+0.3 - +3.6	+1.7
Giant Campbell System	12	+0.0 - +3.6	+2.0
Parallel Shear Zone	10	0.0 - +3.6	+2.8

FIGURE 14

Sulfur isotope distribution in granodiorite and metamorphic facies of the Yellowknife greenstone belt.

FIGURE 15

Sulfur isotope distribution in gold-quartz lenses, surrounding carbonate-sericite schist, chlorite schist and rocks of epidote-amphibolite facies, Yellowknife.

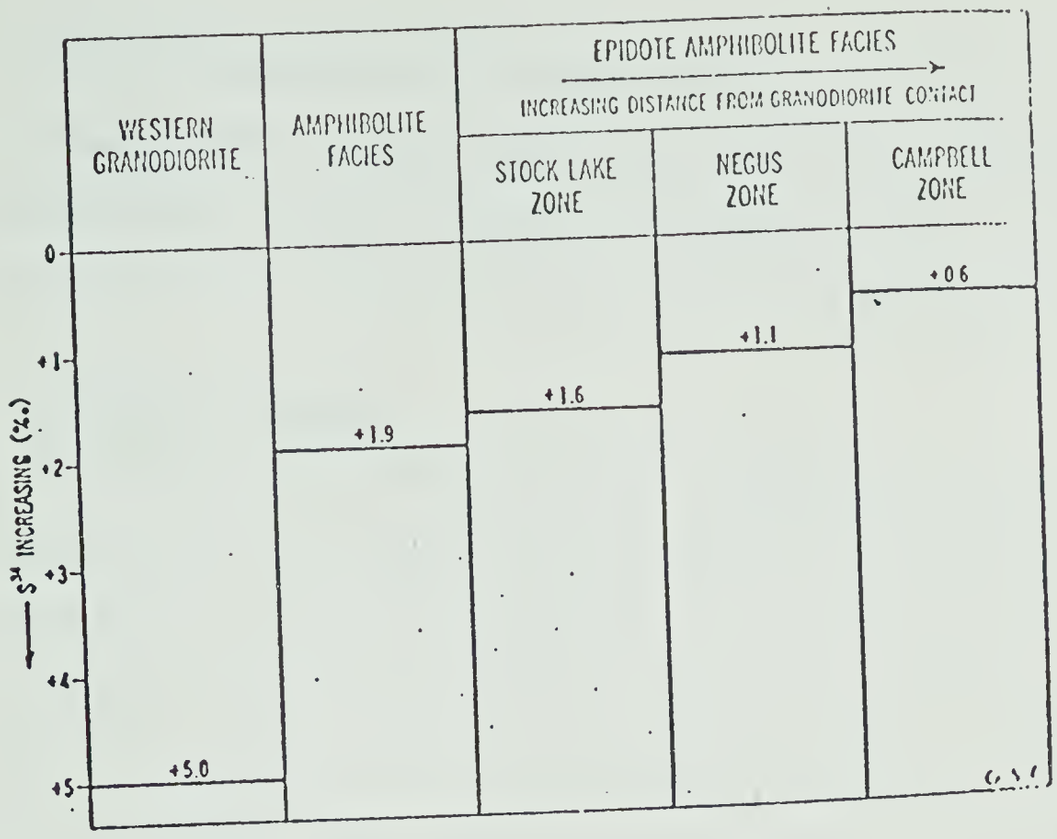
EPIDOTE AMPHIBOLITE FACIES
INCREASING DISTANCE FROM GRANODIORITE CONTACT
WESTERN GRANODIORITE
AMPHIBOLITE FACIES
STOCK LAKE ZONE
NEGUS ZONE
CAMPBELL ZONE
S^{34} INCREASING (‰)
0
+1
+2
+3
+4
+5
+5.0
+1.9
+1.6
+1.1
+0.6
G.S.C.

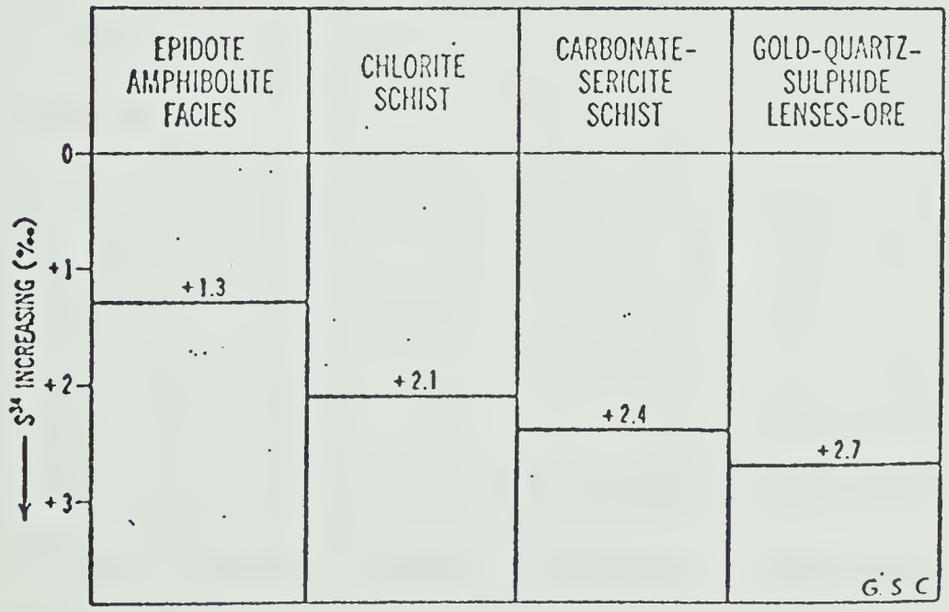
EPIDOTE AMPHIBOLITE FACIES
CHLORITE SCHIST
CARBONATE-SERICITE SCHIST
GOLD-QUARTZ-SULPHIDE LENSES-ORE
S^{34} INCREASING (‰)
0
+1
+2
+3
+1.3
+2.1
+2.4
+2.7
G.S.C.

Recent observations by McConnell (1964), Green (1968), and Robertson and Cumming (1968) and the author's discussions and experiences with the mine geologists strongly suggest a hydrothermal theory. For more discussions on this topic the reader is directed to the pertinent literature cited.

5.2 PRESSURE ESTIMATES

It is extremely difficult to make a reasonable estimate of the pressure of formation for the Campbell shear system from the sparse data concerning overburden at the time of mineralization. The total pressure in the system at any given temperature might be derived by a number of independent methods, namely: (a) from the plot of the relationship between temperature and pressure at a given weight % salt content in aqueous solutions, obtained by analyzing the fluid phases of fluid inclusions for the H_2O-NaCl system (Ohmoto and Rye 1970), or (b) from the geobarometric determinations based upon sphalerite compositions coexisting with pyrrhotite or pyrite (Smith 1963) or (c) from the experimental plots based upon the degree of filling in fluid inclusions vs. the temperature at a given pressure (Lemmlein and Klevtsov 1961).

When the temperature-pressure-density relationship plot of 10 wt % NaCl solution (Ohmoto 1970) is considered, the minimum pressure at 350°C could be circa 150 atmospheres which would represent the minimum pressure in the mineralizing system. Boyle (1954) determined the decrepitation temperatures of fluid inclusions in quartz collected from the Campbell shear system and obtained primary decrepitation temperatures in the order of 300°C and secondary decrepitation temperatures around 162°C. By utilizing the filling temperatures derived from them, in conjunction with the plot of Ohmoto (Personal communication), the pressure range obtained is about 850-900 atmospheres. This pressure could thus be treated as the maximum at the time of deposition. The minimum and

maximum pressures obtained are not unrealistic, comparing them with previous pressure estimates published for hydrothermal systems. It is noteworthy that the application of pressure corrections and calculation of the fugacity of water vapour are not greatly affected by this range of pressure.

5.3 PRESSURE CORRECTIONS FOR FILLING TEMPERATURES

In fluid inclusion thermometry, corrections for pressure are absolutely essential in the calculation of the correct temperature of formation for a given ore deposit. Diagramatic correction-plots have been prepared based upon the experimental work of previous authors (Lemmlein and Kletsov 1961), thus enabling the determination of the temperature of formation of a given crystalline substance. The temperature corrections thus obtained for the Campbell shear zone ranges from 20° to 80°C for pressures of 150 atm and 900 atm respectively. When this correction is made for an average pressure of 500 atmospheres, the corrected temperature would thus be around 320-330°C, whereas the corrected temperatures for the maximum pressure of 900 atm would be 360°±10°C. It should be noted that the error resulting from this type of initial assumption, might be within a range of 1-10%. However, the maximum and minimum pressures have been taken into consideration when computing the molarities of the species in aqueous solutions and the effect of temperature and pressure on different sulfur species are discussed.

5.4 DEPTH OF ORE DEPOSITION

For an average pressure of 500 atmospheres, two extreme limits have been considered for the following calculations. It was found that if (a) an overhead fluid column is taken into consideration ($P_t = P_f$) having

a density of 0.93 gm/cc (10 Wt% solution at 350°C), and (b) an average crustal rock overhead is considered, the depths of deposition would be in the order of 5.0-5.5 km and 1.9-2.0 km respectively (using the equation $P_t = pgh$, where P_t is the total pressure in bars, p = the density of the column, g = the acceleration due to gravity and h = the height of the column). When the feasibility of these two values in the light of the existing geological observations is considered, the following points should be mentioned:

If the depth of ore-deposition was 2.0 km, the average rock temperature at that depth would be roughly 80°-90°C and the temperatures of the ore solutions in the range of 340°C-350°C. Under such conditions there would therefore be a tremendous temperature gradient between the ore solutions and the country rock, a phenomenon which would probably be expressed in textural and mineralogical features, such as chilled marginal zones etc. However, such features have never been observed. In such a case a partial fluid phase could be expected in the hydrothermal plumbing system. An estimate of the depth of ore-deposition of 4 km would be quite appropriate to set the model of the hydrothermal system. Furthermore, it is quite unlikely that any considerable pressure gradients could be expected across the ore body except for very local pressure decreases in the Shear Zone.

5.5 FUGACITY OF WATER VAPOR

The fucacity of water vapor within the system relative to the total pressure was obtained by multiplying the fugacity coefficient by the total pressure (Holser 1954). The average fugacity of water vapor during the time of deposition was thus determined as 150-200 atm, a result which is geologically feasible. The influence of f_{H_2O} is discussed in this

thesis later.

5.6 THE APPLICATION OF THERMODYNAMIC DATA TO SOLUTION CHEMISTRY

The application of thermodynamic principles to solution geochemistry permits the study of ore solution processes and the evaluation of various reactions between electrolytes within the aqueous solutions. The theoretical approach of the study of natural systems of coexisting minerals was supported by Goldschmidt (1954). This author pointed out that there exists a relationship between the magnitude of the free energy of the oxides, sulfides, sulfates and carbonates of the various elements and their mode of occurrence in nature. Kordes (1935) indicated that the mineral assemblages within the systems at a given temperature could be mostly influenced by the fugacity of sulfur in the systems.

Recently more quantitative studies have been performed by Holland (1965) who has defined the conditions of deposition of minerals in terms of free energy and given physical parameters such as temperature and pressure. Holland (1959) applied such thermochemical data to oxides, sulfides, sulfates and carbonates which constitute the principal ore and gangue minerals of ore deposits. For any chemical reaction, the change in free energy may be calculated from the entropy and heat of formation of the reactants and products involved in the said reaction and the equilibrium constant is related to the fugacity of ideal gases in the system. Thus the boundary between the mineral assemblages may be defined by equilibrium constants which in turn are related to the fugacity of sulfur and oxygen in the system. From this type of approach it is possible to specify the range of fugacities of the major gases from a knowledge of the mineral assemblages in any given hydrothermal deposit. Fugacities of hydrogen, carbon monoxide, hydrogen sulfide (gas) and SO_3

FIGURE 16 and FIGURE 17

Diagrams showing the relationship between the fugacity of sulfur and oxygen with respect to t e mineral stability fields (specified)

($\log f(O_2)$ - $\log f(S_2)$ - $\log f(CO_2)$ in Fe-O-S-C, Pb-O- , Zn-O-S systems)

(1) at 350°C - figure 16 and (2) at 300°C - figure 17

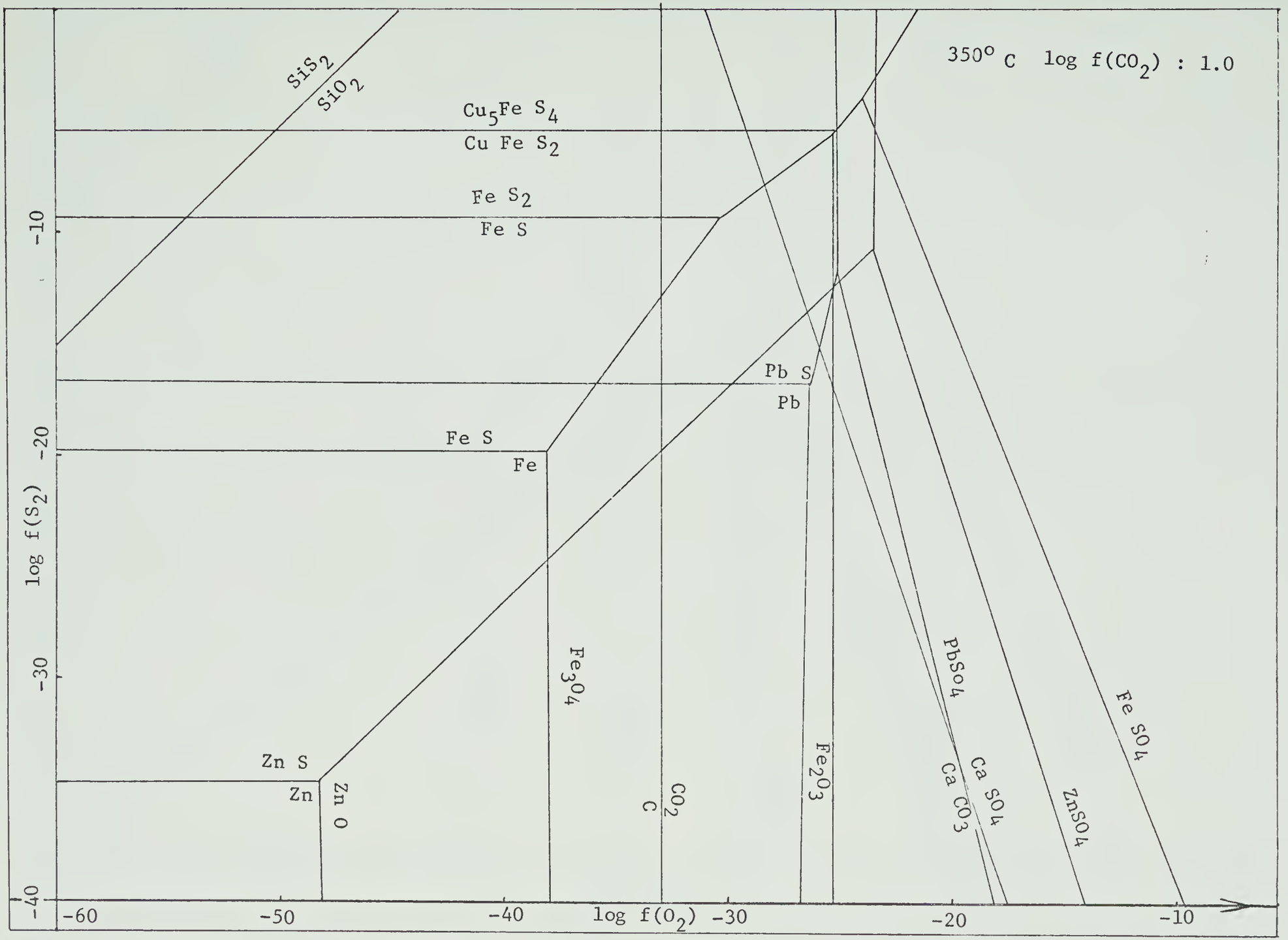
350° C log f(CO2) : 1.0
SiS2
SiO2
Cu5Fe S4
Cu Fe S2
Fe S2
Fe S
Pb S
Pb
Fe S
Fe
Zn S
Zn
Zn O
Fe3O4
CO2
C
Fe2O3
PbSo4
Ca CO3
Ca SO4
ZnSO4
Fe SO4
log f(S2)
log f(O2)
-10
-20
-30
-40
-60
-50
-40
-30
-20
-10

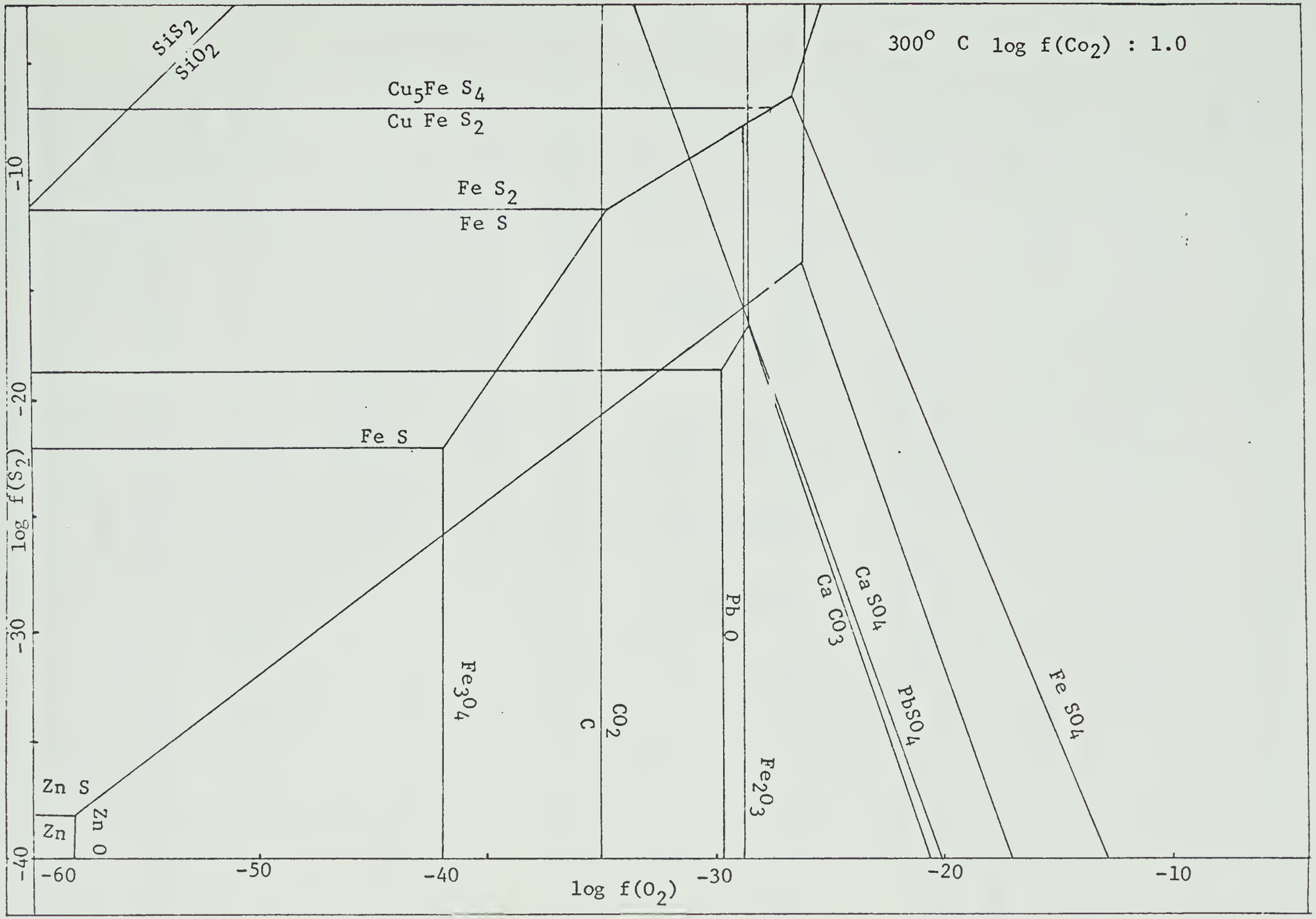
300° C log f(Co2) : 1.0
SiS2
SiO2
Cu5Fe S4
Cu Fe S2
Fe S2
Fe S
Fe S
Fe3O4
C
CO2
Pb O
Fe2O3
Ca CO3
Ca SO4
PbSO4
Fe SO4
Zn S
Zn
Zn O
-10
-20
-30
-40
log f(S2)
-60
-50
-40
-30
-20
-10
log f(O2)

may be calculated relative to the known fugacities of oxygen and sulfur.

5.7 DETERMINATION OF FUGACITIES OF SULFUR AND OXYGEN

From the calculated temperatures of formations, the fugacities of oxygen vs fugacity of sulfur diagrams have been constructed based upon the thermochemical data of Holland (1965, 1959). From the major minerals identified in the Campbell Shear Zone, the maximum and minimum fugacities of oxygen and sulfur have been fixed as follows (Fig. 16 and 17).

Temperature	log $f(O_2)$		log $f(S_2)$	
	Min	Max	Min	Max
350°C	-31.0	-29.0	-10.5	-8.5
300°C	-34.0	-32.0	-11.5	-9.5

The thermochemical data have been applied in the following two equations:

$$\Delta G = AT + BT \log T + CT$$

$$\Delta G = -RT \log k \times 2.303$$

$$\log k = \frac{AT + BT \log T + CT}{-RT \times 2.303} \qquad (1)$$

The A, B and C values are reproduced from Holland (1959, 1965) in Appendix 1.

The maximum and minimum pressures have been considered to be 900 and 150 atmospheres to examine the effect of pressure upon other parameters. The lowermost levels in the mine reach a depth of 4500 ft from the surface. The corresponding corrections for temperature

determinations on primary fluid inclusions from quartz samples would give a correction range of 1 - 10% (which has been taken into consideration in estimating the probable temperature of formation of the fluid inclusions).

5.8 FUGACITY OF CARBON DIOXIDE

Two basic criteria have been applied in estimating the fugacity of carbon dioxide in the mineralizing systems, namely: (a) if the fugacity of carbon dioxide is more than 80 to 100 atmospheres, almost all the fluid inclusions would have shown CO_2 phase volumes as well as gas inclusions. Such features are notably absent in those sections examined, (b) in such a case, if the fugacity of CO_2 is below 50 atmospheres the effect would be negligible in computations of the molalities of the ionic species, as log values would be mostly employed. However, calculations were made to observe the variations in the computed results, but the effect is almost negligible.

5.9 MOLALITIES OF SULFUR SPECIES IN AQUEOUS SOLUTIONS

After calculating the fugacities of sulfur, oxygen, water vapor and CO_2, the fugacities of other gases such as H_2, CO, CH_4 and H_2S were calculated by applying Holland's data, relative to the major species. According to Helgeson (1969), the major aqueous species in acid, chloride-rich solutions, include HCO_3^-, HSO_4^-, HS^-, H_2CO_3 and $CO_{2(aq)}$, $H_2S_{(aq)}$, KCl, NaCl, HCl, $CaSO_4$, $NaSO_4$, H_4SiO_4 and chloride and sulfate complexes of the ore-forming metals. According to Quist et al. (1963) bicarbonate and bisulfate complexes of sodium and potassium are very insignificant below 300°C. Owing to the fact that the necessary thermodynamic data, as well as experimental data, is not presently available, certain assumptions have to be taken into consideration for computational

convenience, the validity of which will be discussed in a subsequent section. The computed results of the molalities of the major species for varying physical parameters are presented in Tables 5 and 6.

5.10 pH OF THE SOLUTIONS

High temperatures-pH controls-CO_2 equilibria and mica-quartz-kaolinite buffer relationships would enable the construction of diagrams for a given ionic strength of hydrothermal temperature at any specified temperature. Firstly the carbonate buffer could be operated on the following equations:

$$a_{H_2CO_3}\,(app) = B.f_{CO_2} = \frac{55.5}{H_{K\,CO_2}} \cdot f_{CO_2} \qquad (2)$$

H_K = Henry's law constant

$$H_2CO_3 \rightleftharpoons H^+ + HCO_3^-, \quad K_1 = \frac{a_{H^+}\, a_{HCO_3^-}}{a_{H_2CO_3}} \qquad (3)$$

$$HCO_3^- \rightleftharpoons H^+ + CO_3^{=}, \quad K_2 = \frac{a_{H^+}\, a_{CO_3^{=}}}{a_{HCO_3^-}} \qquad (4)$$

$$(CaCO_3) \rightleftharpoons K_c = a_{Ca^{++}}\, a_{CO_3^{=}} \qquad (5)$$

$$H_2O \rightleftharpoons H^+ + OH^- \quad K_H = a_{H^+} \cdot a_{OH^-} \qquad (6)$$

$$2\mathfrak{M}_{Ca^{++}} \approx \mathfrak{M}_{HCO_3^-} \qquad (7)$$

$$\mathfrak{M}_{(Ca^{++})^3} = \frac{K_1 K_c \,.\, B \,.\, f(CO_2)}{4K_2 \cdot (\gamma_{HCO_2})^2 \cdot \gamma_{Ca^{++}}} \qquad (8)$$

Substituting and dividing; from the above relationships:

$$(a_{H^+})^3 = \frac{K_1 K_2 . B^2 f(CO_2)^2 . \gamma_{Ca^{++}}}{^2Kc . \gamma_{HCO_3^-}} \qquad (9)$$

Relationship between pH and $f(CO_2)$ could thus be calculated from Eqn 8. The activity coefficients could be calculated from the relationship of the so-called 'Delta approximation' (Helgeson 1969). The Delta approximation is based upon the assumption that the effect of ion hydration upon individual ion activity coefficients calculated from electrostatic theory can be represented by the activity coefficient of a neutral species in the supporting electrolyte. Helgeson's selection of the CO_2 molecule as the hydrated molecule H_2CO_3, has been applied as the neutral species. Thus, Delta approximation is expressed in the following Eq:

$$\log i_{(I, T)} = \frac{-Zi^2 A (T) I^{1/2}}{1 + a^\circ B (T) I^{1/2}} + \log \gamma_{H_2CO_3(I, T)} \qquad (10)$$

where γ_i is the activity coefficient of i th species, $\gamma_{H_2CO_3}$ is the activity coefficient of H_2CO_3 in the supporting electrolyte, a° is the effective diameter of the ion (assumed to be independent of temperature), I is the ionic strength of the solution, A and B are the Debye-Hückel parameters, expressed by:

$$A (T) = \frac{1.8246 \times 10^6 \rho^{1/2}}{[\varepsilon (T) T]^{3/2}} . H_2O \underline{\quad (T)} \qquad (11)$$

$$B (T) = \frac{50.29 \times 10^8 \rho^{1/2}}{[\varepsilon (T)]^{1/2}} H_2O \underline{\quad (T)} \qquad (12)$$

where ρ is the density of the fluid, and ϵ is the dielectric constant of water. Values of A and B are taken from Helgeson (1967c). In the plot of Fig 18 the relationships between temperature-pH and $f(CO_2)$ have been given. Secondly the silicate buffer could be expressed by two equations:

$$3\ KAlSi_3O_8 + 2H^+ \rightleftharpoons \underset{\text{(k mica)}}{KAl_3Si_3O_{10}(OH)_2} + 2K^+ + 6(SiO_2)_{qtz} \qquad (13)$$

$$2\ \underset{\text{(k mica)}}{KAl_3Si_3O_{10}(OH)_2} + 2H^+ + 3H_2O \rightleftharpoons \underset{\text{(kaol)}}{3Al_2Si_2O_5(OH)_4} + 2K^+ \qquad (14)$$

When K feldspar - k mica, k mica - kaolinite buffer systems are taken into consideration, the following simplified equilibrium relations could be applied:

$$a_{H^+} = [(a_{K^+})^2/K]^{1/2} \qquad a_{H_2O} \simeq 1.0 \qquad (15)$$

By varying pH in the above equation, a relationship could be represented between temperature and pH. When these plots are superimposed on the carbonate buffer plot, the composite plot is shown in Fig. 18, and the position of the equilibrium for sericite-quartz-carbonate is selected at the given temperature which would satisfy the maximum number of parameters in question. However, the variations in ionic strengths would show very minor shifts in the equilibrium positions. From the plot (Fig. 18) the pH of the ore fluids at 350°C, is fixed at 6.0-6.5. This infers therefore a very weak acidic to neutral pH for the ore-bearing solutions at 350°C.

FIGURE 18

Temperature - pH controls - CO_2 equilibria - and K-feldspar - K-mica - Kaolinite - quartz buffer plot.

K-feldspar - K-mica, K-mica - Kaolinite, Carbonate buffer

Ionic Strength 3·0

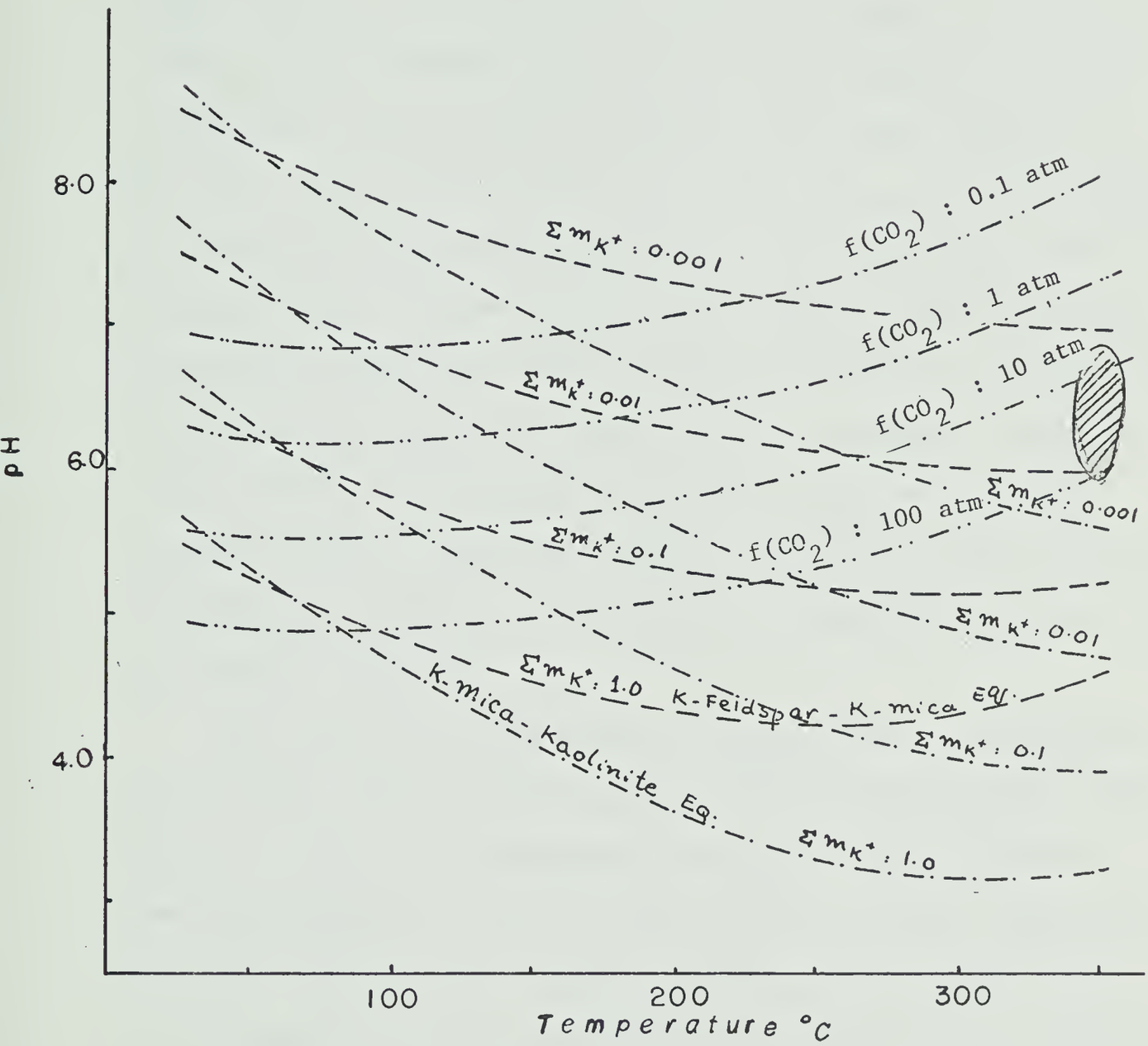

5.11 K/Na RATIOS: INTERPRETATIONS

Na/K (atomic) ratios for various groups of analyses of connate brines and fluid inclusion extracts have been compiled by Sawkins (1968) and the frequency distribution of these fluids varies quite significantly from one type of solution to the other (compiled in Fig. 19). On the basis of these plots the nature of the Yellowknife ore-bearing solutions were interpreted. The distribution of Na/K vs. frequency (Fig. 19) shows that the Na/K ratios in connate waters are greater than those of sea water, whereas the reverse is true for fluid from inclusions and volcanic spring waters. An overall comparison of the results of the present study with the published frequency diagrams reveals a similarity between the providencia fluid inclusion determinations on quartz and the present determinations on quartz from the Campbell shear zone.

The variations of K/Na ratios in natural fluids, in equilibrium with systems containing igneous melts have been given by White (1968) (Fig. 20). Some of the experimental results of Gammon (1968) have been superimposed on the plot of White (1968) at higher temperatures. This plot signifies the necessary conditions for the fluids at any given temperature to be in equilibrium with igneous melts. Any point which lies far away from the equilibrium line (shown in White 1968) could be explained in terms of environments and history of ore deposition. In other words, selective concentration or depletion of either K or Na could be explained on the basis of the geological history and evidences in the region.

Two possible explanations could be considered in the light of the existing experimental data. Firstly, higher K/Na ratios would probably indicate initially higher temperatures (Rye and Haffty 1969). Had the hydrothermal fluids been in contact with the granitic rocks, which were at temperatures higher than the temperatures of ore deposition, existence of such critical higher temperatures could be easily explained. Except for the higher K/Na ratios and a possible source from the western granodiorite intrusion (as a geological factor) there is no positive evidence to support higher temperatures in the initial stages, i.e. secondary inclusions should indicate fairly high temperatures. Secondly, if K is introduced during a process of latter metamorphic and metasomatic effect, it is quite likely that the analyses of the secondary inclusions would have shown higher K concentrations. However, it is highly impossible at this stage to separate primary and secondary fluid inclusions when a sample of 25 grams (approximately) is prepared. A third factor, though indirect, would have contributed a higher contamination, namely presence of fine particles of muscovite in the form of dust, associated with quartz. This could not have been avoided under any circumstances. Higher K/Na ratios in the fluids could be expected when a salinity of the initial fluids in higher and

FIGURE 19

Compiled frequency diagrams of Na/K ratio distributions in different natural aqueous solutions.

a) Na/K ratios of connate waters and field brines

b) Na/K ratios of subsurface waters of the Illinois Basin

c) Na/K ratios of subsurface water from the Michigan Basin

d) Na/K ratuios from inclusion fluids in Mississippi Valley-type deposits

e) Na/K ratios of Providencia inclusions

f) Na/K ratios of spring waters from volcanic environments

g) Na/K ratios of Con Mine inclusion fluids from quartz

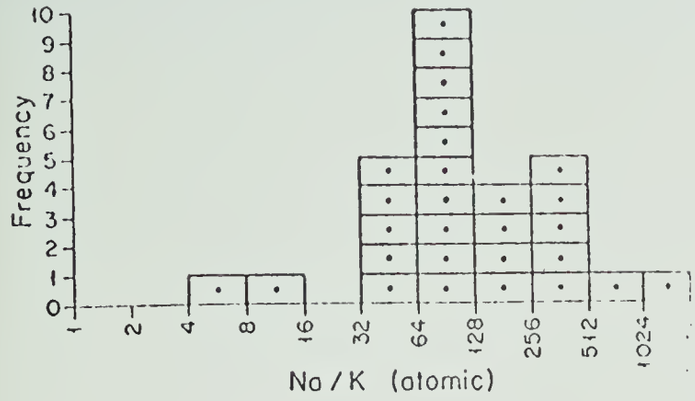

Fig.19a (Top). Na/K ratios of connate waters and ... field brines. Weighted average = 42.3. Data from Wh... Hem and Waring tables 12, 13 and 14 (1963). (Analy... with less than 5,000 ppm total ionic concentration ...

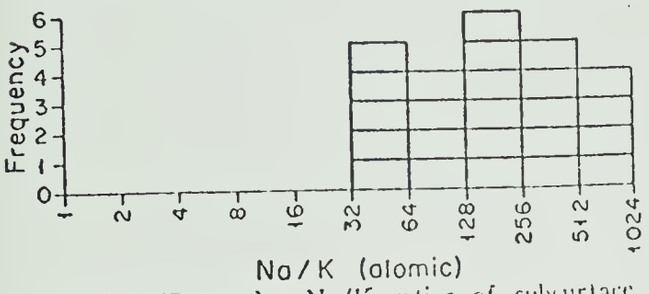

Fig.19c. (Bottom). Na/K ratios of subsurface wa... from the Michigan Basin. Weighted average = 94.6. D... from Graf et al. (1966).

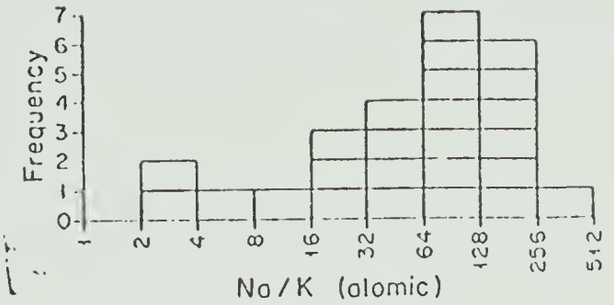

Fig.19b (Middle). Na/K ratios of subsurface waters ... the Illinois Basin. Weighted average = 249. Data fr... Graf et al. (1966).

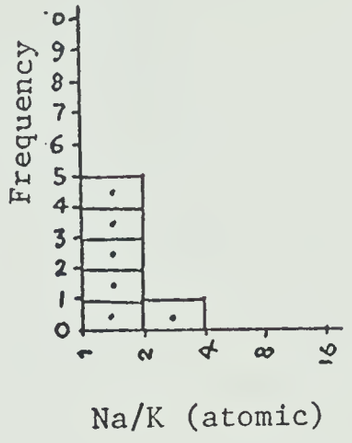

19.g Present Study

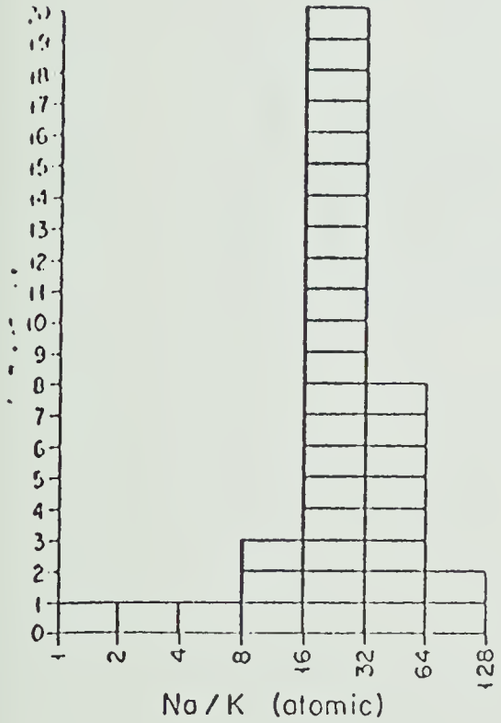

Fig.19d (Left). Na/K ratios from inclusion fluids in Mississippi Valley-type deposits. Average (not weighted *) 26.9. Data from Hall and Friedman (1963) and Sawkins (1966a).

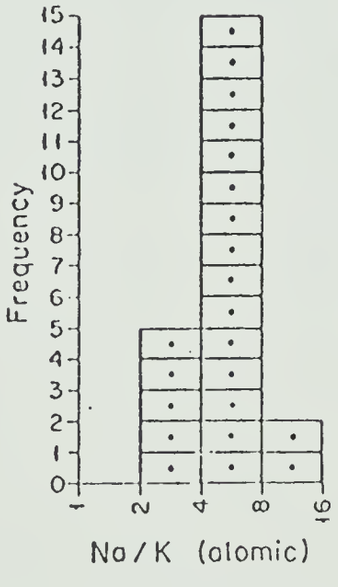

Fig.19e (Middle). Na/K ratios of Providencia inclusions. ...eighted average Na/K = 3.4. Data from Rye and Hafty (1968).

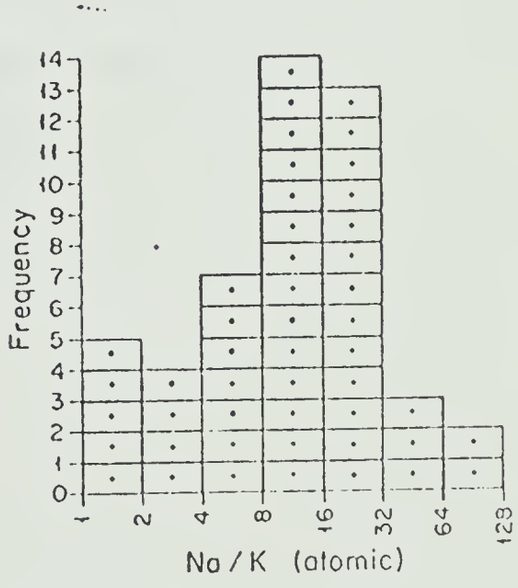

Fig.19f (Right). Na/K ratios of spring waters from volcanic environments. Weighted average = 13.1. Data from White, Hem and Waring, tables 17, 18, 19, 20 and 21 (1963).

Note: Many of these waters exhibit low total ionic concentration in comparison with sedimentary brines and fluid inclusions. This dilution is the result of admixture with groundwater of very low ionic concentration. The Na/K ratios are thus considered to be reasonably representative of waters containing higher ionic concentrations in the deeper parts of volcanic spring systems.

FIGURE 20

Ratios of K/Na in fluid phase vs temperature, from experimental data and natural waters [modified from White (1968) and Gammon et al. (1968)]

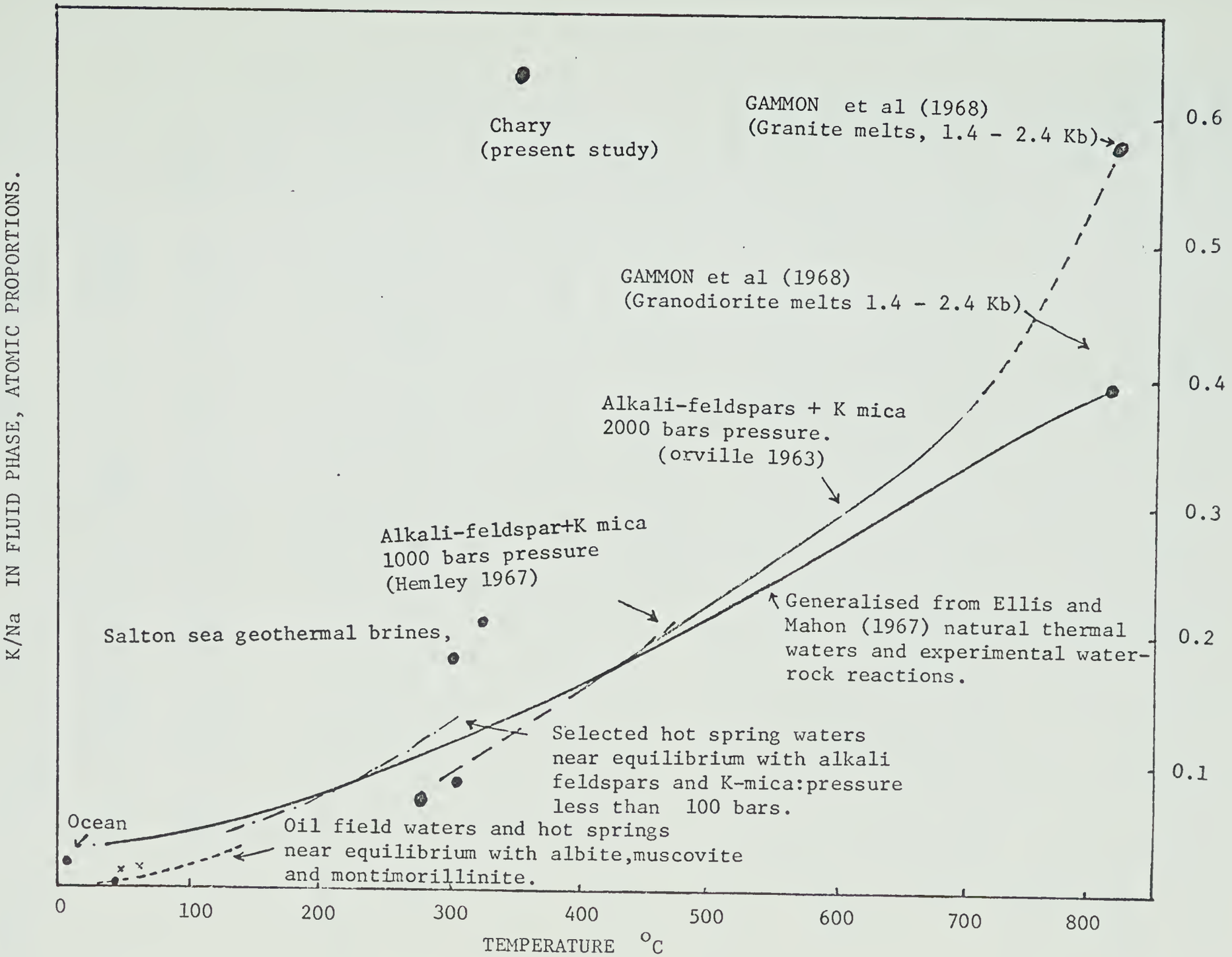
K/Na IN FLUID PHASE, ATOMIC PROPORTIONS.
Chary
(present study)
GAMMON et al (1968)
(Granite melts, 1.4 - 2.4 Kb)
GAMMON et al (1968)
(Granodiorite melts 1.4 - 2.4 Kb)
Alkali-feldspars + K mica
2000 bars pressure.
(orville 1963)
Alkali-feldspar+K mica
1000 bars pressure
(Hemley 1967)
Salton sea geothermal brines,
Generalised from Ellis and
Mahon (1967) natural thermal
waters and experimental water-
rock reactions.
Selected hot spring waters
near equilibrium with alkali
feldspars and K-mica:pressure
less than 100 bars.
Ocean
Oil field waters and hot springs
near equilibrium with albite,muscovite
and montimorillinite.
0.6
0.5
0.4
0.3
0.2
0.1
0
100
200
300
400
500
600
700
800
TEMPERATURE °C

subsequent reactions might change the salinities locally during the process of deposition. Higher K/Na ratios indicate that the hydrothermal solutions have not mingled with sea water or any other percolating solutions during their transport through the Shear Zone. Otherwise the K/Na ratios would have been much lower than they are at present. Thus a more probable interpretation of the K/Na results would be that the chemistry of the solutions did not change during the transport of the ore-bearing fluids through the Shear Zone; i.e., ore deposition has taken place by magmatic or juvenile waters and little contamination has occurred. Consistency in the K/Na ratios in all the samples might indicate that the temperature did not decrease very much during the depositional history.

5.12 ISOTOPIC COMPOSITION OF SULFUR SPECIES

The isotopic composition of sulfides deposited from aqueous solutions is greatly influenced by the dominant sulfur species present in the aqueous solution at the given condition. The chief sulfur species in aqueous solutions at temperatures of 300-360°C are H_2S, HS^-, $S^=$, So_4^-, HSO_4^-, KSO_4^-, $NaSO_4^-$, $KHSO_4^-$, $NaHSO_4$ and H_2SO_4 are minor (Ohmoto, in press). The isotopic composition of total sulfur in the fluids with respect to the $S^=$ from the theoretical considerations of Sakai (1968) may be expressed as follows:

$$\delta S^{34}_{\Sigma S} = (\delta S^{34}_{H_2S} \cdot X_{H_2S}) + (\delta S^{34}_{HS^-} \cdot X_{HS^-}) + (\delta S^{34}_{S^=} \cdot X_{S^=}) +$$

$$(\delta S^{34}_{SO_4^=} \cdot X_{SO_4^=}) + (\delta S^{34}_{HSO_4^-} \cdot X_{HSO_4^-}) + (\delta S^{34}_{KSO_4^-} \cdot X_{KSO_4^-})$$

$$+(\delta S^{34}_{NaSO_4^-} \cdot X_{NaSO_4^-}) + (\delta S^{34}_{KHSO_4^-} \cdot X_{KHSO_4^-}) + (\delta S^{34}_{NaHSO_4^-} \cdot X_{NaHSO_4^-})$$

$$+(\delta S^{34}_{H_2SO_4^-} \cdot X_{H_2SO_4^-}) + \ldots + \ldots + \ldots + \ldots \qquad (16)$$

where δS^{34} is the isotopic composition of i species in aqueous solution, and X_i is the mole fraction of the species i with respect to the total sulfur species.

$$X_i = m_i/(m_{H_2S} + m_{HS^-} + m_{S^=} + m_{SO_4^=} + m_{HSO_4^-} + \ldots\ldots\ldots) \quad (17)$$

The isotopic compositions of H_2S, HS^-, and $SO_4^=$ were theoretically calculated (Sakai 1968) and related to $S^=$ in terms of the reducing function ratios. At present, since the activity coefficients and isotope compositions of these minor species are not available, the published and calculated values of HSO_4^- and $SO_4^=$ have been employed in the computations. Thode and Monster (1965) suggested that there is only a very small fractionation between $SO_4^=$ and sulfate minerals. Ohmoto (personal Communication) has assumed the isotopic compositions of HSO_4^-, KSO_4^-, $NaSO_4^-$, $KHSO_4^-$, $NaHSO_4^-$ to be of the same order as $SO_4^=$.

Sufficient research has been done to demonstrate that chemical equilibrium is possible among coexisting sulfur species and precipitating sulfides at any given temperature (Rye 1969; Kajiwara 1969; Grootenboer 1969). However, many laboratory-controlled systems remain to be analyzed in order to explain certain natural environments of sulfide-sulfate precipitation and their mutual influence upon the isotopic compositions of the precipitating phases. However, the present existing isotopic work on sulfur isotope fractionation does enable one to appreciate the natural phenomena.

Mole fractions, mentioned above, may be calculated if the salt concentration is known, by employing the following relationships at any particular temperature (Helgeson 1969).

$$H_2S \rightleftharpoons H^+ + HS^- \qquad K_1 = \frac{a_{H^+} \cdot a_{HS^-}}{a_{H_2S}} \qquad (18)$$

$$HS^- \rightleftharpoons H^+ + S^= \qquad K_2 = \frac{a_{H^+} \cdot a_{S^=}}{a_{HS^-}} \qquad (19)$$

$$S^= + 2(O_2) \rightleftharpoons SO_4^= \qquad K_3 = \frac{(a_{SO_4^=})}{a_{S^=} \cdot f(O_2)^2} \qquad (20)$$

$$HSO_4^- \rightleftharpoons H^+ + SO_4^= \qquad K_4 = \frac{a + \cdot a_{SO_4^=}}{a_{HSO_4^-}} \qquad (21)$$

$$KSO_4^- \rightleftharpoons K^+ + SO_4^= \qquad K_5 = \frac{a_{K^+} \cdot a_{SO_4^=}}{a_{KSO_4^-}} \qquad (22)$$

$$NaSO_4^- \rightleftharpoons Na^+ + SO_4^= \qquad K_6 = \frac{a_{Na^+} \cdot a_{SO_4^=}}{a_{NaSO_4^-}} \qquad (23)$$

$$KHSO_4 \rightleftharpoons K + HSO_4 \qquad K_7 = \frac{a_{K^+} \cdot a_{HSO_4^-}}{a_{KHSO_4}} \qquad (24)$$

$$NaHSO_4 \rightleftharpoons Na^+ + HSO_4^- \qquad K_8 = \frac{a_{Na} \cdot a_{HSO_4}}{a_{NaHSO_4}} \qquad (25)$$

$$H_2O \rightleftharpoons H^+ + OH^- \qquad K_9 = \frac{a_{H^+} \cdot a_{OH^-}}{a_{H_2O}} \qquad (26)$$

$$H_2SO_4 \rightleftharpoons H^+ + HSO_4^- \qquad K_{10} = \frac{a_{H^+} \cdot a_{HSO_4^-}}{a_{H_2SO_4}} \tag{27}$$

$$a_i = m_i \cdot \gamma_i \, . \tag{28}$$

where K_1, K_2, ... are the equilibrium constants for reactions at the given temperature (Helgeson 1969) and a_i, γ_i, m_i represent the activity, activity coefficient and molality respectively. Computational data in the calculation of the activity coefficients of different species, by using Delta approximation have been given in the appendix 2.

Recent work on the isotopic composition of sulfur species (Ohmoto, personal communication) indicates that the factors influencing the isotopic composition of various species and mineral phases being precipitated from these solutions, are temperature, fugacity of oxygen, hydrogen ion concentration, ionic strength of the solutions, concentration of K and Na in solution, and isotopic composition of total sulfur.

For the present study on the hydrothermal model, with the established data derived from the experimental work, theoretical calculations and other reasonable assumptions, the effect of these parameters on the molalities of the species and on the isotopic composition of the sulfides in aqueous solutions have been examined. The molalities of the sulfur species, H_2S, HS^-, $S^{=}$, $SO_4^{=}$, KSO_4^-, $NaSO_4^-$, $KHSO_4^-$, $NaHSO_4^-$ and H_2SO_4, have been given in the tables 6 and 7 for the parameters specified. The major computational procedures to calculate the individual molalities, thereby calculating the isotopic composition of sulfides in aqueous solution are mainly based on equations 16 to 28. The computational procedures are

outlined in Appendix 3.

From Tables 6 and 7, it can be shown that a decrease in temperature would move the stability fields of minerals towards lower fugacities of oxygen and sulfur. The molalities of the constituents would also vary considerably.

Within the range of interest, the molalities of H_2S, HS^- increase slightly, whereas the molalities of the rest of the sulfur species decrease considerably with a lowering of the temperature and the retention of remaining factors at a constant level, except a corresponding change in the fugacities of oxygen and sulfur with reference to the stability fields of sulfides.

The molalities of the sulfur species are not directly related to the pressure except that the fugacity of water vapor in the system is related to the total pressure by a fugacity coefficient. However, the effect of the partial pressure of water vapor is quite small in computing the molalities of the constituents. Thus all the computations are for an average pressure of 500 atmospheres.

At constant temperature, ionic strength, hydrogen ion concentration, and pressure, decreasing both fugacities of oxygen and sulfur would result in a decrease of the molalities of H_2S, HS^- and $S^=$ and other sulfate species. But at constant factor of $f(O_2)$, a decrease in $f(S_2)$ would decrease the molalities of H_2S, HS^-, $S^=$ and other sulfate species and at constant $f(S_2)$, a decrease in $f(O_2)$ would increase the molalities of other sulfide species.

Ionic strength has no considerable effect upon the molalities of the constituents. Changes in the molalities are so small that the individual percentages of the species would not vary considerably. Since

TABLE 6 and TABLE 7

Computed molalities of the sulfur species considered in aqueous solutions at 350°C and 300°C. pH 3.0 and 6.0 (rest of the parameters specified).

N.B.: A pH of 3 is selected to show the variations in the molalities of the species with pH

Molalities in log values	350°C				300°C			
I = 3.0 pH = 3.0	log $f(O_2)$=-31		log $f(O_2)$=-29		log $f(O_2)$=-34		log $f(O_2)$=-32	
log $f(S_2)$	-10.5	-8.5	-10.5	-8.5	-11.5	-9.5	-11.5	-9.5
*								
H_2S	-3.22	-2.22	-4.22	-3.22	-2.76	-1.76	-3.76	-2.76
HS	-7.71	-6.71	-8.7.	-7.71	-7.14	-6.14	-8.14	-7.14
S	-9.24	-8.24	-10.24	-9.24	-10.51	-9.51	-11.51	-10.51
SO_4	-12.19	-11.19	-9.19	-8.19	-13.88	-12.88	-10.88	-9.88
HSO_4	-9.49	-8.49	-6.49	-5.49	-11.60	-10.60	-8.60	-7.60
KSO_4	-11.37	-10.37	-8.37	-7.37	-13.38	-12.38	-10.38	-9.38
$NaSO_4$	-10.99	-9.99	-7.99	-6.99	-13.07	-12.07	-10.07	-9.07
$KHSO_4$	-8.67	-7.67	-5.67	-4.67	-14.67	-10.61	-8.61	-7.61
$NaHSO_4$	-8.29	-7.29	-5.29	-4.29	-11.29	-10.29	-8.29	-7.29
H_2SO_4	-13.93	-12.93	-10.93	-9.93	-15 72	-14.72	-12.72	-11.72

* log values

NOTE: All these values are relative quantities, not absolute values.

I = 3.0 pH = 6.0	350°C				300°C			
	log $f(O_2)$=-31		log $f(O_2)$=-29		log $f(O_2)$=-31		log $f(O_2)$=-29	
log $f(S_2)$	-10.5	-8.5	-10.5	-8.5	-11.5	-9.5	-11.5	-8.5
H_2S^*	-3.22	-2.22	-4.22	-3.22	-2.76	-1.76	-3.76	-2.76
HS^-	-4.71	-3.71	-5.71	-4.71	-4.14	-3.14	-5.14	-4.14
$S^=$	-3.24	-2.24	-4.24	-3.24	-4.51	-3.51	-5.51	-4.51
$SO_4^=$	-6.19	-5.19	-3.19	-2.19	-7.88	-6.88	-4.88	-3.88
HSO_4^-	-6.49	-5.49	-3.49	-2.49	-8.60	-7.60	-5.60	-4.60
KSO_4^-	-5.37	-4.37	-2.37	-1.37	-7.38	-6.38	-4.38	-3.38
$NaSO_4^-$	-4.99	-3.99	-1.99	-0.99	-7.07	-6.07	-4.07	-3.07
$KHSO_4^-$	-5.67	-4.67	-2.67	-1.67	-8.61	-7.61	-5.61	-4.61
$NaHSO_4^-$	-5.29	-4.29	-2.29	-1.29	-8.29	-7.29	-5.29	-4.29
H_2SO_4	-13.93	-12.93	-10.93	-9.93	-15.72	-14.72	-12.72	-11.72

* Molalities in the log values

NOTE: All these values are relative quantities, not absolute values.

this effect would change the percentages imperceptibly, for the present computational purposes, an ionic strength of 3.0 is selected (Helgeson 1969).

At constant temperature, pressure, ionic strength, fugacities of oxygen and sulfur, a decrease in the hydrogen ion concentration or an increase in pH would not bring about a change in the molalities of H_2S within the range of interest, i.e., 3.0 to 6.0, but a considerable increase in the molalities of HS^-, $S^=$ and all other sulfate ions.

With regard to the K/Na ratios, different values for these ratios would influence the molalities of potassium and sodium complex sulfates and would thus change their individual molalities. However, this effect is quite negligible when considering all other major factors.

5.13 THE INFLUENCE OF PHYSICO-CHEMICAL FACTORS ON THE ISOTOPIC COMPOSITION OF SULFIDES

As discussed previously, at any given temperature, the hydrogen ion concentration and fugacity of oxygen are the major factors influencing the isotopic composition of sulfides in aqueous solutions as the molalities of the individual species are greatly modified by changing the pH and fugacity of oxygen. According to Sakai's theoretical calculations when $S^=$ is assumed to be zero at all instances, the isotopic composition of H_2S, HS^-, pyrite and $SO_4^=$ would be 4.8, 3.7, 4.5 and 23.5 permil heavier than the isotopic composition of $S^=$ at 350°. Based upon this assumption, the isotopic compositions of sulfides in aqueous solutions have been calculated at varying pH and $f(O_2)$ and the plot presented in Figure 20. From these calculated isotopic compositions the isotopic composition of pyrite would have varied considerably. The ranges of oxygen fugacity were fixed with reference to Holland's data. Actually the lower limit for pH

is fixed from Helgeson (1967) of the aqueous solutions. The upper limit is taken from the silica, mica and carbonate buffer (Fig. 18). The plot clearly shows that the isotopic composition of pyrite would assume positive values towards the end phases of deposition if the physico-chemical conditions varied accordingly. It is not very essential that the temperature vary considerably to bring about major changes in the isotopic composition of the species. Even slight changes would bring considerable changes in the isotopic composition.

There are thus three factors that clearly indicate that the initial pH would have been greater than 3.0. As Helgeson stated (1967) that a pH of 3.0 is unrealistic geologically if carbonate minerals are considered to have been deposited simultaneously with the gold quartz bodies. Secondly, if the pH is considered to be 3.0 at the specified maximum of fugacity of oxygen, the fugacity of sulfur is comparatively very high. If the corresponding fugacities of oxygen and sulfur are taken into consideration, the pH of the solutions would have been around 6.0 and the isotopic composition of aqueous sulfides would be -23.5‰. Had pyrite been precipitated from these aqueous solutions of isotopic composition -23.5%, it would show an isotopic composition of -19.0 at a fugacity of oxygen of 10 exp. -29.0 and $f(S_2)$ 10 exp. -8.5. Even a slight decrease in fugacities of sulfur, oxygen or pH would shift the isotopic composition of aqueous sulfides to much heavier values and consequently resulting in much heavier isotopic composition for pyrite.

In this critical region, increase of pH by 1 unit, decrease of the fugacity of oxygen by two units (log) and the fugacity of sulfur by two log units would change the isotopic composition of sulfides in aqueous solution by 23.0‰ and a corresponding shift could be expected in the

FIGURE 21

Computed plot showing the relationship between the fugacity of oxygen and S^{34}‰ on an iso-pH projection

T=35.0 C. I=3.0. K/NA=0.66. LOG FS2=-100

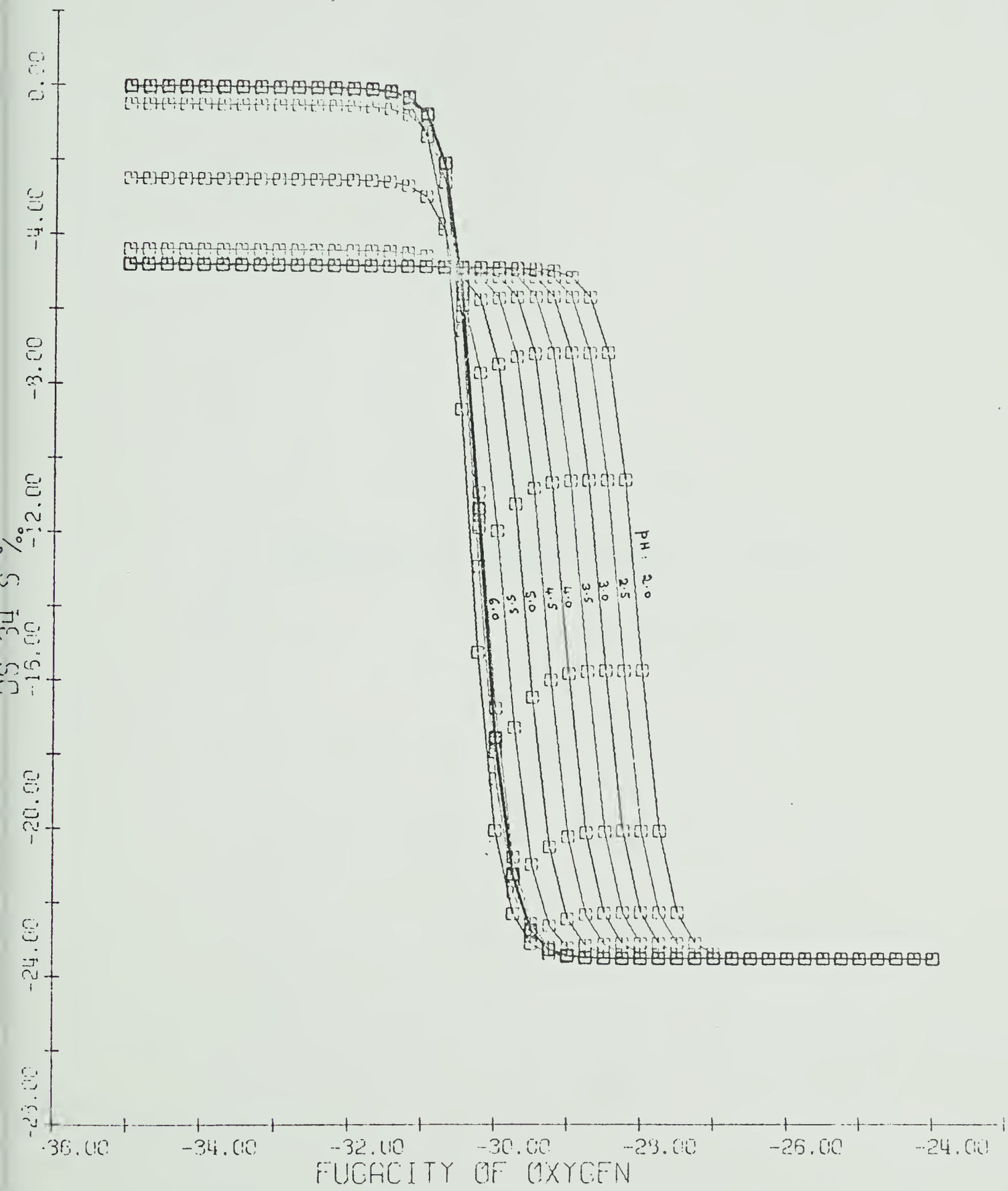

FIGURE 22

Computed pH - fugacity of oxygen - S^{34}‰ plot

PH - FUGACITY OF OXYGEN - DS34S PLOT δS^{34} in permil notation.

T = 350 C., I = 3.0, K/NA = 0.66 TS FIXED 10^{-2}

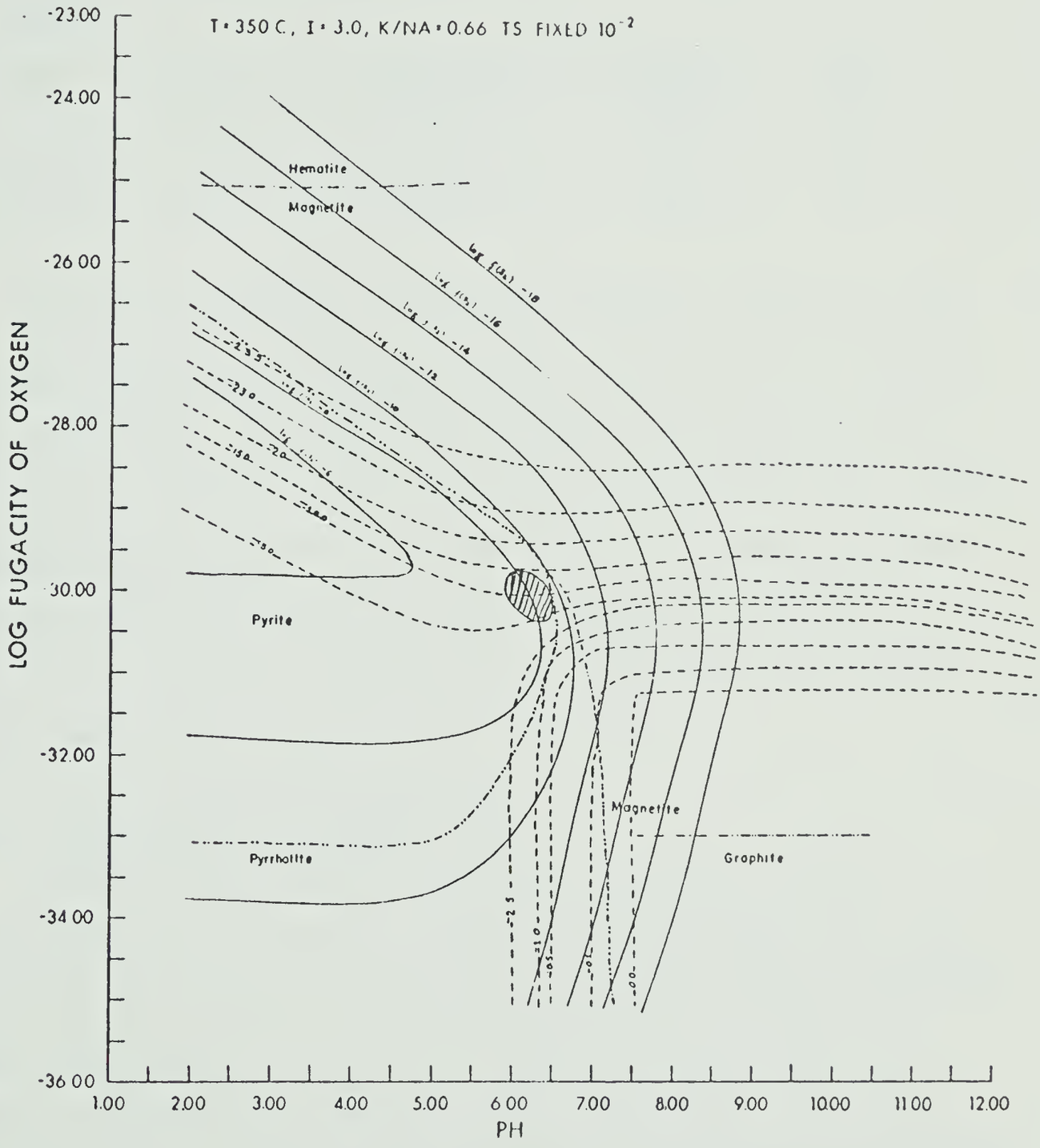

isotopic composition of pyrite and other sulfides deposited from the solutions (Fig. 21). If galena and sphalerite are assumed to have been co-precipitated along with pyrite, the corresponding minimum and maximum isotopic composition for galena would be as follows:

δS^{34} ‰

$S^{=}$	Pyrite	Sphalerite	Galena	pH
-21.0	-16.5	-18.0	-20.2	3.0
-0.3	+4.2	+2.7	+0.5	6.0

This would have been a more probable reason for variations in the isotopic compositions of different sulfides collected from the Campbell Shear Zone system. Temperature would not have been a major factor as the variations in the isotopic compositions are relatively small. From the experimental data, it could be interpreted that fugacity of oxygen would not have changed quite noticeably, otherwise an abrupt change in the isotopic composition would have been occurred from a very negative permil value to more positive values (Fig. 19).

5.14 OXYGEN ISOTOPES: INTERPRETATIONS

From the oxygen isotopic compositions determined on CO_2 gas extracted from the carbonates, the oxygen isotopic compositions of the quartz and the mineralizing waters were calculated, assuming equilibrium among the carbonates, quartz and ore-fluids at a given temperature. Samples with high and low values have been selected for calculating extreme values. Clayton's (1967) empirical equations have been employed:

$$\Delta_{(\text{quartz-water})} = 1000 \ln \alpha = 3.57 \ (10^6 \ T^{-2}) - 2.73 \qquad (29)$$

$$\Delta_{(\text{calcite-water})} = 1000 \ln \alpha = 2.80 \ (10^6 \ T^{-2}) - 3.40 \qquad (30)$$

$$1000 \cdot \ln \alpha_{\text{min-water}} = \delta O^{18}_{\text{min}} - \delta O^{18}_{\text{water}} \qquad (31)$$

The values of hypothetical H_2O coexisting with a given mineral assemblage (Viz. quartz and calcite) at a given temperature were calculated, based upon the mineral-water fractionation curves.

$\delta O^{18}_{\text{calcite}}$	$\delta O^{18}_{H_2O}$	$\delta O^{18}_{\text{quartz}}$	temp
8.7-10.6‰	5.0-6.8‰	21.4-19.6‰	350°C

As no temperature gradient during ore deposition has been recognised, it might be assumed that there were no changes in the isotopic composition during cooling. In the observed mineral assemblages, quartz is invariably rich in O^{18} because of isotopic-exchange reactions, where the frequency shifts on isotopic substitution of O^{18} for O^{16} are similar to two compounds, O^{18} should be concentrated by the compound whose oxygen atoms have the highest vibrational frequencies.

Clayton and Epstein (1961) found that calculated δO^{18} values for hydrothermal waters have a mean of 6‰. O'Neil and Clayton (1964) indicated that the isotopic composition of vapor phases, presumed to have been in equilibrium with various igneous rock types, falls in a narrow range near 8‰. The Providencia fluids (Rye 1966) have been reported to be magmatic waters. The isotopic composition obtained for the Gilman ore body waters was 8.6-6.8‰ which were interpreted to be normal magmatic waters (Engel et al. 1958). An analogy could be drawn between the Gilman

ore body and the Campbell shear system considering the geological setting of the deposits. Furthermore the following generalizations were interpreted based on the experimental data from a number of ore deposits. Taylor (1967) (1) magmatic waters are relatively uniform in O^{18}/O^{16} ratio, with values of 7.5 to 9.0 permil. (2) Hydrothermal waters very commonly have δ values similar to those of magmatic waters with a very few exemptions. (3) Metamorphic waters, particularly those in contact with meta sediments, generally are higher in O^{18} than magmatic waters (10-14‰). (4) Oceanic water is very uniform at -0.5 to +0.5‰. (5) Meteoric and surface fresh waters generally show -10 to -4‰.

5.15 CARBON ISOTOPES: INTERPRETATIONS

Assuming that the major fluid components carrying carbon are CO_2 and CH_4 in aqueous solutions, the fugacities of CO_2 and CH_4 have been utilized in computing the total carbon isotopic composition by using the following relationship:

$$\delta C^{13}_{\Sigma C_T} = (X_{CO_2} \cdot \Delta^{C^{13}}_{CO_2}) + (X_{CH_4} \cdot \Delta^{C^{13}}_{CH_4})$$

The parameters used in the calculations are the fugacity of carbondioxide, the fugacity of methane (in atmospheres), the total pressure, the temperature and the derived isotopic composition of carbondioxide from carbonates. The fugacity of CH_4 may be calculated from the relationship:

$$2H_2O + (CO_2) \rightleftharpoons CH_4 + 2(O_2) \qquad \text{[Holland 1965]}$$

The isotopic compositions of CO_2 and CH_4, relative to $CaCO_3$ are taken from Bottinga's (1969) calculated values for 1000 $\ln \alpha$ for C^{13} exchange relationships among carbondioxide, calcite graphite and methane.

The computed values of isotopic compositions of total carbon in

aqueous solution, range from -4.4 to -0.6‰ for two extreme values obtained on the carbonates, viz. (-4.2‰ and -0.5‰). With the limited amount of data, it is not possible to establish any trends of δC^{13} during calcite precipitation. The most obvious temperature dependent reaction during calcite deposition was the isotopic fractionation of carbon between the hydrothermal fluids and precipitating calcites. If the calculated values are correct, they fall near the range recorded for materials believed to represent juvenile carbon. Craig (1953) estimated a δC^{13} of terrestrial carbon to be -7% from material-balance considerations of the carbon cycle in nature. δC^{13} values reported for diamonds range from about -2.0 to -9.0‰ and average about -6‰ (Wickman 1956). δC^{13} determinations in carbonatite ejecta in pleistocene tuffs from the Laacher See district, Germany, which are believed to represent primary igneous carbonatite derived from a gabbroic magma, give a range of -6.6 to -8.4‰ (Taylor et al. 1965). Similarly, Providencia hydrothermal fluids have been interpreted to contain deep-seated carbon in the fluids (Rye 1966).

The possibility of a juvenile source for the carbon in the hydrothermal fluids at Yellowknife is in substantial agreement with the geological picture of the area having the western granodiorite intrusive as the major source. The uncertainties in determining the fugacities of oxygen and water vapor or the experimental uncertainties in determining the carbon isotopic composition would be the major factors of error. However, detailed work is planned for further studies. Since carbon isotopic composition also falls within the range of magmatic carbon isotopic composition, it is more justifiable to state that the source of carbon as well as the ore solutions is from a magmatic entity.

5.16 THEORETICAL ASSUMPTIONS, UNCERTAINTIES AND SOURCES OF ERRORS

Before evaluating the validity of the results, it is essential to discuss the sources of errors in the computations.

1. In the theoretical calculations of Sakai (1968) the equilibrium among the given set of sulfur species is assumed, but in nature, reactions tend to reach equilibrium.

2. The computed values of the isotopic compositions of the sulfur compounds (log f) are approximations.

3. In nature, closed system reactions are rare.

4. Since the isotopic compositions of HSO_4^-, KSO_4^-, $NaSO_4^-$, $KHSO_4^-$, $NaHSO_4^-$ at a given temperature are not theoretically calculated, for the present purposes it is assumed that they are almost of the same order of $SO_4^=$ (Ohmoto, personal communication).

5. Since bicarbonate and bisulfate complexes of sodium and potassium are very insignificant, they are not considered in the computations.

6. The molalities of the different species calculated are relative quantities rather than absolute values.

7. Equilibrium reactions are assumed among hydrothermal fluids, quartz, and calcite.

8. The major carbon species considered are CO_2 and CH_4 in equilibrium within the system.

9. Uncertainties in the equilibrium constants and activity coefficients.

5.17 SOURCE OF ORE CONSTITUENTS

According to White (1968) the following sources for a given ore deposit may be discussed in the light of the geology and geochemistry of the area: (a) metals dispersed in products of weathering and sediments,

(b) metals undergoing metamorphism, (c) metals in rocks of the deep crust or the mantle, or (d) metals present in earlier-formed ore deposits. Two of the sources mentioned above seem pertinent to the Con Mine deposits, namely, (1) rocks being metamorphosed, or (2) rocks of the deep crust or mantle. The first case is supported by Boyle (1961) whereas Ames (1962), Coleman (1957) and McConnell (1964) supported the second theory.

The observation by McConnell (1964), of narrow veinlets within the granitic rocks West of the Yellowknife greenstrone belt, containing small amounts of sulfides, (pyrite, minor galena and sphalerite) and erratic gold values is perhaps pertinent to the present discussion. Green's work (1968) strongly supports the theory that the Western Granodiorite might not have formed by the granitization process. In the light of Boyle's (1961) lateral secretion theory, it is difficult to explain the presence of the ore deposit in the granite body. Thus McConnell strongly feels that the gold-quartz deposits in the Yellowknife area were formed and localised due to the ascending hydrothermal solutions through the Shear Zones, resulting in alteration haloes surrounding the lenses.

5.18 THE CHEMICAL NATURE OF THE ORE-FLUIDS

The chemistry of the ore-fluids depends principally upon the dominent factor influencing the chemical composition as well as the dominent chemical constituent of the solutions. Sulfide complexes of As, Sb and Hg are highly soluble at high pH's and at concentrations of total sulfide (Dickson 1961). The bisulfate complexes of Cu, Zn, Cd, Pb, Ag, Hg, Sb and As seem to be adequately stable (Barnes and Czamanski 1967) at reasonable pH. Regarding the character of the ore-bearing solutions, Ridland (1941) stated that the main constituents in the ore

fluids are Ta, Mn, Fe, As, Sb, Zn, Ca, Cu, Te, Au, Ag, Pb, Si, S and H_2O. As has been calculated from the silicate and carbonate buffer system (Fig. 18) a pH of 5.5-6.5 would quite adequately explain the isotopic variations in sulfides. These weak acid solutions would have influenced the formation of the alteration zones surrounding the lenses. Geological and isotopic evidence shows that the source was magmatic but to obtain possible evidence regarding this conclusion and contrary to Boyle's theory of lateral secretion (1961), Deuterium, Sr, Pb isotope work is obviously necessary to facilitate comparison between the possible 'parental' granite body and the ore deposits. Oxygen isotope work on carbonates and other silicate phases would hopefully augment such information.

The solutions are thought to have percolated through the Shear Zone and filled the dilation sectors. The mechanism of transport could be expected as due to (1) the regional geothermal gradient, or (2) the pressure potential within the ore solutions.

Age of Mineralization

The problem of age of mineralization presently rests in the state of a logical speculation. Ridland (1941) related the gold mineralization in the Yellowknife area to one of the following possibilities: (a) as the gold deposits are found in the youngest pre-Cambrian rocks of the district, they may have been formed during the late pre-Cambrian orogenies in which the younger sedimentary rocks were folded and metamorphosed; (b) a giant quartz vein, 185 miles Northwest of Yellowknife, containing pitchblende, has been dated by lead-uranium ratios as late Ordovician and the mineralization may be related to this period, and (c) the Franklin Mountains, 140 miles West of Yellowknife, were formed during Laramide revolution. It is

possible that the Yellowknife gold-quartz deposits were formed during this orogeny. Robertson and Cumming (1966) obtained the lead model date 2900 m.y. on sulfides from veins in the metavolcanics, and Green (1968) obtained K-Ar and R-Sr data for the granodiorites, the date 2610 ± 58 m.y. and metavolcanics 2625 ± 60 m.y. There is a slight discrepancy in the results obtained by these two approaches. However, it is suggested that the out-pouring of volcanic rocks took place only slightly before the intrusion of granodiorite batholiths, to which mineralization in the district could be attributed. McConnell's (1964) observations also support this conclusion.

CHAPTER VI

SUMMARY - CONCLUSIONS AND INDICATED FURTHER RESEARCH

From the data gained from the sulfur isotope fractionation studies and fluid inclusion studies it is concluded that mineralization in the gold quartz veins of Yellowknife area took place at a temperature of 350°-300°C. The general nature of the gold-ore-bodies, the persistence of ore with increasing depth and the character of the major mineral constituents, suggest that p-T conditions during the mineralization were possibly uniform and rank in medium to high grade. In the light of the thermodynamic data it is shown that the isotopic composition of the sulfides is a function of physico-chemical conditions during precipitation. From the microscopic paragenetic studies, it is postulated that mineralization most likely took place in two stages, this fact being augmented by the isotopic compositions of the sulfides (the earlier pairs exhibiting lighter isotopic composition compared with the later pairs).

Calculated oxygen isotopic compositions of the hypothetical ore fluids, as well as the isotopic compositions of the carbon in the ore solutions, fall within the limits of the isotopic compositions of the respective constituents of the magmatic fluids. Furthermore, the K/Na ratio frequency distribution diagrams indicate a comparison with the compositions of magmatic fluids.

The probable concentration of hydrogen ions in the aqueous solutions at 350°C was determined by adopting the silica - K-mica - carbonate

buffer system. The pH of the mineralizing solutions was thus determined to be in the range of 5.5-6.0. The mineralizing fluids of pH 5.5-6.0, when passing through the Shear Zone, might have reacted with the country rock, as a result of which sericite-carbonate schist has formed, enveloping each quartz lens.

The variation of the molalities of different sulfur species in the aqueous mineralizing solutions have been demonstrated by computed plots and the conclusion is drawn that pH, fugacity of oxygen and temperature of formation would have influenced the minor variations in the isotopic compositions of the sulfides in the aqueous solutions to a major extent in the case of Campbell shear system whereas the influence of ionic strength, K and Na ratios and partial pressure of water vapor is negligible.

From the techniques used in deciphering the nature of the ore solutions and their chemistry, it is felt that further research to clarify some of the unsolved and critical questions, is quite essential. Particular mention may be made of more detailed work on the stable isotope geochemistry within the alteration zone; i.e., a study of the variations of sulfur, oxygen and carbon isotopic compositions in the ore bodies, the surrounding alteration zones and the country rocks, would perhaps enable one to detect the source of the ore constituents and their ultimate mode of emplacement. Similarly the following further research is suggested: (a) electron microprobe studies on element partition during the ore forming processes, viz; K, Na, Sr, etc., (b) a study of deuterium isotope variations to further investigate the nature of the ore forming processes, (c) geochemical studies on the sericitic micas from the alteration zones, (d) the determination of chlorine concentrations which

might be a geochemical indicator of potential ore zones, and (e) based on the empirical studies on the solubilities of gold, quartz, pyrite and calcite, quantitative studies of the gold, enriched in each lens from the known data of the dimension of the quartz lenses.

REFERENCES

Baragar, W.R.A. (1966): Geochemistry of the Yellowknife volcanic rocks; Can. Jour. Earth. Sci. 3, pp. 9-30.

Barnes, H.L. and Kilerud, (1961): Equilibrium in sulfur containing aqueous solutions; Eco. Geol. Vol. 56, pp. 648-688.

Bateman, J.D. (1952): Some geological features at Giant Yellowknife; Proc. Geol. Assoc. Can. Vol. 5, pp. 95-107

Borina, A.F. (1963): Aqueous salt solutions at high pressures and temperatures as possible media of transport of ore-forming elements in hydrothermal processes; Geoch. International Vol. 7, pp. 681-690.

Bottinga, Y. (1969): Calculated fractionation factors for carbon and hydrogen isotope exchange in the system calcite-carbondioxide-graphite-methane-hydrogen-water vapor; Geoch. Cosmo. Acta, Vol. 33, No. 1, pp. 49-64.

Boyle, R.W. (1964): A decrepitation study of quartz from the Campbell and Negus-Rycon Shear Zone Systems, Yellowknife, N.W.T.; Geol. Surv. Can. Dept. Mines & Tech. Surv. Bull. 30.

_____. (1961): The geology, geochemistry and origin of the gold deposits of Yellowknife district; Geol. Surv. Can. Mem. 310, Dept. Mines & Tech. Surveys.

_____. (1968): The source of metals and gangue elements in epigenetic deposits; Min. deposita. 3, 174-177.

_____., Wanless, R.K. and Lowden, (19): The origin of gold-quartz deposits, Yellowknife, N.W.T.; Econ. Geol., Vol. 58, pp. 804-807.

Brown, C.E.G. and Dadson, A.S. (1953): Geology of the Giant Yellowknife Mine; Tran. Can. Inst. Min. Met., Vol. 56, pp. 59-76.

_____, Dadson, A.S. and Wriggleworth, L.A. (1959): On the ore-bearing structures of the Giant Yellowknife gold mine; Trans. Can. Inst. Min. Met., Vol. 62, pp. 107-116.

Buryak, V.A. (1966): Relation between auriferous veins and gold sulfide host rock mineralization in pre-cambrian gold-ore deposits (Lena gold field); DOKI. Acad. Sci. U.S.S.R., Vol. 165, 79-81.

Burkay, V.A., Kashcheyeva, T.V. and Khmelevskaya, I.M. (1966): Influence of host rock composition on the development of pre-cambrian gold mineralization; Tran. DOKI. Akad. Nauk. U.S.S.R., Vol. 169, pp. 405-408.

Campbell, N. (1949): West Bay Fault, in structural geology of Canadian deposits; Can. Inst. Min. Met., Jubilee Volume, pp. 244-259.

Clayton, R.N. and Epstein, S. (1961): The use of oxygen isotopes in high temperature geothermometry; Jour. Geol., Vol. 69, pp. 447-452.

Cobble, J.W. (1964): The thermodynamic properties of high temperature aqueous solutions VI: Application of entropy correspondence to thermodynamics and kinetics; J. Am. Chem. Soc., Vol. 86, pp. 5394-5401.

_____. (1966): High temperature aqueous solutions: Science; Vol. 152, pp. 1479-1485.

Coleman, L.C. (1957): Mineralogy of Giant Yellowknife gold mineralization, Yellowknife, N.W.T.; Econ. Geol., Vol. 52, pp. 400-425.

Craig, H. (1953): Geochemistry of stable carbon isotopes; Geoch. Cosmo. Acta, Vol 3, pp. 53-92.

Dadson, A.S. (1949): Giant Yellowknife; Western Miner, Vol. 22, No. 10, pp. 82-90.

_____. and Bateman, J.D. (1948): Giant Yellowknife Mine, in Structural Geology of Canadian Ore Deposits; Can. Inst. Min. Met., Jubilee Volume, pp. 273-283.

Ellis, A.J. and Golding, R.M. (1963): The solubility of carbon dioxide above 100°C in water and in sodium chloride solutions; Am.Jour. Sci., Vol. 261, No. 1, pp. 47-60.

Engel, A.E.J,, Clayton, R.N. and Epstein, S.(1958): Variations in oxygen isotopic composition of carbon and oxygen in Leadville limestone (Mississippiraon, Colorado) and its hydrothermal and metamorphic phases; J. Geol. 66, pp. 374-393.

Folinsbee, R.E. (1947): Preliminary map, Lac de Gras, Northwest Territories; Geol. Surv. Canada, paper 47-5.

Fortier, Y.O. (1947): Rose Lake, Northwest Territories: Geol. Surv. Canada, paper 47-16.

Goldschmidt, V.M. (1954): Geochemistry; Muir, A. ed., Oxford.

Green, D.C. (1968): Pre-Cambrian Geology and Geochronology of the Yellowknife Area, N.W.T.; Ph.D. Thesis, Univ. of Alberta (unpublished).

Grinenko, L.N., Andreyeva, M.G. and Gavrilov, A.M. (1965): Isotopic composition of sulfur in the sulfides of the Baleysk gold deposits; Geoch. Int. 2, pp. 223-232.

Grootenboer, J. and Schwarcz, (1969): Experimental sulfur isotope fractionations between sulfide minerals; Earth and Plan. Sci. Letters, Vol. 7, pp. 162-166.

Grooves, D.I. and Soloman, M. (1968): Fluid inclusion studies at Mount Bischoff, Tasmania; Tran. Inst. Min. and Met., pp. B1-B12

Gross, W.H. and Thode, H.G. (1965): Ore and the source of acid intrusives using sulfur isotopes; Econ. Geol., Vol. 60, pp. 576-589.

Harvey, R.D. and Vitaliano, C.J. (1961): Wall rock alteration in the goldfield district, Nevada; Geol. Soc. Am. Spec. Pap. 68, pp. 194.

Helgeson, H.C. (1967a): Solution Chemistry and metamorphism; Abelson, P.H. ed. Researches in Geochemistry, pp. 362-404.

_____. (1967b): Silicate metamorphism in sediments and the genesis of hydrothermal ore solutions. 'Genesis of stratiform lead-zinc-barite-fluirite deposits'; Brown, ed., Econ. Geol. Monograph. 3, pp. 333-341.

_____. (1967c): Thermodynamics of complex dissociates in aqueous solution at elevated temperatures; Jour. Phy. Chem., Vol. 71, pp. 3121-3136.

_____. (1968a): Geologic and thermodynamic characteristics of the Scatton Sea geothermal system; Am. Jour. Sci., Vol. 266, pp. 129-166.

_____. (1969): Thermodynamics of hydrothermal systems at elevated temperatures and pressures; Am. Jour. Sci. Vol. 267, pp. 729-804.

_____. (1970): Description and interpretation of phase relations in geochemical processes involving aqueous solutions; Am. Jour. Sci., Vol. 268, pp. 415-438.

_____., Garrels, R.M. and Mackenzie, F.T. (1969): Evaluation of irreversible reactions in geochemical processes involving minerals and aqueous solutions, II: Applications; Geoch. Cosmo. Acta, Vol. 33, pp. 455-481.

Hemley, J.J. and Jones, W.R. (1964): Chemical aspects of hydrothermal alteration with emphasis on hydrogen metasomatism; Econ. Geol., Vol. 159, pp. 538-569.

_____. and Mayer, C. (1967): 'Wall Rock Alteration'; Barnes, H.L. ed., Geochemistry of hydrothermal ore deposits, chapter 6, pp. 166-234.

Henderson, J.F. (1939): Beaulieu River Area, Northwest Territories; Geol. Surv. Canada, paper 39-1.

_____. and Brown, I.C. (1949): Yellowknife, Northwest Territories; Geol. Surv. Canada, paper 50-34.

_____. (1950): Structure of Yellowknife Greenstones Belt, N.W.T., Tran. Can. Inst. Min. Met., Vol. 53, pp. 427-434.

_____. (1952): The Yellowknife Greenstone Belt; Geol. Surv. Canada, paper 52-28.

_____. (1966): Geology and Structure of the Yellowknife Greenstone Belt, District Mackenzie; Geol. Surv. Canada - Dept. Mines & Tech. Surverys, Bull. 141.

Holland, H.D. (1959): Some applications of thermodynamic data to problems of ore deposits: 1. Stability relations among the oxides, sulfides, sulfates and carbonates of ore and gangue minerals, Econ. Geol., Vol. 54, pp. 184-233.

_____. (1965): Mineral assemblages and composition of ore-forming fluids; Econ. Geol., Vol. 60, pp. 1101-1166.

Holser, W.T. (1954): Fugacity of water at high temperatures and pressures; Jour. Phy. Chem., Vol. 58, pp. 316-317.

Jensen, M.L. (1959): Sulfur isotopes and hydrothermal deposits; Econ. Geol. Vol. 54, pp. 374-394.

Jolliffe, A.W. (1936): Yellowknife River Area, Northwest Territories; Geol. Surv. Canada, paper 36-5.

Kajiwara, Y. Krous; H.R. and Sasaki, A. (1969): Experimental study of sulfur isotope fractionation between coexistent sulfide minerals; Earth and Plane. Sci. Letters, 7, pp. 271-277.

Kajiwara, Y. (1970): Personal communication.

Kordes, E. (1935): Die Beziehunges zwischen den Dissoziationsdampfdrücken von sulfiden und ihrer Ausscheidungsfolge auf magmatogenen Erzlagerstätten; Min. Pet. Mitt., V. 46, pp. 256-288.

Kretz, R. (1968): Study of pegmatite bodies and enclosing rocks Yellowknife Beaulieu Region, District of Mackenzie; Geol. Surv. of Canada, Bull. 159.

Leech, A.P. (1965): A Reconnaissance: Basic intrusive rocks of the pre-Cambrian Shield, Canada; M.Sc. Thesis (U. of Alberta), unpublished.

Lemmlein, G.G. and Klevtsov, P.V. (1961): Relations among the principal thermodynamic parameters in a part of the system H_2O-NaCl; Geochem. No. 2, pp. 148-158.

Lord, C.S. (1942): Snare River and Ingray Lake Map Areas, Northwest Territories; Geol. Surv. Canada, Memoir 235.

McConnell, G.W. (1964): Yellowknife gold quartz deposits; Econ. Geol., Vol. 59, pp. 328-330.

_____. (1964): Notes on similarities between some Canadian gold deposits and the Homestake deposits of South Dakota; Econ. Geol., Vol. 59, pp. 719-720.

Moore, J.C.G. (1956): Courageous-Matthews Lake, District of Mackenzie, Northwest Territories; Geol. Surv. Canada, Memoir 283.

Ohmoto, H. and Rye, R.O. (1970): The Bluebell Mine, British Columbia. I: Mineralogy, paragenesis, fluid inclusions and the isotopes of hydrogen, oxygen and carbon; Econ. Geol., Vol. 65, pp. 417-437.

O'Neil, J.R. and Clayton, R.N. (1964): Oxygen isotope geothermometry in Isotopic and cosmic chemistry; Craig. H. et al. eds., Amsterdam, North Holland, Pub. Co., pp. 157-168.

Orville, P.M. (1963): Alkali ion exchange between vapor and feldspar phases; Am. Jour. Sci., Vol. 261, pp. 201-237.

Pryor, T. (1924): The underground geology of the Kolar gold field; Tran. Inst. Min. & Met., Vol. 33, pp. 95-135.

Quist, A.S., Frank, E.V., Jolley, H.R. and Marshall, W.L. (1963): Electrical conductances of aqueous solutions at high temperature and pressure. I: The conductance of potassium sulfate water-solution from 25° to 800° and at pressures up to 4000 bars; Jour. Phy. Chem., Vol. 67, pp. 2453-2459.

Ridland, G.C. (1941): Mineralogy of Negus and Con Mines, Yellowknife, N.W.T., Canada; Econ. Geol., Vol. 36, pp. 45-70.

Robertson, D.K. and Cumming, G.L. (1968): Lead and sulfur isotope ratios from the Great Slave Lake area, Canada; Can. Jour. Earth. Sci., Vol. 5, pp. 1269-1276.

Roedder, E. (1967): Fluid inclusions as samples of ore deposits; Barnes, H.L. ed., Hold Riener and Winston Inc.k pp. 515-574.

_____. (1963): Studies of fluid inclusions II: Freezing data and their interpretation, Econ. Geol, Vol. 58, pp. 167-211.

_____. (1963): Studies of fluid inclusions III: Extractions and quantitative analysis of inclusion the milligram range; Econ. Geol., Vol. 58, pp. 353-375.

Rye, R.O. (1966): The carbon, hydrogen and oxygen isotopic composition of the hydrothermal fluids responsible for the lead zinc deposits at Providencia Zacatecas, Mexico; Econ. Geol., Vol. 61, No. 8, pp. 1399-1427.

Sakai, Hitoshi (1968): Isotopic properties of sulfur compounds in hydrothermal processes; Geoch. Jour., Vol. 2, pp. 29-49.

Sawkins, F.J. (1966): Ore genesis in the North Pennine ore field in the light of fluid inclusion studies.

_____. (1968): Na/K and Cl/SO_4 ratios in fluid inclusions; Econ. Geol., Vol. 63, pp. 935-942.

Smith, F.G. (1963): Physical Geochemistry; Addison Welbey, New York.

Sproule, W.R. (1952): Control of ore deposition, Con Rycon and Negus Mines, Yellowknife, Northwest Territories; M.Sc. Thesis, Queen's University, Kingston (unpublished).

Tatsumi, T. (1965): Sulfur isotopic fractionation between coexisting sulfide minerals from Japanese ore deposits; Econ. Geol., Vol. 60, pp. 1645-1659.

Taylor, H.P. Jr. (1967): Oxygen isotope studies of hydrothermal mineral deposits in Geochemistry of Hydrothermal Deposits; Barnes, H.L. ed., Holt, Rinehart and Winston, Inc., New York, pp. 109-142.

_____., Freechen, J. and Degens, E.T. (1965): Oxygen and carbon isotope studies of carbonatites from Laacher See district, Germany (abs); Geol. Soc. Am. Spec. Paper 82, pp. 205-206.

_____. (1967): Oxygen isotope studies of hydrothermal mineral deposits in Geochemistry of hydrothermal ore deposits; Barnes, H.L. ed., pp. 108-142.

Wanless, R.K., Boyle, R.W. and Lowden, J.A. (1960): Sulfur isotopic investigation of the gold quartz deposits of the Yellowknife district; Econ. Geol., Vol. 55, pp. 1591-1621.

White, D.E. (1968): Environment of generation of some base metal ore deposits; Econ. Geol., Vol. 63, pp. 301-335.

Wickman, F.E. (1956): The cycle of carbon and stable carbon isotopes; Geoch. Cosmo. Acta, V. 9, pp. 136-153.

APPENDIX 1

Thermodynamic Data (Holland 1965, 1959)

		A	B	C	D	Ref.
1.	$3/2[Fe] + (O_2)$ $1/2[Fe_3O_4]$	-133900		41.10	298-833	1
2.	$2[Fe] + (S_2)$ $2[FeS]$	-71820		25.12	412-1179	1
3.	$4[Fe_3O_4]+(O_2)$ $6[Fe_2O_3]$	-114700		67.8	300-1200	2
4.	$Fe_2O_3+(S_2)+5/2(O_2)$ $2[FeSO_4]$	-275000		147.1	300-1000	1
5.	$2[FeS]+(S_2)$ $2[FeS_2]$	-71000		71.9	600-1000	2
6.	$[FeS_2]+2(O_2)$ $[FeSO_4]+1/2(S_2)$	-162600		57.8	300-1000	1
7.	$2[Zn]+[S_2]$ $2[ZnS]$	-127300	-9.2	73.4	298-693	1
8.	$2[Zn]+(O_2)$ $2[ZnO]$	-168200	-13.8	88.3	298-693	1
9.	$[ZnS]+2(O_2)$ $[ZnSO_4]$	-185710	-7.37	105.0	298-1000	2
10.	$[ZnO]+1/2(S_2)+3/2(O_2)$ $[ZnSO_4]$	-166200		80.5	300-1000	1
11.	$2[Pb]+S_2$ PbS	-72280		41.3	600-1200	2
12.	$2[Pb]+(O_2)$ $2[PbO_2]$	-109900	-16.1	100.2	600-1150	1
13.	$[PbS]+2(O_2)$ $[PbSO_4]$	-197000		84.3	300-1000	2
14.	$[PbO]+1/2(S_2)+3/2(O_2)$ $[PbSO_4]$	-182600		81.7	300-1000	1
15.	$[Si]+O_2$ $[SiO_2]$	-210600	-3.0	52.22	298-1700	1
16.	$[Si]+(S_2)$ $[SiS_2]$	-80000		39.7	298-1000	2
17.	$[SiO_2]+(S_2)$ $[SiS_2]+(O_2)$	130000	3.0	-12.5	298-1000	2
18.	$[C]+(O_2)$ $[CO_2]$	-94200		-0.2	298-2000	2
19.	$[CaSO_4]+(CO_2)$ $[CaCO_3]+1/2(S_2)$ $+3/2(O_2)$	+163500		-46.3	300-1000	1
20.	$[CuFeS_2]+S_2$ $[Cu_5FeS_4]+4[FeS_2]$	-50728		56.95	525-775	2
21.	$(H_2O)+1/2(S_2)$ $(H_2S)+1/2(O_2)$	37145	-0.86	1.61	298-1750	2
22.	$S_2+2(O_2)$ $2(SO_2)$	-173240		34.62	298-2000	2

1 Holland (1959) 2 Holland (1965)

Molal Values of the Debye-Hückel Electrostatic Parameters A and B from 25 to 350° C and the Values of the Dielectric Constant (Akerlof and Oshry, 1950) and Density (Keenan and Keyes, 1936) of Water Employed in the Calculations*

Temperature °C	A	$B \times 10^{-8}$	ϵ_{H_2O}	ρ_{H_2O}
25	0.5095	0.3284	78.420	0.9968
30	0.5144	0.3292	76.618	0.9956
40	0.5244	0.3310	73.125	0.9919
50	0.5354	0.3329	69.800	0.9882
60	0.5471	0.3347	66.629	0.9833
70	0.5596	0.3366	63.604	0.9779
75	0.5661	0.3376	62.144	0.9750
80	0.5729	0.3386	60.718	0.9720
90	0.5871	0.3406	57.965	0.9656
100	0.6019	0.3425	55.336	0.9580
110	0.6180	0.3447	52.826	0.9512
120	0.6347	0.3468	50.427	0.9428
125	0.6435	0.3479	49.268	0.9390
130	0.6525	0.3490	48.134	0.9346
140	0.6715	0.3512	45.939	0.9259
150	0.6915	0.3536	43.838	0.9169
160	0.7129	0.3559	41.824	0.9076
170	0.7354	0.3583	39.891	0.8974
175	0.7472	0.3595	38.953	0.8921
180	0.7595	0.3608	38.033	0.8870
190	0.7851	0.3632	36.244	0.8758
200	0.8127	0.3659	34.519	0.8645
210	0.8427	0.3686	32.852	0.8530
220	0.8746	0.3714	31.238	0.8401
225	0.8919	0.3728	30.449	0.8338
230	0.9099	0.3744	29.671	0.8274
240	0.9484	0.3775	28.145	0.8140
250	0.9907	0.3807	26.655	0.7993
260	1.0385	0.3845	25.196	0.7852
270	1.0905	0.3879	23.762	0.7679
275	1.1198	0.3900	23.052	0.7599
280	1.1502	0.3919	22.347	0.7506
290	1.2185	0.3962	20.947	0.7321
300	1.2979	0.4010	19.557	0.7126
310	1.3900	0.4059	18.170	0.6905
320	1.5003	0.4116	16.782	0.6669
325	1.5625	0.4144	16.086	0.6533
330	1.6315	0.4173	15.388	0.6392
340	1.7933	0.4237	13.982	0.6086
350	1.9936	0.4300	12.558	0.5721

* The numbers shown above apply to the liquid phase along the boiling curve for water.

Values of $\mathring{a}_i$ for Some Individual Ions in Aqueous Solutions

$\mathring{a}_i \times 10^8$	Ion
2.5	Rb^+, Cs^+, NH_4^+, Tl^+, Ag^+
3.0	K^+, Cl^-, Br^-, I^-, NO_3^-
3.5	OH^-, F^-, HS^-, BrO_3^-, IO_4^-, MnO_4^-
4.0–4.5	Na^+, HCO_3^-, $H_2PO_4^-$, HSO_3^-, Hg_2^{++}, SO_4^{--}, SeO_4^{--}, CrO_4^{--}, HPO_4^{--}, PO_4^{3-}
4.5	Pb^{++}, CO_3^{--}, SO_3^{--}, MoO_4^{--}
5.0	Sr^{++}, Ba^{++}, Ra^{++}, Cd^{++}, Hg^{++}, S^{--}, WO_4^{--}
6	Li^+, Ca^{++}, Cu^{++}, Zn^{++}, Sn^{++}, Mn^{++}, Fe^{++}, Ni^{++}, Co^{++}
8	Mg^{++}, Be^{++}
9	H^+, Al^{3+}, Cr^{3+}, trivalent rare earths
11	Th^{4+}, Zr^{4+}, Ce^{4+}, Sn^{4+}

SOURCE: Adapted from I. M. Klotz, *Chemical Thermodynamics*. Englewood Cliffs, N.J., Prentice-Hall, 1950, p. 331.

Appendix III

```
C        CALCULATION OF  ISOTOPIC COMPOSITIONS OF AQUEOUS SOLUTIONS
C        CALCULATION OF MOLALITIES OF SULFUR SPECIES AND ISOTOPIC
C        COMPOSITON OF SULFUR WITH MOLE FRACTIONS OF SULFUR SPECIES
C           (A) CALCULATE NPH NFO2
      DIMENSION XP (1000),XFO2(1000),X1(1000),X2(1000),X3(1000),X4(1000)
     .,X5(1000),X6(1000),X7(1000),XP(1000),X9(1000),X10(1000),X11(1000),
     .X12(1000),X13(1000),X14(1000),X15(1000),X16(1000),X17(1000),
     .X18(1000)
      DIMENSION X(13),Y(3),Z(3),PH(40),FO2(100)
      DIMENSION DPLOT(47),APH(25),AFO2(47)
      DIMENSION DPLOTT(47)
C
      DATA X/300.,-11.39,-3.06,-7.72,64.26,-7.06,-2.59,-0.3,29.39,0.5,
     .1.93,1.23,9.104/
      READ(5,100)PHMIN,PHMAX,FO2MIN,FO2MAX
C
      NPH=((PHMAX-PHMIN)/0.5)+1
      NFO2=((FO2MAX-FO2MIN)/0.25)+1
      PH(1)=PHMIN
      FO2(1)=FO2MIN
      DO 1 J=2,NPH
    1 PH(J)=PH(J-1)+0.5
      DO 2 J=2, NFO2
    2 FO2(J)=FO2(J-1)+0.25
      NTOTAL=NPH*NFO2
      JC=0
      DO 5 J=1,NPH
      DO 6 K=1,NFO2
      JC=JC+1
      XP(JC)=PH(J)
    6 CONTINUE
    5 CONTINUE
      NC=0
      DO 7 J=1,NPH
      DO 8 K=1,NFO2
      NC=NC+1
      XFO2(NC)=FO2(K)
    8 CONTINUE
    7 CONTINUE
C
      DO 1111 NNN=1,2
      READ(5,99)(X,FS2)
      DO 111 NN=1,4
      READ(5,99) (Y(J),J=1,9)
      READ(5,99)(Z(J),J=1,3)
   99 FORMAT(3F10.2)
      KC = 1
      DO 3 J=1,NPH
      DO 4 K=1,NFO2
      AH=-PH(J)
      OH =10**(AH-Y(2))
      QOH1=(Y(2)+ALOG10(Y(2)))-(AH+Y(4))
      QOH=10**QOH1
      AS=((0.5*FS2)+(ALOG10(Y(2))-((2.*AH)+X(9)+(0.5*FO2(K)))))
      AHS=(AH+AS)-X(4)
```

```
      AH2S=(AH+AHS)-X(3)
      AS04=X(5)+AS+(2*E02(K))
      AHS04=(AH+AS04)-X(6)
      AH2S04=(AH+AHS04)-X(10)
      OH2S04=10**(AH2S04-Y(9))
      X10(KC)=ALOG10(OH2S04)
      OS=10**(AS-Y(7))
      X2(KC)=ALOG10(OS)
      OHS=10**(AHS-Y(4))
      X2(KC)=ALOG10(OHS)
      OH2S=10**(AH2S-Y(2))
      X1(KC)=ALOG10(OH2S)
      OS04=10**(AS04-Y(6))
      X4(KC)=ALOG10(OS04)
      OHS04=10**(AHS04-Y(5))
      X5(KC)=ALOG10(OHS04)
      T1=(2.*Y(1)-(OHS+OHS04+4.*(OS+OS04)))
      T2=(OOH+OHS+OHS04+2.*(OS+OS04)-OH)
      ONA=(0.5*(T1+T2))/(1+R)
      X15(KC)=ONA
      OK=R*ONA
      X14(KC)=OK
      AKS04=((ALOG10(OK))+Y(3)+AS04)-X(7)
      ANS04=( ALOG10(ONA)+Y(5)+AS04)-Y(7)
      AKHS04=(ALOG10(OK) +Y(3)+AHS04)-Y(8)
      ANHS04=((ALOG10(ONA)+Y(5)+AHS04)-X(8))
      OKS04=10**(AKS04-Y(5))
      X6(KC)=ALOG10(OKS04)
      ONS04=10**(ANS04-Y(5))
      X7(KC)=ALOG10(ONS04)
      OKHS04=10**(AKHS04-Y(5))
      X8(KC)=ALOG10(OKHS04)
      ONHS04=10**(ANHS04-Y(5))
      X9(KC)=ALOG10(ONHS04)
      TS1=OH2S+OHS+OS
      TS2=OS04+OHS04+OKS04+ONS04+OKHS04+ONHS04+OH2S04
      TS=TS1+TS2
      X12(KC)=TS
      XH2S=OH2S/TS
      XHS=OHS/TS
      XS=OS/TS
      XS04=OS04/TS
      XHS04=OHS04/TS
      XKS04=OKS04/TS
      XNS04=ONS04/TS
      XKHS04=OKHS04/TS
      XNHS04=ONHS04/TS
      XH2S04=OH2S04/TS
      XRS=TS1/TS
      XOS=TS2/TS
      X11(KC)=XOS
      DS24S=-1*((XH2S*X(11))+(XHS*X(12))+(XOS*X(13)))
      X18(KC)=DS24S
      OCL=(ONA+OK)-(OKS04+ONS04+T2)
      X16(KC)=OCL
```

```
      TI2=0.5*(ONA+OK+OCL+OHS+OHSO4+OKSO4+ONSO4+4*(OS+OSO4))
      X17(KC)=TI2
      FH2S=(ALOG10(OH2S))+(ALOG10(Z(1)))-(ALOG10(55.5))
      FS=(FH2S+(0.5*F02(K)))-(Z(3)+ALOG10(Z(2)))*2
      X18(KC)=FS
      KC = KC + 1
    4 CONTINUE
    3 CONTINUE
C
      WRITE(6,101)
  101 FORMAT(//2X,'TEMPERATURE     KH2O       KH2S       KHS      KSO4
     .  KHSO4       K  KSO4,(K NASO4)          KHSO4 (NAHSO4)'/2X,'
     .  K FOR  S2 AND  H2O          KH2SO4   DEL H2S-S
     .DEL HS-S          DEL SO4-S' // )
      WRITE(6,102)(X(1),X(2),X(3),X(4),X(5),X(6),Y(7),X(8),X(9),
     .X(10),Y(11),Y(12),X(13))
  102 FORMAT(13F10.3)
      WRITE(6,103)
  103 FORMAT(//2X,'ION STRENGTH          ACT H2O          ACTIVITY COEF
     .OF   (K,CL)  (OH,HS)   (HSO4,NA,KSO4,NASO4,KHSO4,NAHSO4  )'/2X,'
     .SO4          S--          H      (H2S,H2SO4)'//)
      WRITE(6,104)(Y(1),Y(2),Y(3),Y(4),Y(5),Y(6),Y(7),Y(8),Y(9))
  104 FORMAT(9F10.4)
      WRITE(6,105)
  105 FORMAT(//2X'HENRY CONSTANT OF H2S      FUGACITY OF WATER
     .HOLLAND     DATA    OF        H2S   '//)
      WRITE(6,106)(Z(1),Z(2),Z(3))
  106 FORMAT(10X,F10.2,10X,F5.1,10X,F10.2 )
      WRITE(6,107)
  107 FORMAT(//2X,'              K/NA RATIO          FUGACITY OF SULFUR   '//)
      WRITE(6,108)(P,FS2)
  108 FORMAT(10X,F10.3,10X,F10.4)
      WRITE(6,200)
      WRITE(6,201)(XP(N),XF02(N),X1(N),X2(N),X3(N),X4(N),X5(N),X6(N),
     .X7(N),XP(N),X9(N),X10(N),X11(N),N=1,NTOTAL)
      WRITE(6,204)
      WRITE(6,202)
      WRITE(6,203)(XP(N),XF02(N),X12(N),X13(N),X14(N),X15(N),X16(N),
     .X17(N),X18(N),N=1,NTOTAL)
C
  100 FORMAT(4F10.2)
  200 FORMAT(//2X,'PH',3X,'F02',6X,'XH2S',7X,'XHS',9X,'XS',8X,'XSO4',7X
     .'XHSO4',6X,'XKSO4',5X,'XNASO4',5X,'XKHSO4',5X,'XNAHSO4',
     .          4X,'XH2SO4',6X,'XOS'//)
  201 FORMAT(F5.1,1X,F6.2,1X,E10.3,1X,E10.3,1X,E10.3,1X,E10.3,1X,E10.3,
     .1X,E10.3,1X,E10.3,1X,E10.3,1X,E10.3,1X,E10.3,1X,E10.3)
  202 FORMAT(//2X,'PH',4X,'F02',7X,'TS',11X,'FS',9X,'MK',8X,'MNA',9X,'MCL
     .',14X,'I2',9X,'DS34S'//)
  203 FORMAT(F5.1,1X,F6.2,2X,E10.3,2X,E10.3,2X,E10.3,2X,E10.3,2X,
     .E10.3,2X,E10.3,2X,E10.3)
  204 FORMAT('1')
  111 CONTINUE
 1111 CONTINUE
      STOP
      END
```

B29976